IL
NUOVO CIMENTO
ORGANO DELLA SOCIETÀ ITALIANA DI FISICA
SOTTO GLI AUSPICI DEL CONSIGLIO NAZIONALE DELLE RICERCHE
E DEL COMITATO NAZIONALE PER L'ENERGIA NUCLEARE

VOL. XXI, N. 4 *Serie decima* 16 Agosto 1961

# Isotopic Spin Dependence of Nucleon-Nucleon Cross-Sections between 600 and 1000 MeV.

G. MARTELLI, H. B. VAN DER RAAY, R. RUBINSTEIN
and
K. R. CHAPMAN, J. D. DOWELL (*), W. R. FRISKEN (**),
B. MUSGRAVE (***), D. H. READING
*Physics Department, The University of Birmingham - Birmingham*

(ricevuto il 10 Marzo 1961)

**Summary.** — The ratio of the differential cross-section for p-p and p-n scattering at 90° in the c.m.s. has been measured at three different energies, between 600 MeV and 1000 MeV, using fast scintillation counters in conjunction with magnetic momentum analysis. The value of this ratio decreases markedly with increasing energy, from $3.04 \pm 0.56$ at 595 MeV, to $1.00 \pm 0.18$ at 775 MeV and to $0.683 \pm 0.097$ at 1010 MeV, showing an enhancement of the scattering amplitude in the $T = 0$ state above 600 MeV. It is shown how this behaviour may be related to the second resonance in $\pi$-p scattering.

## 1. – Introduction.

Information about isotopic spin dependence of nuclear forces can be obtained from measurements of proton-proton and proton-neutron scattering at the same energy. At 90° in the c.m.s., where only states of even angular

(*) Present address: *CERN*, Geneva.
(**) Present address: Radiation Laboratory, Mc Gill University, Montreal.
(***) Present address: Physics Department, Yale University, New Haven, Conn.

momentum can contribute to the scattering, the isotopic singlet and triplet states do not interfere. Since the proton-proton eleastic scattering occurs in a pure $T=1$ state, whilst the proton-neutron interaction takes place in a known mixture of $T=0$ and $T=1$ states, measurements of these two reactions allow the contribution of the $T=0$ state to be determined. Moreover, if charge independence is valid, the condition

$$\varrho = \frac{\sigma_{pp}(90°)}{\sigma_{pn}(90°)} \leqslant 4 , \tag{1}$$

must be satisfied, since

$$\varrho = 4 \frac{|f_{T=1}(90°)|^2}{|f_{T=0}(90°)|^2 + |f_{T=1}(90°)|^2} , \tag{2}$$

where $f_{T=0}(90°)$ and $f_{T=1}(90°)$ are the scattering amplitudes in the $T=0$ and $T=1$ states respectively.

The differential cross-sections for p-p and n-p scattering have been investigated, at energies below 630 MeV, by several authors ([1,2]). From their measurements the ratio of the p-p to the n-p differential cross-sections at 90° in the c.m.s. can be deduced. In the present experiment this ratio was measured directly at 595 MeV, 775 MeV and 1010 MeV, using fast scintillation counters in conjunction with magnetic momentum analysis.

The yield from the proton-proton interaction was obtained as a difference between counts recorded with polythene and carbon targets, whilst that from the proton-neutron interaction was deduced similarly from results obtained with heavy water and water targets.

## 2. – Experimental method.

The measurements have been carried out using the extracted beam of the Birmingham proton-synchrotron, which produces $10^8$ protons/pulse, the duration of the pulse being 4 ms ([3]).

The experimental arrangement is shown in Fig. 1. After being deflected by the extractor, the beam leaves the vacuum box of the machine through the exit port ($P$), which is fitted with a 0.005 in. stainless steel dome. The beam is then focussed by a system of quadrupole lenses ($Q_1, Q_2, Q_3$) to a 1 in. diameter circle at the target position ($T$). The general background is reduced

([1]) W. N. Hess: *Rev. Mod. Phys.*, **30**, 368 (1958).

([2]) N. S. Amaglobeli and Iu. M. Kazarinov: *Žurn. Èksp. Teor. Fiz.*, **37**, 1587 (1959).

([3]) G. A. Doran, E. A. Finlay, H. R. Shaylor and M. M. Winn: *Nucl. Instr. Meth.*, **7**, 225 (1960).

by heavy concrete shielding walls ($W_1$, $W_2$) provided with clearance channels through which the beam passes. Once the beam has left the vacuum box of the synchrotron, it continues its path in air; no appreciable background from air scattering is observed.

The incident beam intensity was monitored by means of a fixed triple coincidence telescope, which accepted particles scattered through an angle of approximately 45° by a polythene target ($T'$). The resolving time of the monitor telescope was $2\tau = 12$ ns. The beam intensity was further checked by means of an ionization chamber (I.C.) of 9 in. aperture, placed before the scattering target. The total amount of material introduced into the beam path by the chamber was $7 \cdot 10^{-3}$ g/cm² of aluminized melinex.

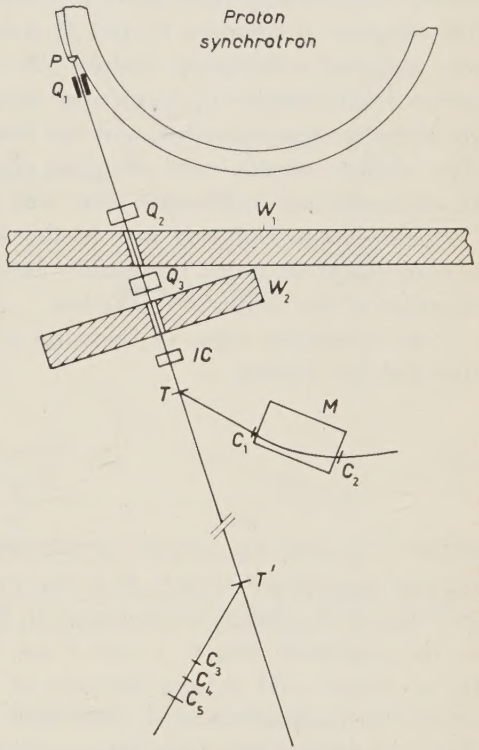


Fig. 1. – Experimental layout.

The four scattering targets (polythene, carbon, heavy water and water) could be interchanged remotely and were aligned to better than 0.5 mm. The polythene target measured $\frac{1}{2}$ in. in the beam direction and was $\frac{3}{4}$ in. high; the carbon target was also $\frac{3}{4}$ in. high and had the same stopping power as the polythene target. The water and heavy water were contained in two 0.03 in. walled vessels accurately machined from solid perspex. Their internal dimensions were $\frac{3}{4}$ in. in the vertical direction and $\frac{1}{2}$ in. in the beam direction. During the experiment the two liquids were frequently interchanged, in order to avoid any systematic error arising from small differences in the two containers.

Protons elastically scattered through 90° in the c.m.s. passed through the defining counter $C_1$ (which subtended $10^{-4}$ sr) and were then deflected through an angle of $\sim 28°$ by a magnet ($M$) and detected by counter $C_2$. The magnet was 120 cm long and had an aperture of $(5 \times 50)$ cm². Its field was adjusted for each of the three incident beam energies and stabilized to better than one part in $10^5$, by means of a nuclear resonance technique. Since the two counters were operated close to the magnet, they were fitted with 50 cm light guides, so that the photomultipliers could be placed well below the median plane of the magnet. The photomultipliers were further placed within two concentric

magnetic shields, the inner being of $\frac{1}{16}$ in. mu-metal and the outer of $\frac{1}{4}$ in. mild steel.

The random background could not be calculated, as the beam intensity varied considerably from pulse to pulse, and had to be measured directly. The outputs of counters $C_1$ and $C_2$ were split into two channels and fed into two identical coincidence circuits ($2\tau = 16$ ns). In one of these channels the pulses from counter $C_2$ (say) were suitably delayed, so that only accidental coincidences were recorded, and the true counting rate could thus be deduced. The random counts were recorded alternately in the two coincidence units, to eliminate any systematic error due to slight differences between them.

The random counting rate in the monitor was completely negligible over a wide range of beam intensities: this was verified by comparison with the readings of the ionization chamber.

The numerical value of the ratio $\varrho$, obtained from our measurements can therefore be written as

$$\varrho = \frac{[t_{(CH_2)_n} - \gamma t_C]K}{[t_{D_2O} - \delta t_{H_2O}]}, \tag{3}$$

where $t$ indicates the number of coincidences ($C_1C_2$), corrected for background, for the appropriate target; $K$ is the ratio of the number of deuterium atoms per cm$^2$ in the heavy water target to the number of hydrogen atoms per cm$^2$ in the polythene target; $\gamma$ and $\delta$ are correction factors for slight differences in the carbon and oxygen contents of the two pairs of targets. As a further check, the measurement at 1010 MeV was repeated replacing the water and heavy water targets with lithium hydride and lithium deuteride targets to determine the proton-neutron yield. Good agreement was found, and the result quoted for this energy represents an average of these two sets of measurements.

To verify that all the elastically scattered particles were detected by the system, a counter of 2 cm width ($C_2$ in Fig. 1) was used to scan across the back of the magnet. Typical curves, obtained at 1010 MeV, are shown in Fig. 2*a* and 2*b*. The effect of the internal momentum of the bound nucleons is evident from the broadening of the momentum spectrum obtained from the interaction with deuterium as compared with that found when using a « hydrogen » target. The full width at half height of the distribution found for the proton-proton interaction, corresponds to a momentum spread of 200 MeV/c. This is in good agreement with results of a simple calculation taking into account the angular acceptance of the system.

In performing the actual cross-section measurements, the 2 cm counter ($C_2$) was replaced by a $(10 \times 8)$ cm$^2$ counter and the full width of the momentum spectrum was covered by placing this counter in three adjacent positions.

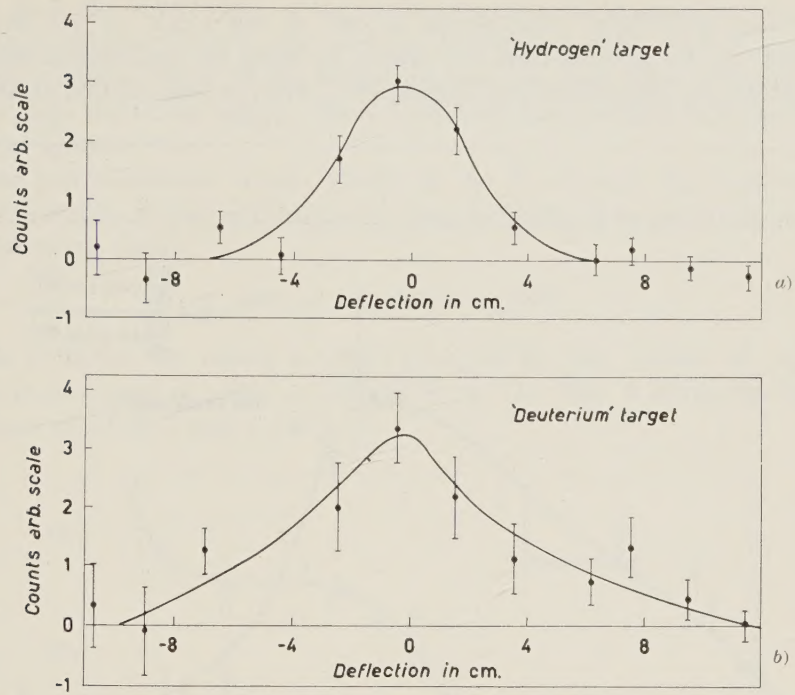


Fig. 2. – *a*) Momentum distribution of protons scattered by a « hydrogen » target; *b*) momentum distribution of protons scattered by a « deuterium » target.

Extreme care was taken to ensure that no region of the spectrum was omitted or measured twice. The complete scan was repeated several times for each of the four targets and good consistency was obtained.

## 3. – Experimental results.

The final values of $\varrho$, given in Table I and Fig. 3, represent the mean of numerous complete runs and should be free from any systematic error; consequently the errors quoted are based on counting statistics only.

TABLE I.

| Energy (MeV) | $\varrho$ |
|---|---|
| 1010 | $0.683 \pm 0.097$ |
| 775 | $1.00 \pm 0.18$ |
| 595 | $3.04 \pm 0.56$ |

The n-p differential cross-section at 90° in the c.m.s. at 775 MeV and 1010 MeV can be deduced from the ratio $\varrho$ by using the appropriate measured values of the p-p differential cross-section ([4,5]). The n-p cross-section at 600 MeV

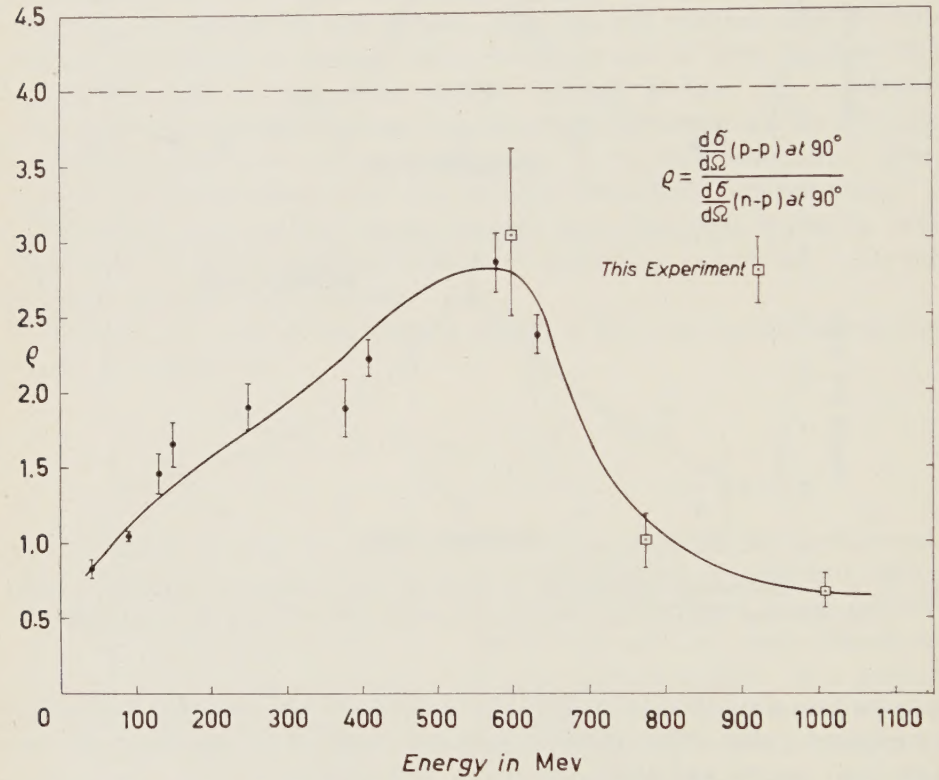


Fig. 3. – Energy dependence of the ratio of elastic p-p to p-n cross-sections at 90° in the c.m.s.

has already been measured directly by KAZARINOV *et al.* ([6]). The value of $\sigma_{np}(90°)$ obtained at 775 MeV is subject to a small error, since we used the p-p differential cross-section obtained by SMITH *et al.* ([4]) at 800 MeV.

## 4. – Discussion.

In the present experiment we have treated the p-n collisions as occurring between free nucleons. This seems justified since at nucleon energies of several

([4]) L. W. SMITH, A. W. MC REYNOLDS and G. SNOW: *Phys. Rev.*, **97**, 1186 (1955).
([5]) J. D. DOWELL, W. R. FRISKEN, G. MARTELLI, B. MUSGRAVE, H. B. VAN DER RAAY and R. RUBINSTEIN: *Nuovo Cimento*, **18**, 818 (1960).
([6]) IU. M. KAZARINOV and IU. N. SIMONOV: *Žurn. Èksp. Teor. Fiz.*, **31**, 169 (1956).

hundred MeV the wavelength of the incident particle is considerably less than the average distance between the nucleons in the deuterium nucleus; furthermore, the screening effect of the bound nucleons on each other becomes negligible at large scattering angles. These facts have been verified experimentally by several authors [7-9].

As the p-p interaction occurs wholly in the $T=1$ state, the contribution of the $T=0$ state to the n-p interaction may be deduced by re-writing eq. (2) in the following form:

$$\sigma_{T=0}(90°) = 4\sigma_{np}(90°) - \sigma_{pp}(90°) . \tag{4}$$

Table II shows the values $\sigma_{T=1}(90°)$ $(\equiv \sigma_{pp}(90°))$, the values of $\sigma_{np}(90°)$ deduced from $\varrho$, and $\sigma_{T=0}(90°)$ as defined in eq. (4). Fig. 4 shows the energy dependence of $\sigma_{pp}(90°)$ and $\sigma_{np}(90°)$.

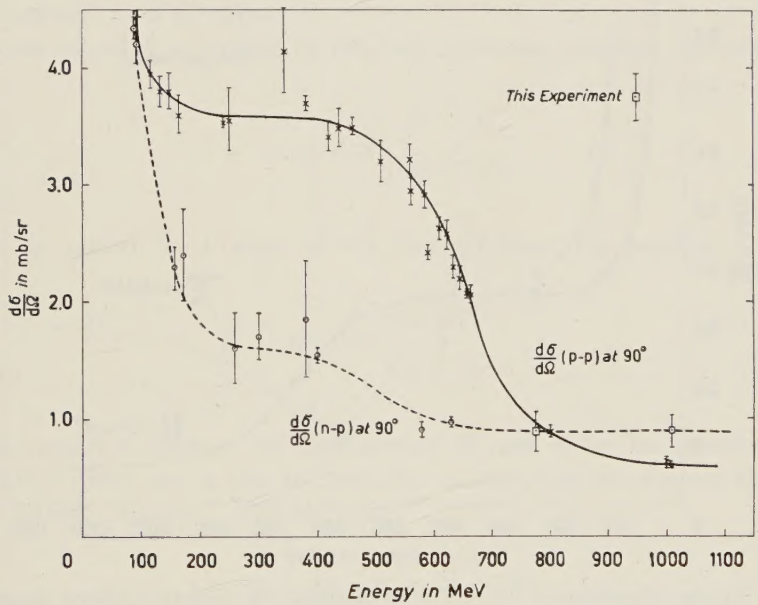


Fig. 4. – Energy dependence of the p-p and n-p elastic cross-sections at 90° in the c.m.s.

The values of $\varrho$ (Fig. 3) at 595 MeV, 775 MeV and 1010 MeV were measured directly in the present experiment, while the others were deduced from published results [1,2].

(7) G. A. Leksin: *Žurn. Éksp. Teor. Fiz.*, **32**, 440 (1957).

(8) V. P. Dzelepov, B. M. Golovin, Iu. M. Kazarinov and N. N. Semenov: *CERN Symposium* (1956), Vol. II, 115.

(9) A. P. Batson, B. B. Culwick, H. B. Klepp and L. Riddiford: *Proc. Roy. Soc.*, A **251**, 233 (1959).

TABLE II.

| Energy (MeV) | $(\sigma_{pp}(90°)$ (mb/st) | $\sigma_{np}(90°)$ (mb/st) | $\sigma_{T=0}(90°)$ (mb/st) |
|---|---|---|---|
| 1010 | $0.608 \pm 0.030$ | $0.89 \pm 0.13$ | $2.95 \pm 0.54$ |
| 775 | $0.89 \pm 0.05$ | $0.89 \pm 0.17$ | $2.66 \pm 0.67$ |

The value of $\varrho$ never exceeds 4: this is to be expected if charge independence is valid. The feature of interest in Fig. 3 is the marked decrease of $\varrho$ from 600 MeV to 1000 MeV. Since the contribution from the $T=1$ state is known, the behaviour of $\varrho$ shows that $\sigma_{T=0}(90°)$ is greatly enhanced with increasing energy (see Fig. 5 and Table II).

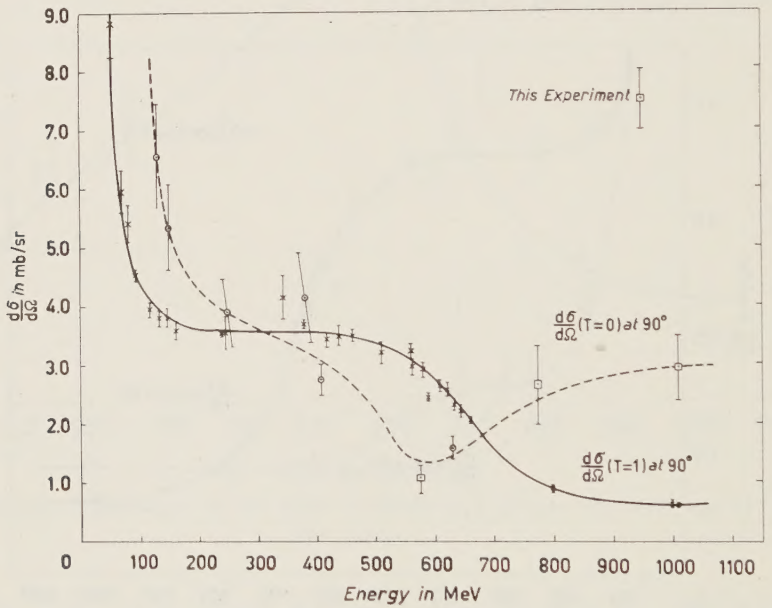


Fig. 5. – Energy dependence of the cross-sections for nucleon-nucleon scattering in in the $T=0$ and $T=1$ states, at 90° in the c.m.s.

The observed increase of $\sigma_{T=0}(90°)$ above 600 MeV can probably be interpreted in terms of shadow effects. Low energy pion scattering is dominated by the well known $T=\frac{3}{2}, J=\frac{3}{2}$ resonance. A second resonance occurs $\sim 300$ MeV (in the c.m.s.) above the first, and this and other higher order resonances are dominated by the $T=\frac{1}{2}$ state ([10]). Similarly, nucleon-nucleon

([10]) R. F. PEIERLS: *Phys. Rev.*, **118**, 325 (1960).

inelastic interactions may be pictured as proceeding through the formation of a pion-nucleon resonant system (isobar), which can occur in the $T=\frac{3}{2}$ state from an initial $T=1$ state, but with increasing energy we approach the value at which it is possible to form an isobar corresponding to a higher resonance, in a $T=\frac{1}{2}$ state, and here the $T=0$ state of the initial nucleons can contribute to the process (*).

Although our mesurements are limited to 90° in the c.m.s., we have attempted a comparison between the behaviour $\sigma_{T=0}(90°)$ and $\sigma_{T=1}(90°)$ with the $\pi$-p resonances in the $T=\frac{3}{2}$ and $T=\frac{1}{2}$ states respectively. In order to make this comparison, an equivalent energy for the two interactions had to be defined. This has been done by using an approximate model to describe the inelastic interaction of the two nucleons.

Let us call $\mathcal{N}^+$ the isobar ($\pi$-$\mathcal{N}$) with spin $\frac{3}{2}$, isotopic spin $\frac{3}{2}$ and even parity, created in a $p_{\frac{3}{2}}$ state, and $\mathcal{N}^{++}$ the isobar with spin $\frac{3}{2}$, isotopic spin $\frac{1}{2}$ and odd parity, created in a $d_{\frac{3}{2}}$ state.

For an initial $T=1$ state of the two nucleons, consider the reaction

$$\mathcal{N}+\mathcal{N}\begin{cases}\nearrow \mathcal{N}+\mathcal{N} \\ \searrow \mathcal{N}+\mathcal{N}^+\end{cases} \tag{5}$$

and for an initial $T=0$ state of the two nucleons, the reaction

$$\mathcal{N}+\mathcal{N}\begin{cases}\nearrow \mathcal{N}+\mathcal{N} \\ \searrow \mathcal{N}+\mathcal{N}^{++}\end{cases} \tag{6}$$

First consider reaction (5), and assume $\mathcal{N}$ and $\mathcal{N}^+$ to be produced at rest in the c.m.s. (they are in fact in a relative $S$-state, and we neglect about 10 or 20 MeV kinetic energy). We can write

$$M+M+T'=M+M^+,$$

where $M$ is the nucleon rest mass and $T'$ the total kinetic energy of the interacting nucleons in the c.m.s.

Then

$$T'+M=M^+=(k^2+M^2)^{\frac{1}{2}}+(k^2+\mu^2)^{\frac{1}{2}},$$

(*) Two isobars in a $T=\frac{3}{2}$ state could also be formed. However, there is strong experimental evidence (see, for instance [9]) that, at these energies, double pion production is very small.

where $k$ is the momentum of the pion in the c.m.s. and $\mu$ is the pion mass.

Furthermore

$$(k^2 + \mu^2)^{\frac{1}{2}} = t' + \mu ,$$

where $t'$ is the kinetic energy of the pion in the c.m.s.

Let us now consider pion-nucleon scattering and let the kinetic energy of the pion in the c.m.s. also be $t'$. Under the above assumptions, $t'$ can be defined as the energy « equivalent » to $T'$ in the nucleon-nucleon collisions.

In an identical manner an equivalence can be defined between the energy $t''$ of the pion in the $d_{\frac{3}{2}}$ resonance and the energy $T''$ corresponding to reaction (6).

These definitions of energy equivalence allow us to compare the energy dependence of the total cross-sections for $\pi$-p scattering $\sigma_t(T=\frac{3}{2})$ with that of $\sigma_{T=1}(90°)$ (see Fig. 6) and the energy dependence of $\sigma_t(T=\frac{1}{2})$ with that of $\sigma_{T=0}(90°)$ (see Fig. 7). In order to remove the effect of geometrical factors, $\sigma_{T=1}(90°)$ and $\sigma_{T=0}(90°)$ have been divided by $\lambda^2$ ($2\pi\lambda$ being the wave length of the incident nucleon in the lab. system).

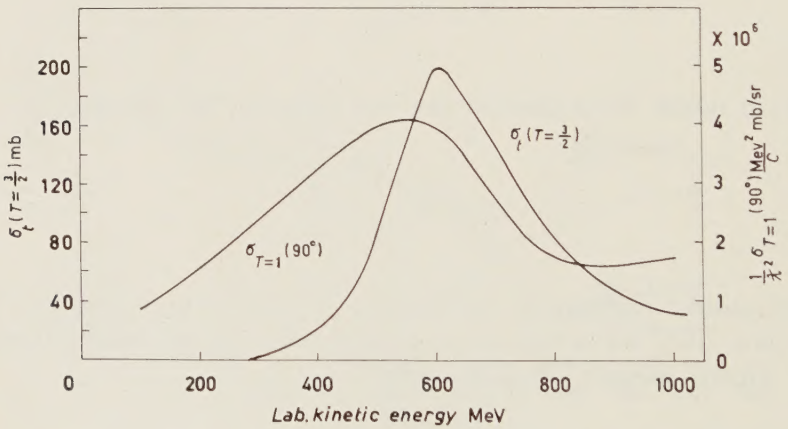


Fig. 6. – Comparison between the energy dependence of the total $\pi$-p cross-section $\sigma_t(T=\frac{3}{2})$ and that of the nucleon-nucleon elastic scattering in the $T=1$ state at 90° in the c.m.s.

The values of $\sigma_t(T=\frac{1}{2})$ have been deduced from the relation

$$\sigma_t(T=\tfrac{1}{2}) = \tfrac{3}{2}\sigma_t(\pi^-) - \tfrac{1}{2}\sigma_t(\pi^+) ,$$

where $\sigma_t(\pi^-)$ and $\sigma_t(\pi^+)$ are the total cross-sections for $\pi$-p scattering [11].

[11] L. C. L. YUAN: *CERN Symposium* (1956), Vol. II, 195.

To draw a detailed comparison between these curves, a knowledge of the individual amplitudes for the two scattering processes would be required. Although we only know the cross-sections at 90 , our results confirm that the

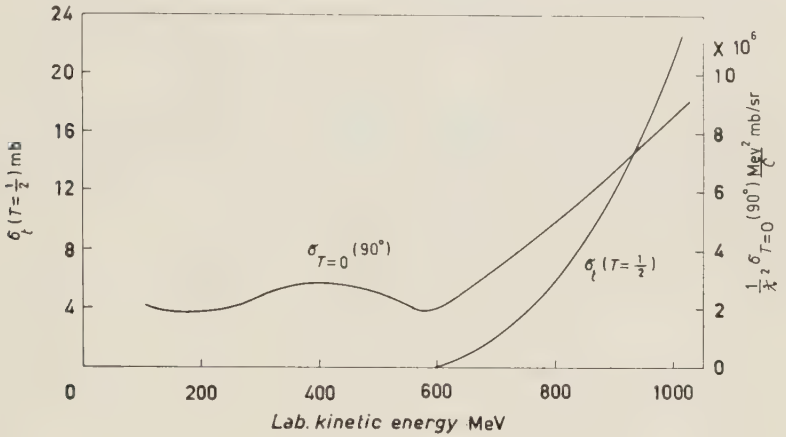


Fig. 7. – Comparison between the energy dependence of the total $\pi$-p cross-section $\sigma_t(T=\frac{1}{2})$ and that of the nucleon-nucleon elastic scattering in the $T=0$ state at 90 in the c.m.s.

final state interaction between the pion and the nucleon in the inelastic process $\mathcal{N}+\mathcal{N}\rightarrow\mathcal{N}+\mathcal{N}+\pi$ has a marked effect on the elastic cross-section, and this seems to show up strongly at 90° in the c.m.s.. Indeed, this effect appears not only in the results obtained in the $T=1$ initial state of the two nucleons, but also for the $T=0$ state, and this seems due to the onset of the $T=\frac{1}{2}$ pion-nucleon resonance. Nevertheless, the mechanism cannot be identical for both cases.

Let us first consider reaction (5), which occurs in the $T=1$ state. If the isobar is produced in a $l=0$ state relative to the nucleon, then, because of conservation of total angular momentum, isotopic spin and parity, the only possible initial state is $^1D_2$. This state has a non-zero amplitude at 90°, and this provides a plausible explanation of the maximum shown by $\sigma_{T=1}(90°)$ at 600 MeV (see Fig. 6).

If we now consider reaction (6), which occurs in the $T=0$ state, a $l=0$ relative state between $\mathcal{N}^{++}$ and $\mathcal{N}$ can only occur for a $^1P_1$ initial state of the two nucleons. This state has zero amplitude at 90° and therefore cannot explain the observed rise of $\sigma_{T=0}(90°)$ in Fig. 7. However, if the $\mathcal{N}^{++}$ is being produced in a $l=1$ state, this might account for the rise of $\sigma_{T=0}(90°)$, since the $l=1$ state is associated with $^3S_1$, $^3D_1$, $^3D_2$, $^3D_3$, $^3G_3$ initial states, which have a non-zero contribution at 90°.

However, one would then expect that the observed rise of $\sigma_{T=1}(90^\circ)$ would be shifted towards higher energies, or perhaps have a slow initial rise. For this reason it would be interesting to check whether the curve $\sigma_{T=0}(90^\circ)$ has a maximum which coincides with the $d_{\frac{3}{2}}$ resonance in pion scattering, or whether this maximum occurs at higher energies.

* * *

The authors are deeply indebted to Mr. L. CASTILLEJO and Dr. R. F. PEIERLS, of the Mathematical Physics Department of this University, for most valuable discussions and comments. They would like to thank the Synchrotron crew, under Dr. P. D. WHITAKER, for cheerful co-operation, and Mr. H. R. SHAYLOR for providing the stabilized bending magnet.

R.R. and D.H.R. are grateful to D.S.I.R. for Research Studentships.

## RIASSUNTO

Si è misurato il rapporto fra le sezioni d'urto differenziali per scattering p-p e p-n a 90° nel centro di massa a tre differenti energie, fra 600 MeV e 1 000 MeV, mediante l'uso di contatori a scintillazione e analisi magnetica. Il valore di questo rapporto diminuisce notevolmente col crescere dell'energia, da $3.04 \pm 0.56$ a 595 MeV, a $1.00 \pm 0.18$ a 775 MeV e a $0.683 \pm 0.097$ a 1 010 MeV, e questo indica un aumento della ampiezza di scattering nello stato $T=0$ al di sopra di 600 MeV. Questo risultato è posto in relazione con la seconda risonanza nello scattering $\pi$-p.

IL NUOVO CIMENTO Vol. XXI, N. 4 16 Agosto 1961

# Some Analytic Properties of a Decay Amplitude with Final State Interactions.

## I. - The Vertex Diagrams in $K \to 3\pi$ Decay.

G. Barton (*)

*Institute for Advanced Study - Princeton, N. J.*

C. Kacser (**)

*Palmer Physical Laboratory, Princeton University - Princeton, N. J.*

(ricevuto il 14 Aprile 1961)

**Summary.** — The simplest vertex-type diagrams for $K \to 3\pi$ decay contain an internal double pion line; when the total rest-mass parameter $\lambda$ of this line is taken as discrete, the amplitude possesses on the physical sheet an anomalous branch point above the normal one, subject to the condition $(M^2 - \mu^2)/2 < \lambda^2 < (M - \mu)^2$, with $M$ the kaon and $\mu$ the pion mass. On integrating over $\lambda^2$ this singularity is eliminated. In order to understand the amplitude fully, we must consider it temporarily as a function of two complex variables, in which a double dispersion representation is found to hold. The spectral functions are examined in semi-closed form to exemplify these statements, and to give a perturbation-theory illustration of some of the popular approximations in calculations on this decay.

### 1. – Introduction.

The basic mechanism responsible for $K \to 3\pi$ decay is not fully understood. It is commonly assumed however that in the absence of any coupling between the emergent pions the matrix element would be essentially constant,

(*) On leave of absence from Christ Church, Oxford. Supported by a grant to the Institute from the National Science Foundation.

(**) On leave of absence from Magdalen College, Oxford. Supported in part by the U.S.A.F. Office of Scientific Research, Air Research and Development Command.

and that the structure it actually posssesses is due to the final state interactions. Recently several dispersion-theoretic considerations of such effects have appeared ([1-4]); one of their common features is the effort to find an approach as closely analogous as possible to that which one would naturally follow in dealing with a hypothetical scattering process $K-\pi \to \pi-\pi$. SAWYER and WALI ([2]) discuss this from the viewpoint of the Mandelstam representation of a scattering process for stable masses, and then restrict themselves explicitly to that component of the decay amplitude which is independent of the K-meson mass $M$, and which can therefore be obtained by a trivial reinterpretation of such a discussion. By contrast, KHURI and TREIMAN ([1]) make no such assumption about the $M$-dependence of the matrix element, which they begin by writing as

$$\langle \pi_1 \pi_2 \pi_3 \text{ (out)} \,|\, \mathscr{H}_w \,|\, K \rangle$$

and which, by suitable contractions, they then manipulate into a form reminiscent of a scattering amplitude. Here, $\mathscr{H}_w$ is the weak (decay-inducing) Hamiltonian density. Its appearance in first (but no higher) order is essential since otherwise the single K-meson state $K$ cannot be given any well defined meaning. Once the amplitude is written in this form the weak coupling is imagined to be switched off, so that $K$ becomes a stable single particle state.

The presence of an extra operator $\mathscr{H}_w$ as compared with a true scattering process between stable particles entails that the «absorptive part» of the heuristic dispersion relation can no longer be identified with the imaginary part of the amplitude, so that the spectral function is now not necessarily real.

Another common approximation of these calculations is the restriction to that part of the amplitude which can be expressed as a sum of terms each depending on only one of the covariant variables $s_i = -(K-k_i)^2$, $K$ and $k_i$ being the momenta of the K-meson and of the $i$-th pion respectively (*).

The main purpose of the present paper is to illustrate the import and interconnections of these approximations from the viewpoint of perturbation theory by examining the simplest Feynman diagrams for $K \to 3\pi$ decay, paying attention not only to the analytic properties but also to the spectral functions of the corresponding amplitudes.

In Section 2 we comment on the ideas underlying the perturbation approach; in Section 3 we give the results of the standard method for locating the sin-

([1]) N. N. KHURI and S. B. TREIMAN: *Phys. Rev.*, **119**, 1115 (1960).
([2]) R. F. SAWYER and K. C. WALI: *Phys. Rev.*, **119**, 1429 (1960).
([3]) S. FUBINI and R. STROFFOLINI: *Nuovo Cimento*, **17**, 263 (1960).
([4]) Cf. also the Proceedings of the 1960 Rochester Conference.
(*) We use the metric $(+, +, +, -)$.

gularities of the Feynman amplitudes as functions of $s$ and $M$, and point out the mechanism which, in perturbation theory, prevents the identification of the spectral function with the imaginary part. Finally in Section **4** we find semi-closed expressions for, and comment on, the simplest non-trivial spectral functions.

## 2. – Perturbation approach.

From the viewpoint of unadulterated perturbation theory it is clear that nucleon loops ought to figure prominently in our diagrams, since they are certainly involved both in the weak $K \to 3\pi$ vertex and in the subsequent $\pi\pi$ interactions. Nevertheless for a variety of reasons we shall omit them. Thus, all momentum transfers in the decay are low compared with the nucleon mass and it is intuitively appealing, though not rigorously justifiable, that after renormalization it is the low-momentum regions which predominate also for the virtual particles (5). In other words, we think of the loops as contributing primarily to the effective $K\pi^3$ and $\pi^4$ coupling constants. However, the strongest motivation for including only pions as internal lines is the desire to parallel as closely as possible the conventional dispersion-theoretic treatment.

The couplings we envisage are therefore $Gq_K q_\pi^3$ (occuring once only; from now on we drop the factor $G$) and $gq_\pi^3$; the isotopic structure is irrelevant to our purposes and is ignored (*).

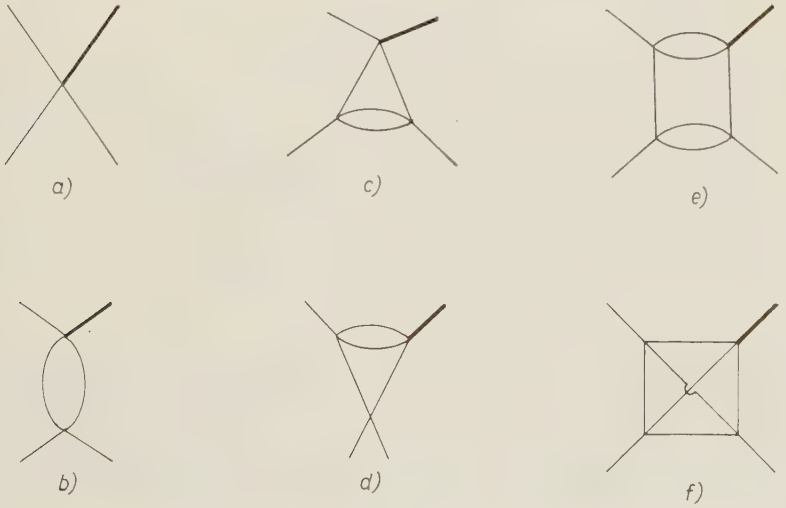


Fig. 1.

(5) A similar idea has been exploited in a different context by Y. Fujii and S. Furuichi: *Prog. Theor. Phys.*, **23**, 251 (1960).

(*) No qualitatively new features appear if one introduces also a $\varphi_K^2\varphi_\pi^2$ coupling.

The leading diagrams are of the type shown in Fig. 1. The heavy line represents the K-meson; all other lines represent pions. Proceeding anticlockwise from the K line we label the external pion lines by their momenta $k_1$, $k_2$, $k_3$. The first diagrams to depend on two of the $s_i$ are those of type (*e*) and (*f*) which are at least of order $g^3$; thus for $g$ to be small is a sufficient but by no means necessary justification of the restriction to single-$s$-dependent terms [3] (*).

We shall confine ourselves to such diagrams and pick out those depending on $s_1 = -(K-k_1)^2 = -(k_2+k_3)^2$, from which we now drop the suffix. The only diagram of order $g$, *i.e.* (*b*), is of the self-energy type and evidently depends only on $s$ but not on $M$. Thus a small $g$ is sufficient also to ensure that $M$-independent terms predominate.

The vertex-type diagrams (*c*) and (*d*), both of order $g^2$, are the first ones capable of showing non-trivial characteristics of decay processes. Actually (*c*) is still independent of $M$ and only (*d*) depends on both $s$ and $M$.

We must note at the outset that as they stand the amplitudes for all these diagrams diverge, although they have the same structure as those of ordinary $\varphi^4$ theory and are therefore renormalizable in principle. The double pion line carrying a total momentum of square $-s$ (*e.g.* the entire diagram (*b*)) has the representation

$$\Delta(s) = \int_4^\infty \mathrm{d}s' \sigma_0(s')(s' - s - i\varepsilon)^{-1}; \qquad \sigma_0(s') = \{(s'-4)/s'\}^{\frac{1}{2}}, \tag{2.1}$$

which already diverges logarithmically. (Here and henceforth the $\pi$ mass is set equal to unity.) If, in diagrams (*c*) to (*e*), we leave this $s'$ integration to be performed at the end of the calculation, then the integral over the remaining circulating momentum converges. On the other hand, a conventional renormalization procedure essentially replaces $\Delta(s)$ by $\Delta'(s) = \Delta(s) - \Delta(4)$; the $s'$ integration then converges but the integral over the other circulating momentum diverges logarithmically and must be renormalized in a second, independent, step.

However, as explained above, the $\varphi^4$ coupling itself is only an approximation; moreover the entire perturbation approach is of course being taken with a grain of salt. Hence, instead of renormalizing formally, we adopt an easy way of eliminating the divergence in an equally covariant manner: $\sigma_0$ is imagined to be replaced by some function $\sigma$ that decreases fast enough at

(*) *Note added in proof.* – In a second paper (submitted to *Nuovo Cimento*) we consider diagrams of type (*e*). We find complex singularities occur simultaneously in both of the two natural $s$ variables; however one-dimensional dispersion relations with only the normal threshold cuts do hold.

infinity for (2.1) to converge. This would be the case if either or both of the $K\pi^3$ and $\pi^4$ vertices had some covariant cut-off mechanism built into them; in view of the closed nucleon loops hidden in both types of vertex such a cut-off could reasonably be expected to be effective in the vicinity of the nucleon mass.

With this point of view, diagrams (*c*) and (*d*) are approached by first replacing the double pion line with a single line of rest mass $\lambda$, and then integrating over $\lambda^2$ with the weight function $\sigma(\lambda^2)$. On this prescription both diagrams converge without further manipulation. The analytic properties of our amplitudes are certainly unaffected by this method of securing convergence; the spectral functions themselves of course do depend on how the infinities are removed, although as regards the final outcome, namely the variation of the matrix element with $s$, this quantitative dependence is, at an educated guess, quite weak.

## 3. – Analytic structure.

3·1. *Introduction.* – In the spirit of the preceding remarks, and otherwise following standard methods (6), we write the contribution of diagram (*d*) as follows:

$$F(s, M^2) = \int_4^\infty \mathrm{d}\lambda^2 \sigma(\lambda^2) f(s, M^2, \lambda^2) , \tag{3.1}$$

where

$$f = \int_0^1 \mathrm{d}\alpha_1 \mathrm{d}\alpha_2 \mathrm{d}\alpha_3 \, \delta(1 - \alpha_1 - \alpha_2 - \alpha_3) \Delta^{-1} , \tag{3.2}$$

with

$$\Delta = \{\alpha_1\lambda^2 + \alpha_2 + \alpha_3 - \alpha_1\alpha_2 - \alpha_2\alpha_3 s - \alpha_3\alpha_1 M^2 - i\varepsilon\} . \tag{3.3}$$

Recall that the pion mass is unity and that the physical K mass lies between 3 and 4.

It is clear from the structure of these equations that the singularities of $F$ will coincide with those of $f(s, M^2, \lambda^2)$ at $\lambda^2 = 4$, the end point of the $\lambda^2$ integration. However, in order to gain some feeling for the spectral functions we shall first consider $f$ for general discrete $\lambda^2 > 4$.

(6) J. M. Jauch and F. Rohrlich: *The Theory of Photons and Electrons* (Cambridge, Mass., 1955).

3·2. *Analytic structure for given* $\lambda^2$. – We immediately encounter the fundamental difficulty, characteristic of decay processes with final state interactions, that for given real $M^2$ and $\lambda^2$ the amplitude $f$ cannot mathematically speaking be regarded as the boundary value of a function of a single complex variable $s$. To see this, consider $\Delta$ with the Feynman $i\varepsilon$ incorporated into the (now complex) variable $s$, and perform the $\alpha_1$ integration in (3.2). Then, independently of $s$, $\Delta$ vanishes at two points along the $\alpha_2 = 0$ boundary of the region of integration in the $(\alpha_2\alpha_3)$ plane, subject only to the condition that $\lambda < (M-1)$. At these points therefore the integration is ill defined; to make it unambiguous either $\lambda^2$ or $M^2$ must also be assigned an infinitesimal imaginary part, so that in principle $f$ must be regarded as a function of *two* complex variables. The end result is independent of which is chosen; we adopt $M^2$ as the second variable, because the discussion then proceeds in close analogy to that of more familiar cases, and because at the end we can establish some correspondence with certain properties of production amplitudes.

Of course from the physical point of view $s$ and $M^2$ are radically different kinds of quantities, since $M^2$ is a constant parameter whose numerical value is dictated by nature, while $s$ is a variable chosen for describing the decay process. Nevertheless, in order to gain a complete understanding of the amplitude $f$ we are forced to treat them, mathematically, on a comparable footing; we go on therefore to investigate the analytic properties of $f$ as a function of these two complex variables. It will appear later that such a procedure does after all come into some contact with physics.

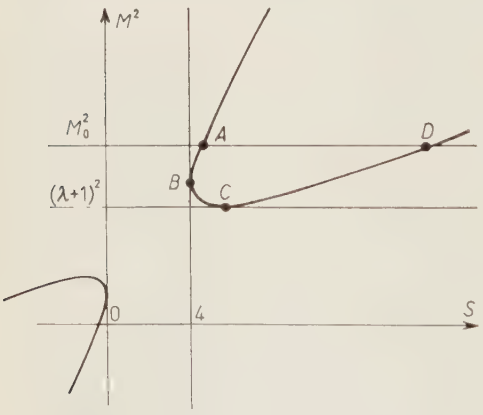


Fig. 2.

On the physical sheet $f$ always possesses normal thresholds (endpoint singularities) as $s = 4$ and at $M^2 = (\lambda+1)^2$. The equation for the surface of coincident singularities is

$$(3.4)\quad Q(s, M^2) = \{\lambda^2 s^2 + \lambda^2(\lambda^2 - M^2 - 3)s + (M^2-1)^2\} = 0 .$$

The intersection of $Q = 0$ with the real $(s, M^2)$ plane, which we shall call $\Gamma$, is the hyperbola shown in Fig. 2. The line $AD$ should be ignored at this stage. The point $B$ lies at $M^2 = (2\lambda^2+1)$, and $C$ at $s = (\lambda+2)$.

Following standard methods [7,8] we find that on the physical sheet none

(7) J. TARSKI: *Journ. Math. Phys.*, **1**, 149 (1960).

(8) M. FOWLER, P. V. LANDSHOFF and R. W. LARDNER: *Nuovo Cimento*, **17**, 956 (1960).

of the arcs of $\Gamma$ are singular; in particular, there are no singularities on the physical sheet for complex $s$ or $M^2$. This result hinges on the physically imposed condition $\lambda > 2$; for $\lambda < 2$, the conic $\Gamma$ is an ellipse, one of its arcs is singular, and complex singularities do appear ([8,9]). (For $\lambda = 2$, $\Gamma$ degenerates into a straight line and must necessarily be discussed as the limiting case with $\lambda$ tending to 2 from above or from below.)

This information is sufficient to establish for the amplitude corresponding to our particular diagram (*d*) a two-dimensional representation, with cuts only along the real axes, of the type conjectured by BONNEVAY ([10]):

$$f(s, M^2, \lambda^2) = \int_{(\lambda+1)^2}^{\infty} \frac{\mathrm{d}M'^2}{M'^2 - M^2 - i\varepsilon} \int_4^{\infty} \frac{\mathrm{d}s'}{s' - s - i\varepsilon} \beta(s', M'^2, \beta^2) , \tag{3.5}$$

and

$$F(s, M^2) = \int_9^{\infty} \frac{\mathrm{d}M'^2}{M'^2 - M^2 - i\varepsilon} \int_4^{\infty} \frac{\mathrm{d}s'}{s' - s - i\varepsilon} B(s', M'^2) , \tag{3.6}$$

where

$$B(s, M^2) = \int_4^{\infty} \mathrm{d}\lambda^2 \, \sigma(\lambda^2) \beta(s, M^2, \lambda^2) . \tag{3.7}$$

The signs of the $i\varepsilon$ are determined by comparison with the equations for the Feynman amplitude, (3.2) and (3.3). The lower limits on the integrals in (3.5) and (3.6) are actually deceptive; thus the spectral function $\beta$ is non-zero only within the upper branch of $\Gamma$ (cf. Section **4**).

We are now in a position to give meaning to a single-variable dispersion relation in $s$ by performing the $M'^2$ integration in (3.5):

$$f(s, M^2, \lambda^2) = \int_4^{\infty} \frac{\mathrm{d}s'}{s' - s - i\varepsilon} \varrho(s', M^2, \lambda^2) , \tag{3.8}$$

$$\varrho(s', M^2, \lambda^2) = \int_{(\lambda+1)^2}^{\infty} \frac{\mathrm{d}M'^2}{M'^2 - M^2 - i\varepsilon} \beta(s', M'^2, \lambda^2) . \tag{3.9}$$

([9]) P. V. LANDSHOFF and S. B. TREIMAN: Cambridge preprint (1960).

([10]) G. BONNEVAY: *Proceedings of the 1960 Rochester Conference*, p. 523; but cf. also the report on the subsequent discussion.

A similar representation exists for $F$, whose spectral function $P$ is given by

$$P(s', M^2) = \int_4^\infty \mathrm{d}\lambda^2\, \sigma(\lambda^2)\, \varrho(s', M^2, \lambda^2)\,. \tag{3.10}$$

Actually of course we are interested in $f$ only when $M^2$ has its physical value, which for the rest of this subsection we shall denote by $M_0^2$. The line $AD$ in Fig. 2 shows the position of $M_0^2$ for $\lambda$ such that $4 < \lambda^2 < (M_0^2 - 1)/2$. For $(M_0^2 - 1)/2 < \lambda^2 < (M_0 - 1)^2$, the line $AD$ intersects the upper branch of $\Gamma$ at a level between $B$ and $C$, while for $\lambda^2 > (M_0 - 1)^2$ it lies below the normal threshold and fails to intersect the upper branch at all. Eq. (3.9), combined with the restriction on $\beta$ anticipated from the next section, shows that $\varrho$ will be complex when $s$ lies between the points $A$ and $D$, which exists only if $M_0 < (\lambda + 1)$. (It is clear that the only feature marking $f$ as a decay amplitude is just this external instability condition.)

Finally, we anticipate from the next section the conclusion that, subject to the condition $(M_0^2 - 1)/2 < \lambda^2 < (M_0 - 1)^2$, $f$ as a function of $s$ has an anomalous branch point ($ABP$) at $A$; this $ABP$ invariably lies above the normal branch point at $s = 4$.

3·3. *General comments.* – Since the $ABP$ of $f$ at $A$ has disappeared from the physical sheet by the time $\lambda$ has decreased to 4, it is clear that the final amplitude $F$ has no corresponding singularity, but only the normal branch point at $s = 4$. In a manner of speaking which will be substantiated further in the next section, the $ABP$ of $f$ is significant, from the point of view of $F$, only in that it is connected with the mechanism whereby the spectral function becomes complex when $M$ becomes unstable.

The necessity of integrating over $\lambda^2$ with a continuous weight function is not of course coincidental: since the corresponding internal line carries the same quantum numbers as two pions, and does actually interact with two pions at one extremity, its mass value must be distributed continuously. Note that any approximation to $\sigma(\lambda^2)$ by means of $\delta$-functions (as could conceivably be inspired by a $\pi\pi$ resonance) runs the risk of introducing spurious singularities into $F$.

The circumstance that $f$, for discrete $\lambda < 2$, acquires singularities for complex $s$ and real $M^2$, has been noted by Fowler, Landshoff and Lardner [8]. (Such a situation would arise if there existed a bound state of two pions.) Its physical significance has been elaborated by Landshoff and Treiman [9], who show that diagrams of the kind we have been considering contribute to production processes, in which $M^2$ is identifiable as the total energy of the initially colliding particles. For such a production process with $\lambda < 2$ one has external

instability combined with internal stability; as we pass to $\lambda > 2$ the internal stability is lifted, a change which is known to favor a simplification of the analytic structure.

In this connection it is profitable to observe in general that our decay amplitudes have at least as much in common with production as with scattering processes.

It may be worth-while to make two further observations. The first diagram whose contribution to $\varrho$ develops an imaginary part is also the first in which all three pions emerging from the $K\pi^3$ vertex interact at least once more. This is the perturbation-theoretic illustration of a point already made on general grounds by FUBINI and STROFFOLINI ([3]). Lastly, the similarity between the diagrams for $K \to 3\pi$ and those of ordinary $q^4$ theory makes it evident that the complete decay amplitude regarded as a function of $M^2$ will have (at least) all the singularities possessed by the pion propagator as a function of negative squared momentum.

## 4. – The spectral functions.

We have already noted that for $g$ to be small is sufficient but not necessary to justify one of the popular approximations to the matrix element. It is much less clear whether the approximation making the amplitude independent of $M$ is justifiable on any other grounds. In order to gain some limited insight into the likelihood of this conjecture we shall compare the spectral functions of diagrams (*c*) and (*d*), which are on an equal footing in that both are of order $g^2$ and have representations of the type (3.7) and (3.8). If the spectral function $\varrho'$ of (*c*) should turn out to exceed appreciably the spectral function $\varrho$ of (*d*), then we would have some indication that this approximation can be independent of the magnitude of $g$; otherwise the only hope in sight for maintaining the approximation would be to suppose $g$ small, so that diagrams (*c*) and (*d*), though competitive, would both be dominated by (*b*).

It is admittedly conceivable that even for large $g$ diagram (*b*) dominates both (*c*) and (*d*) merely by possessing a sufficiently larger spectral function. However, it seems unlikely to us that $M$-independent terms could continue to predominate on grounds such as these as more and more higher order diagrams were taken into account.

The calculation of $\varrho$ is carried out in the Appendix. The resultant closed form is to be used in the sense of the representation (3.8) and (3.9); this reminds us, when encountering singularities of $\varrho$ on the real $s$-axis, to circumvent them by giving $M^2$ an infinitesimal positive imaginary part. We find:

$$\varrho = \frac{\theta(s-4)}{2\Sigma^{\frac{1}{2}}} \log \left\{ \frac{(s + 2\lambda^2 - M^2 - 3) + [\Sigma(s-4)/s]^{\frac{1}{2}}}{(s + 2\lambda^2 - M^2 - 3) - [\Sigma(s-4)/s]^{\frac{1}{2}}} \right\}, \tag{4.1}$$

where

$$\Sigma = [s-(M-1)^2][s-(M+1)^2]\,. \tag{4.2}$$

It is trivial to verify that the zeros of $\Sigma$ do not entail singularities of $\varrho$: when $\Sigma$ is negative, $\Sigma^{\frac{1}{2}}$ can be replaced by $\pm i\,(-\Sigma)^{\frac{1}{2}}$ as long as the same sign is adhered to throughout. (The logarithm merely changes to an inverse sine at these points.)

Similarly we find for the spectral function $\varrho'$ of diagram (*c*):

$$\varrho' = \frac{\theta(s-4)}{2[s(s-4)]^{\frac{1}{2}}} \log\left\{\frac{s+\lambda^2-4}{\lambda^2}\right\}. \tag{4.3}$$

As $s\to\infty$ for constant $\lambda^2$, both $\varrho$ and $\varrho'$ behave like $(1/2s)\log(s/\lambda^2)$; but in the important vicinity of the physical region they differ appreciably. The behavior of $\varrho'$ being quite transparent, we comment only on $\varrho$. Part of our purpose is to exhibit in terms appropriate to the explicit form of $\varrho$ the analytic properties of $f$ deduced by general arguments in Section 3, and verify the existence of the *ABP*.

The potentially interesting points are those at which the denominator $D$ or the numerator $N$ of the argument of the logarithm in (4.1) vanishes for $s>4$. We know from the Appendix that $sND=Q$, so that the locus of such points is just the upper branch of the hyperbola $\Gamma$ as shown in Fig. 2. Let us denote by $s_+$ and $s_-$ respectively the larger and smaller values of $s$ corresponding to a given $M^2$; they are encountered in the path of the $s'$ spectral integral only if $\lambda<(M-1)$. Clearly $s_+$ and $s_-$ are both branch points of $\varrho'$; but recalling the standard representation (3.8) we see that only if they lie infinitesimally below the real axis will they lead to branch points of $f$, for only then is the contour of integration pinched between singularities of the integrand. The imaginary part of $s^+$ is always positive, but that of $s_-$ is negative subject to the familiar condition $(M^2-1)/2<\lambda^2<(M-1)^2$. Note that the argument of the logarithm in (4.1) is positive for $4<s<s_-$, negative for $s_-<s<s_+$, and positive for $s>s_+$ until the zeros of $\Sigma$ are reached; these always lie to the right of $s_+$. The imaginary part of the logarithm between $s_-$ and $s_+$ turns out to be $+i\pi$.

From (3.9) we see that the imaginary part of $\varrho/\pi$ is just the Bonnevay double spectral function, which we have therefore identified as

$$\beta = \begin{cases} (2\Sigma^{\frac{1}{2}})^{-1} & \text{when } (s,\,M^2) \text{ lies within } \Gamma, \\ 0\,, & \text{otherwise.} \end{cases} \tag{4.4}$$

The region where the total Bonnevay function $B$ fails to vanish is that covered by the family of all $\Gamma$ with $\lambda\geqslant 2$. This region is bounded by the line $s=4$

on the left, and by the upper edge of the enveloping curve, namely the parabola $\Sigma = 0$, from below. $P$ is complex up to the maximum value of $s_1$, which is $(M-1)^2$, *i.e.* throughout the physical decay region.

Detailed inspection fails to reveal any reason to suppose that $\varrho$ and $P$ are negligible compared with $\varrho'$ and the corresponding $P'$. Hence, according to the narrowly limited criterion applied here, the neglect of the $M$-dependence of the decay amplitude remains unwarranted except by appeal to the smallness of the pion-pion coupling constant $g$.

* * *

We welcome this opportunity to acknowledge discussions with Professor S. B. Treiman, Dr. Jan Tarski, and Dr. J. P. Lascoux. The first-named author is grateful also to the Governing Body of Christ Church for their continued leave of absence, to the National Science Foundation for support, and to Professor J. R. Oppenheimer for extending to him the splendid hospitality of the Institute for Advanced Study.

## Appendix

In order to calculate the spectral function $\varrho$ for $M < 3$, we recall that $\pi\varrho$ is here identical with the imaginary part of $f$. By performing the $\alpha_1$ integration in (3.2) we find

$$\varrho(s) = \int_0^1 \mathrm{d}\alpha_2 \int_0^{1-\alpha_2} \mathrm{d}\alpha_3 \, \delta(\Lambda),$$

where

$$\Lambda = \{\alpha_2^2 + M^2\alpha_3^2 - (s - M^2 - 1)\alpha_2\alpha_3 - \lambda^2\alpha_2 - (M^2 + \lambda^2 - 1)\alpha_3 + \lambda^2\}.$$

In the $(\alpha_2\alpha_3)$ plane the conic $\Lambda = 0$ intersects the boundary of the region of integration only if $s > 4$, this taking place at two points along the line $\alpha_2 + \alpha_3 = 1$, (and nowhere else). It is convenient to rotate axes by $\pi/4$: defining $\alpha = 2^{-\frac{1}{2}}(\alpha_2 + \alpha_3)$, $\beta = 2^{-\frac{1}{2}}(\alpha_2 - \alpha_3)$, we have

$$\varrho = \int_0^{2^{-\frac{1}{2}}} \mathrm{d}\alpha \int_{-\alpha}^{\alpha} \mathrm{d}\beta \, \delta(R).$$

For brevity we put $R = s(\beta - \beta_1(\alpha))(\beta - \beta_2(\alpha))$, so that

$$\varrho = \int_0^{2^{-\frac{1}{2}}} \mathrm{d}\alpha \int_{-\alpha}^{\alpha} \mathrm{d}\beta \, \frac{1}{s\,|\beta_1(\alpha) - \beta_2(\alpha)|} \{\delta(\beta - \beta_1) + \delta(\beta - \beta_2)\}.$$

Let $\alpha_+$ be the value of $\alpha$ at which $\beta_1(\alpha) = \beta_2(\alpha)$. The equation $Q = 0$ then has two roots in $\beta$ for $\alpha_+ < \alpha < 2^{-\frac{1}{2}}$ and none for $0 < \alpha < \alpha_+$. Evaluating $\beta_1$ and $\beta_2$ we find

$$\varrho = 2^{\frac{1}{2}} \int_{\alpha_+}^{2^{-\frac{1}{2}}} \mathrm{d}\alpha S^{-\frac{1}{2}} ,$$

where

$$S = \{2\Sigma\alpha^2 + 2.2^{\frac{1}{2}}\alpha[s(M^2 + 2\lambda^2 - 1) - (M^2 - 1)^2] + [(M^2 - 1)^2 - 4s\lambda^2]\} \cdot$$

$$\cdot 2\Sigma(\alpha - \alpha_-)(\alpha - \alpha_-) .$$

$\Sigma$ is defined in (4.2). The integration is now straightforward and yields

$$\varrho = \frac{1}{2\Sigma^{\frac{1}{2}}} \log \left\{ \frac{s^{\frac{1}{2}}(s + 2\lambda^2 - M^2 - 3) + [\Sigma(s-4)]^{\frac{1}{2}}}{2[\lambda^2 s^2 + \lambda^2(\lambda^2 - M^2 - 3)s + (M^2 - 1)^2]^{\frac{1}{2}}} \right\} .$$

The radicand in the denominator of the logarithm is familiar from (3.4). The last step is to note that

$$4[\lambda^2 s^2 + \lambda^2(\lambda^2 - M^2 - 3)s + (M^2 - 1)^2] =$$

$$= \{s^{\frac{1}{2}}(s + 2\lambda^2 - M^2 - 3) + [\Sigma(s-4)]^{\frac{1}{2}}\}\{s^{\frac{1}{2}}(s + 2\lambda^2 - M^2 - 3) - [\Sigma(s-4)]^{\frac{1}{2}}\} ,$$

which enables us to rewrite $\varrho$ in the form (4.1).

Perhaps we should mention that the same expression for $\varrho$ is obtainable also by applying the so-called unitarity condition (11). From this point of view it is more natural to regard $f$ and $\varrho$ as functions of the variables $s$ and $\lambda^2$; the final results are the same. We have opted for the other method because, although it is slightly more elaborate to carry through, it involves less heuristic theorizing.

(11) R. BLANKENBECLER and Y. NAMBU: *Nuovo Cimento*, **18**, 595 (1960).


## RIASSUNTO (*)

I più semplici diagrammi del tipo a vertice per il decadimento $K \to 3\pi$ contengono una linea interna per il doppio pione: se si prende come quantità discreta il parametro $\lambda$ della massa totale di riposo di questa linea, l'ampiezza possiede sul foglietto fisico, al di sopra di quello normale, un punto anomalo di branching, sottoposto alla condizione $(M^2 - \mu^2)/2 < \lambda^2 < (M - \mu)^2$, in cui $M$ è la massa del kaone e $\mu$ quella del pione. Per integrazione in $\lambda^2$ si elimina questa singolarità. Per comprendere appieno l'ampiezza, dobbiamo considerarla temporaneamente come funzione di due variabili complesse, in cui si trova che è valida una rappresentazione con doppia dispersione. Per fare un esempio di queste affermazioni e per dare una illustrazione in teoria della perturbazione di alcune delle approssimazioni più comuni nei calcoli di questo decadimento, si esaminano le funzioni spettrali in forma semichiusa.

(*) *Traduzione a cura della Redazione.*

IL NUOVO CIMENTO Vol. XXI, N. 4 16 Agosto 1961

# A New Technique in the Statistical Model of Particle Production.

T. Ericson (*)

*CERN - Geneva*

(ricevuto il 7 Giugno 1961)

**Summary.** — A new method is introduced to account for conservation laws in the statistical model of particle production. The approach becomes exact in the limit of high multiplicities; it leads to simple analytical expressions which allow immediate estimates of the influence of the various conservation laws under different circumstances. Momentum conservation is shown to have little influence on the energy spectra of the emitted particles; its consequences for the angular correlation of particles are studied. The statistical weight factors, which result from the coupling of the isospin vectors of the emitted particles with isospin conservation imposed, are shown to be well represented by semi-classical expressions; the dependence of the weight factors on total isospin and multiplicity becomes obvious. The general effects of angular momentum conservation in the statistical model are studied; the angular distributions are forward-backward symmetric in the c.m. system, a prediction specific to the model and a suitable test to its validity. In the classical approximation the angular distribution is forward-backward peaked, though not more than a limiting distribution $1/\sin\theta$, where $\theta$ is the angle of the particle with the beam direction. Angular momentum conservation leaves energy spectra nearly unchanged, while multiplicities are strongly affected by it; the effective interaction volumes in nucleon-antinucleon annihilation and nucleon-nucleon collisions are shown to be approximately the same, when this effect is taken into account.

## 1. – Introduction.

It is a standard procedure in strong interaction studies to use the predictions of the statistical model (SM) as a reference to which experimental

(*) On leave from the Institute of Theoretical Physics, Lund, Sweden.

results are compared. When this model was first introduced by FERMI [1], it was extremely simple: momentum and angular momentum effects were neglected, and it was mainly applied to «low energy» reactions, which have low multiplicities. At present, the SM is applied to energies at which the number of energetically possible reactions is very large; so that for this reason alone the calculations tend to become very laborious. In addition, momentum conservation is included as a rule and great progress has been made towards the incorporation of angular momentum conservation in the last year [2,3]. This increases the labour even further and it has become necessary to turn to high speed computers to obtain results in reasonable time. In the process the original simplicity of the SM has largely been lost. It is thus most desirable to find an approximation technique which at least partly enables us to restore simplicity and which will keep the computing to within reasonable limits.

A satisfactory approximation should aim at fulfilling the following criteria:

1) it should have a simple physical interpretation, so that its region of validity can be determined from physical considerations;

2) its predictions should be particularly good for large multiplicities, as these are handled only with difficulty by present methods;

3) the structure of its results should be such as to facilitate the insight into the dependence of cross-sections on the variables and to permit rapid qualitative estimates;

4) it should be possible to use it to generalize the SM to include effects only little discussed so far, angular momentum effects for example.

In this paper we present an approximation, the random coupling approximation (RCA), which seems to meet all of these requirements. The method is sufficiently flexible, that it can be applied with equal ease to momentum phase space integrals, to the statistical weights due to isospin conservation and to angular momentum effects. One of the main problems of the SM is the evaluation of the momentum phase space of $n$ particles with given total energy $E$ and given total momentum $\boldsymbol{P}$. We will therefore outline the principal idea of the RCA for this case.

The method of random coupling simply observes that the net effect of momentum conservation is equivalent to the requirement that the $n$ momentum vectors add randomly to the given total momentum $\boldsymbol{P}$; this momentum is obtained with a certain *a priori* probability, that is described to a good ap-

(1) E. FERMI: *Progr. Theor. Phys.* (*Japan*), **5**, 570 (1950).
(2) L. F. COOK: UCRL-8841 (1959).
(3) Z. KOBA: *Nuovo Cimento*, **18**, 608 (1960).

proximation by a Gaussian distribution. As the *a priori* probability singles out no direction in space, the problem now depends only on the absolute values of the momenta, which immediately cuts down the number of integrations from $3n$ to $n$. The detailed application of the RCA to momentum phase space is studied in Section 2. As a byproduct of that discussion and as a non-trivial application we will estimate the angular correlation of two particles in nucleon-antinucleon annihilation.

The statistical weight factors due to isospin conservation are essentially nothing but the *a priori* probability that $n$ isospin vectors couple to given total isospin $T$ and a given projection of it, $T_z$. The exact formal solution can be given by Clebsch-Gordan techniques ([4-6]) or by projection operator technique ([7]); while this is sufficient for numerical calculations of statistical weights, it does not readily provide insight into their behaviour. Starting from a semiclassical picture we obtain in Section 3 the *a priori* probability for random coupling of the $n$ isospin vectors in complete analogy to the corresponding problem for momentum vectors. The semiclassical result is obtained in a very simple analytical form which reproduces the exact solution excellently. It should be advantageous for application to problems, for which numerical values of statistical weights are not available.

The conservation of total angular momentum and its projection on the $z$-axis imposes restrictions on the phase space available for the emitted particles. Until recently, it was customary to assume that the restrictions imposed by angular momentum conservation were negligible. Cook ([2]) and Koba ([3]) have recently taken it formally into account by Clebsch-Gordan techniques, but the expressions obtained are still rather awkward for practical use. Because the angular momenta in high energy processes are quite large, it should be very appropriate to apply classical arguments to the angular momentum conservation, in particular as this is known to work in compound nuclear processes, even for relatively low angular momenta ([8,9]). In Section 4 we take angular momentum conservation into account by considering it as due to the *a priori* probability that the $n$ angular momenta couple to given total angular momentum. The typical influence of angular momentum on branching ratios and angular distributions becomes qualitatively very simple. The most important feature of a statistical angular distribution is its forward—backward symmetry in the CM, which is due to the fact that interference between

([4]) Y. Yeivin and A. de-Shalit: *Nuovo Cimento*, **1**, 1147 (1955).
([5]) V. S. Barašenkov and B. M. Barbašev: *Suppl. Nuovo Cimento*, **7**, 19 (1957).
([6]) F. Cerulus: *Suppl. Nuovo Cimento*, **15**, 402 (1960).
([7]) F. Cerulus: *Nuovo Cimento*, **19**, 528 (1961).
([8]) T. Ericson and V. Strutinski: *Nucl. Phys.*, **8**, 284 (1958); **9**, 689 (1958-59).
([9]) T. Ericson: *Adv. in Phys.*, **9**, 425 (1960).

different partial waves has no place in a statistical description. Furthermore, we discuss the limiting cases of the angular distribution in the SM and show that the emitted particles must be expected to be forward-backward peaked. The multiplicity depends strongly on angular momentum. We show that this influence can be approximately represented by a scale factor in the interaction volume. When angular momentum conservation is included the interaction volumes of nucleon-antinucleon annihilation and multiple production processes become the same within a factor 2.

## 2. – Momentum phase space.

The SM is a phase space description of the strong interaction reactions in which all appropriate quantum numbers have to be imposed. The phase space is strongly dominated by the accessible volume in momentum phase space: it has been customary to disregard the influence of angular momentum as this greatly complicates the problem. We return to this point in Section **4**: we will here study the momentum phase space integrals, which occur in the ordinary treatments. The momentum integrals are of the form

$$(1) \qquad \varrho_n^*(E, \boldsymbol{P}) = \int \dots \int \mathrm{d}\boldsymbol{p}_1 \dots \mathrm{d}\boldsymbol{p}_n \cdot f(p_1, \dots, p_n) \delta^{(3)}\Big(\sum_i \boldsymbol{p}_i - \boldsymbol{P}\Big)\Big(\sum_i \varepsilon_i - E\Big).$$

In eq. (1) we denote by $\boldsymbol{p}_i$ the momentum of the $i$-th particle, by $\varepsilon_i = \sqrt{p_i^2 + m_i^2}$ its energy, by $\boldsymbol{P}$ and $E$ the total momentum and energy of the system. The weight function $f(p_1, \dots, p_n)$ takes into account the exact version of the SM, which is considered. It is unity for the non-covariant formulation of the SM ([1,10]), and equals $\prod_{i=1}^{n} (p_i^2 + m_i^2)^{-\frac{1}{2}}$ for the covariant formulation ([11]). We will not specify it any further, but note that it depends only on the absolute value of the particle momenta, not on their direction. The exact form of the weight function is completely irrelevant for the further discussion, which deals with effects due to the angular dependence of the momenta.

In order to obtain a simple approximation to eq. (1) we first observe that it depends on the direction of the particle momenta $\boldsymbol{p}_i$ only through the volume elements $\mathrm{d}\boldsymbol{p}_i$ and through the momentum conserving factor $\delta^{(3)}\Big(\sum_i \boldsymbol{p}_i - \boldsymbol{P}\Big)$. Therefore, if we keep the lengths of the momentum vectors, $p_i$, fixed and for a moment neglect momentum conservation, the angular integration yields a factor $(4\pi)^n$. The momentum vectors couple randomly in space to a wide

([10]) *E.g.*, R. Hagedorn: *Nuovo Cimento*, **15**, 434 (1960).
([11]) P. P. Srivastava and E. C. G. Sudarshan: *Phys. Rev.*, **110**, 765 (1958).

range of different total momenta $\boldsymbol{P}$. The effect of the momentum conservation is simply to single out just those combinations of the momentum vectors $\boldsymbol{p}_i$, which couple to the given total momentum $\boldsymbol{P}$. To account for momentum conservation, we should therefore multiply $(4\pi)^n$ by the *a priori* probability $P(p_1, \ldots, p_n; \boldsymbol{P})$ that $n$ momentum vectors of given lengths $p_i$ add randomly to the total momentum $\boldsymbol{P}$. This factor is identically

$$P(p_1, \ldots, p_n; \boldsymbol{P}) = \frac{1}{(4\pi)^n} \int \ldots \int \mathrm{d}\boldsymbol{n}_1 \ldots \mathrm{d}\boldsymbol{n}_n \delta^{(3)}\Big(\sum_i p_i \boldsymbol{n}_i - \boldsymbol{P}\Big), \tag{2}$$

where $\boldsymbol{n}_i$ are unit vectors. We notice in passing that the integration of the *a priori* probability over all $\boldsymbol{P}$ in eq. (2) yields unity as should be. We can thus identically rewrite eq. (1) in terms of eq. (2) as

$$\varrho_n^*(E, \boldsymbol{P}) \quad (4\pi)^n \int_0^\infty \ldots \int_0^\infty p_1^2 \mathrm{d}p_1 \ldots p_n^2 \mathrm{d}p_n f(p_1, \ldots, p_n) P(p_1, \ldots, p_n; \boldsymbol{P}) \delta\Big(\sum_i \varepsilon_i - E\Big). \tag{3}$$

The importance of identically expressing eq. (1) as eq. (3) in terms of the *a priori* probability is that this probability depends only on the lengths of the momentum vectors, $p_i$. If we therefore can find a reasonably simple expression for $P(p_1, \ldots, p_n; \boldsymbol{P})$ the number of integrations necessary to evaluate the phase space has been reduced from $3n$ to $n$.

The second observation is that the total momentum $\boldsymbol{P}$ in nearly all practical applications is quite small; in most problems it will be the momentum of one or two of the particles only, and when we are interested in the phase space in the CM, we have even $\boldsymbol{P} \equiv 0$. Under these circumstances an asymptotic expression for $P(p_1, \ldots, p_n; \boldsymbol{P})$ valid for large $n$ is readily obtained by the following statistical consideration.

Suppose we have $n$ independent quantities $x_1, \ldots, x_n$ which have probability distributions so that their mean values

$$\langle x_i \rangle = 0 \tag{4}$$

for all of them. The sum $X = \sum_i x_i$ will then have a distribution which tends very rapidly towards a Gaussian with increasing $n$ (the central limit theorem):

$$P_x(X) \simeq \frac{1}{(2\pi\sigma^2)^{\frac{1}{2}}} \exp\left[-X^2/2\sigma^2\right]. \tag{5}$$

The mean square deviation of $X$ from 0, $\sigma^2$, is given by

$$\sigma^2 = \sum_i \langle x_i^2 \rangle. \tag{6}$$

We apply the central limit theorem to the projections of the momentum vectors $p_i$ on some axis, $p_{ix}$. As the direction of $p_i$ is considered to be random in our approximation, either sign is equally probable; thus, $p_{ix} = 0$. Furthermore, no axis in space is preferred, and we have therefore

$$\langle p_{ix}^2 \rangle = \tfrac{1}{3}\langle p_{ix}^2 + p_{iy}^2 + p_{iz}^2 \rangle = p_i^2/3 \,.$$

The sum of the projections is obviously the total momentum component $P_x$ along this axis,

$$P_x = \sum_i p_{ix} \,. \tag{7}$$

Applying eq. (5) and (6) we have immediately

$$P_x(p_1, \ldots, p_n; P_x) \simeq \frac{1}{(2\pi\sigma^2)^{\frac{1}{2}}} \exp\left[-P_x^2/2\sigma^2\right], \tag{8}$$

with $\sigma^2$ given by

$$\sigma^2 = \tfrac{1}{3}\sum_i p_i^2 \,. \tag{9}$$

We could have used any axis in space for this argument, as the prescribed length $p_i$ of each random vector does not impose any restriction on the sign of a projection. The probability of finding a total momentum $\boldsymbol{P}$ is the product of the probabilities in three perpendicular directions. Using the isotropy of the problem:

$$P(p_1, \ldots, p_n; \boldsymbol{P}) \simeq \frac{1}{(2\pi\sigma^2)^{\frac{3}{2}}} \exp\left[-(P_x^2 + P_y^2 + P_z^2)/2\sigma^2\right] = \frac{1}{(2\pi\sigma^2)^{\frac{3}{2}}} \exp\left[-\boldsymbol{P}^2/2\sigma^2\right]. \tag{10}$$

Substitution of eq. (9) and (10) into eq. (3) gives

$$\varrho_n^*(E, \boldsymbol{P}) \simeq (4\pi)^n \int_0^\infty \ldots \int_0^\infty p_1^2 \,\mathrm{d}p_1 \ldots p_n^2 \,\mathrm{d}p_n \frac{f(p_1, \ldots, p_n)}{\left[2\pi \cdot \frac{1}{3}\left(\sum_i p_i^2\right)\right]^{\frac{3}{2}}} \cdot \exp\left[-\boldsymbol{P}^2 \Big/ \tfrac{2}{3}\Big(\sum_i p_i^2\Big)\right] \delta\Big(\sum_i \varepsilon_i - E\Big). \tag{11}$$

The evaluation of eq. (11) is quite straightforward by ordinary computer methods and we have thus obtained a simple approximation to the momentum phase space, $\varrho_n^*(E, \boldsymbol{P})$. It is useful, however, to make further approximations in eq. (11) in order to get a good qualitative understanding of the influence

of momentum conservation and to be able to evaluate $\varrho_n^*(E, \boldsymbol{P})$ simply without the use of a computer.

We observe that the probability function depends on the momenta $p_i$ only through the quantity $\sum_i p_i^2$. This implies that the dependence of $P(p_1, ..., p_n; \boldsymbol{P})$ on any individual one of the $p_i$ is quite weak; the sum $\sum_i p_i^2$ is nearly a constant over the range of combinations $p_i$, which gives the main contribution to the phase space integral (11). We will therefore only commit small errors in replacing the sum by its mean value. The probability function will then not depend on momenta and can be taken outside the integration signs. We denote the phase space without momentum restrictions by $N_n^*(E)$

$$N_n^*(E) = (4\pi)^n \int_0^\infty \dots \int_0^\infty p_1^2 \mathrm{d}p_1 \dots p_n^2 \mathrm{d}p_n f(p_1, ..., p_n) \delta\Big(\sum_i \varepsilon_i - E\Big) . \tag{12}$$

According to the argument above for the near constancy of $\sum_i p_i^2$, we write eq. (11) as

$$\varrho_n^*(E, \boldsymbol{P}) = \left\langle \frac{\exp\left[-\boldsymbol{P}^2/\frac{2}{3}(\sum_i p_i^2)\right]}{\left[2\pi \cdot \frac{1}{3}(\sum_i p_i^2)\right]^{\frac{3}{2}}} \right\rangle N_n^*(E) \simeq \frac{\exp\left[-\boldsymbol{P}^2/\frac{2}{3}\langle \sum_i p_i^2 \rangle\right]}{\left[2\pi \cdot \frac{1}{3}\langle \sum_i p_i^2 \rangle\right]^{\frac{3}{2}}} N_n^*(E) . \tag{13}$$

In the last step in eq. (13) we have everywhere replaced the sum $\sum_i p_i^2$ by a mean value which is defined by

$$\Big\langle \sum_i p_i^2 \Big\rangle N_n^*(E) \quad \sum_i (4\pi)^n \int_0^\infty \dots \int_0^\infty p_i^2 \mathrm{d}p_1 \dots p_i^4 \mathrm{d}p_i \dots p_n^2 \mathrm{d}p_n f(p_1, ..., p_n) \delta\Big(\sum_i \varepsilon_i - E\Big) . \tag{14}$$

The expression for $\varrho_n^*(E, \boldsymbol{P})$ which is approximately obtained in eq. (13) and (14) becomes exact in the limit of large multiplicities. It must, however, be emphasized that eq. (11) is more appropriate for a computer evaluation of $\varrho_n^*(E, \boldsymbol{P})$.

Eq. (13) permits immediately the following statement about the covariant and non-covariant SM: if a cross-section is predicted for the two models, the ratio of the two predictions is insensitive to momentum conservation, since $\langle \sum_i p_i^2 \rangle$ is expected to be nearly the same in the two cases. Differences in predictions of cross-sections can thus be obtained without inclusion of momentum conservation, which is a considerable simplification. Only when absolute cross-sections are calculated is it necessary to include this conservation law.

To estimate the error which typically is associated with the RCA we will compare the approximate evaluation of $\varrho_n^*(E, \boldsymbol{P})$ to limiting cases which can

be exactly evaluated. Two convenient cases of this kind are provided by the non-covariant model in the limit when either all the emitted particles are extremely relativistic (E.R.) or when they are non-relativistic (N.R.). It will be shown that the errors introduced are of order $1/n$ and the they thus vanish as the multiplicity becomes large.

The limiting cases of the non-covariant model with momentum conservation have the exact phase space integrals:

$$\varrho_n^*(E,\boldsymbol{P})_{NR} = \frac{(2\pi)^{(3n-3)/2}\Big(\prod_{i=1}^{n} m_i^{\frac{3}{2}}\Big)\Big[T-\boldsymbol{P}^2/2\Big(\sum_i m_i\Big)\Big]^{(3n-5)/2}}{(\sum_i m_i)^{\frac{3}{2}}\,\Gamma[(3n-3)/2]}\,; \qquad n\geqslant 2\,, \tag{15}$$

where $T = E - \sum_i m_i$ is the total kinetic energy of the system:

$$\varrho_n^*(E,\boldsymbol{P})_{ER} = \left(\frac{\pi}{2}\right)^{n-1}\frac{1}{(2n-1)!}\,\frac{1}{(2n-2)!}\,\frac{\mathrm{d}^n}{\mathrm{d}E^n}\,(E^2-\boldsymbol{P}^2)^{2n-2}\,; \qquad n\geqslant 2\ (^*). \tag{16}$$

We will also need the corresponding phase space without momentum conservation [1]

$$N_n^*(E)_{NR} = \frac{(2\pi)^{\frac{3}{2}n}\Big(\prod_{i=1}^{n}(m_i^{\frac{3}{2}})\Big)T^{\frac{3}{2}n-1}}{\Gamma(\boldsymbol{r}\,\tfrac{3}{2})}\,, \tag{17}$$

and

$$N_n^*(E)_{ER} = (8\pi)^n\,\frac{E^{3n-1}}{(3n-1)!}\,. \tag{18}$$

The approximate results are expected to be most accurate for relatively small $|\boldsymbol{P}|$; we will therefore study the accuracy of the first coefficients in a series expansion in $\boldsymbol{P}^2$. Eq. (13) suggests that we expand

$$\frac{\varrho_n^*(E,\boldsymbol{P})}{N_n^*(E)} = A\left[1-\frac{\boldsymbol{P}^2}{2S_2^2}+\frac{1}{2!}\left(\frac{\boldsymbol{P}^2}{2S_4^2}\right)^2-\ldots\right]. \tag{19}$$

Our approximation implies

$$A \simeq \frac{1}{(2\pi\sigma^2)^{\frac{3}{2}}}\,; \qquad S_2^2 \simeq S_4^2 \simeq \ldots \simeq \sigma^2\,, \tag{20}$$

(*) Eq. (15) and (16) are given by Lepore and Stewart [12] for $\boldsymbol{P}=0$. Eq. (15) is directly obtained from their result by subtracting the energy of c.m. motion from the total kinetic energy $T$; eq. (16) is derived by a generalization of the technique used by Lepore and Stewart

[12] J. V. Lepore and R. N. Stewart: *Phys. Rev.*, **94**, 1724 (1954).

as is immediately evident from eq. (13).

From eq. (15) and (17) we have

$$(21)\qquad \begin{cases} A_{NR} = \dfrac{1}{(2\pi)^{\frac{3}{2}}} \dfrac{1}{(T\sum_i m_i)^{\frac{3}{2}}} \dfrac{\Gamma(\frac{3}{2}n)}{\Gamma[(3n-3)/2]}, \\ (S_2^2)_{NR} = \dfrac{2}{3n-5} T\Big(\sum_i m_i\Big), \end{cases}$$

and similarly from eq. (16) and (18)

$$(22)\qquad \begin{cases} A_{ER} = \dfrac{2}{\pi} \dfrac{(3n-1)(3n-2)(3n-3)}{(2n-1)} 2^{-4n} \binom{4n-4}{2n-2} E^{-3}, \\ (S_2^2)_{ER} = \dfrac{4n-5}{(3n-4)(3n-5)} E^2; \end{cases}$$

To compare the accuracy to which (20) and (22) are approximated, we calculate $\sigma^2$ and use eq. (20):

$$(23)\qquad \begin{cases} \sigma_{NR}^2 = \dfrac{1}{3}\Big\langle \sum_i p_i^2 \Big\rangle_{NR} = \dfrac{2}{3} \dfrac{\big(\sum_i m_i\big)}{n} T, \\ \sigma_{ER}^2 = \dfrac{1}{3}\Big\langle \sum_i p_i^2 \Big\rangle_{ER} = \dfrac{4}{3} \dfrac{E^2}{(3n+1)}, \end{cases}$$

which obtains from the definition of $\langle \sum_i p_i^2 \rangle$ in eq. (14) after elementary integrations.

From eq. (23) together with eq. (21) we obtain the ratio of the exact coefficients to the approximate random coupling coefficients:

$$(24)\qquad \begin{cases} (2\pi\sigma_{NR}^2)^{\frac{3}{2}} A_{NR} = 1 - \dfrac{4}{5}\dfrac{1}{n} + O\left(\dfrac{1}{n^2}\right), \\ \dfrac{(S_2^2)_{NR}}{\sigma_{NR}^2} = 1 + \dfrac{5}{3}\dfrac{1}{n} + O\left(\dfrac{1}{n^2}\right). \end{cases}$$

The same procedure applied to the relativistic limit, eq. (21) and (23) gives

$$(25)\qquad \begin{cases} (2\pi\sigma_{ER}^2)^{\frac{3}{2}} A_{ER} = 1 - \dfrac{33}{16}\dfrac{1}{n} + O\left(\dfrac{1}{n^2}\right), \\ \dfrac{(S_2^2)_{ER}}{\sigma_{ER}^2} = 1 + \dfrac{35}{12}\dfrac{1}{n} + O\left(\dfrac{1}{n^2}\right). \end{cases}$$

It is thus clear from eq. (24) and (25) that the errors introduced by our approximation are of the order $1/n$; the approximation becomes increasingly

exact as $n \to \infty$. The approximation is therefore most useful in the case of high multiplicities, *i.e.* when computer calculations tend to become prohibitively long.

The approximation tested in eq. (24) and (25) is in general the joint effect of introducing a probability distribution instead of using exact momentum conservation (eq. (11)) and that of replacing $\sum_i p_i^2$ by its mean value (eq. (13)). It is therefore interesting to notice that for non-relativistic particles of equal mass $\sum_i p_i^2 = 2mT$, *i.e. no* approximation is involved in assuming the sum to be a constant. In this case the effect of the first approximation is tested separately, and for this case eq. (24) gives the accuracy of eq. (11) directly. A comparison to eq. (25) which involves the additional approximation of eq. (15) seems to indicate that it approximately doubles the error, if conditions are not particularly favourable.

The main advantage of the RCA is that it permits very rapid, though approximate, calculation of the phase space $\varrho_n^*(E, \boldsymbol{P})$ and that it clarifies the extent to which it is important to include momentum conservation. With the exception of very small multiplicities, the phase space is nearly always sufficiently well represented by this method, in particular when it is realized that the inclusion of angular momentum conservation introduces corrections to the relative branching ratios in the SM which are at best of the same order as the errors in our approximation and usually considerably larger (see Section **4**). The influence of angular momentum is usually ignored; it is thus by no means evident that a very exact evaluation of the momentum phase space provides any quantitative advantage over the RCA.

As a simple, but non-trivial, application of the RCA we finally calculate qualitatively the angular correlation between two non-identical particles due to momentum conservation (cf. [13]). We neglect the influence of angular momentum conservation, so that the result applies best to the case of nucleon-antinucleon annihilation for which this correction is rather small (*). For illustration we calculate the mean angular correlation between two particles in the extreme relativistic limit for the non-covariant model. The angular correlation of particles 1 and 2 is determined by the phase space available for the $(n-2)$ remaining particles, which have an energy $E-\varepsilon_1-\varepsilon_2$ and a momentum $-(\boldsymbol{p}_1+\boldsymbol{p}_2)$. This phase space is thus $\varrho_{n-2}^*(E-\varepsilon_1-\varepsilon_2; -(\boldsymbol{p}_1+\boldsymbol{p}_2))$ in the CM of all the particles. To obtain the mean angular correlation $\langle W(\boldsymbol{p}_1, \boldsymbol{p}_2)\rangle$ to a good approximation we simply replace the energies $\varepsilon_1 = p_1$ and $\varepsilon_2 = p_2$ by their mean values $E/n$. We furthermore observe, that only

[13] G. GOLDHABER, S. GOLDHABER, W. LEE and A. PAIS: *Phys. Rev.*, **120**, 2250 (1960).

(*) The consideration can, however, be generalized to include angular momentum conservation.

the factor which imposes restrictions on the length of the total momentum will contribute to the angular correlation. Eq. (13) gives thus

$$\langle W(\boldsymbol{p}_1, \boldsymbol{p}_2)\rangle \propto \langle \exp[-(\boldsymbol{p}_1+\boldsymbol{p}_2)^2/2\sigma^2]\rangle \propto \exp\left[-\frac{\langle p_1\rangle\langle p_2\rangle\cos\theta}{\sigma^2}\right], \tag{26}$$

where $\theta$ is the angle between $\boldsymbol{p}_1$ and $\boldsymbol{p}_2$.

The value of $\sigma^2$ is obtained from eq. (23), and has to be taken for $(n-2)$ particles with a total energy $((n-2)/n)\cdot E$. Neglecting unity as compared to $3n$ we obtain

$$\sigma^2 \simeq \frac{4}{9}\cdot\frac{n-2}{n^2}E^2. \tag{27}$$

This yields immediately on substitution into eq. (26) the approximate and normalized correlation

$$\langle W(\boldsymbol{p}_1, \boldsymbol{p}_2)\rangle \simeq \frac{9}{4(n-2)}\exp\left[-\frac{9}{4}\frac{\cos\theta}{(n-2)}\right]; \qquad n \gg 1, \tag{28}$$

which is in a convenient form for crude estimates. As expected, the angular correlation is an anticorrelation of $\boldsymbol{p}_1$ and $\boldsymbol{p}_2$, which disappears with increasing multiplicity.

## 3. – Statistical weight factors.

Since the branching ratios in the SM are considered directly proportional to the available phase space for the reaction products, we have to calculate the accessible volume in the discrete spin-isospin phase space in addition to that of configuration-momentum phase space.

Suppose $n$ distinguishable particles to be emitted and denote their isospins by $t_i$, their spins by $s_i$. There is an *a priori* statistical weight factor $g_i$ associated with every particle. If the experiment does not ask the charge of the particle, $g_i=(2t_i+1)(2s_i+1)$, which corresponds to the different discrete values of the $z$-components of spin and isospin. If the charge of the particle is determined, the $z$-component of the isospin is known, and the weight factor is $g_i=1\cdot(2s_i+1)$. We have assumed that the polarization of the emitted particles is not studied. Therefore, if no conservation laws impose restrictions on the discrete phase space available, this is simply $\prod_{i=1}^{n} g_i$. We have furthermore to take into account that not all particles are distinguishable in practice; all the permutations of indistinguishable particles correspond to the same configuration and must be counted once only. Members of different isospin

multiplets are always distinguishable. If the experiment measures only the total production of an isospin multiplet, all the particles belonging to the multiplet are indistinguishable; on the other hand, if the experiment studies the charge distribution inside the multiplet, particles of different charge become distinguishable, while those of same charge remain indistinguishable. To count permutations of indistinguishable particles once only, we have to multiply the spin-isospin phase space factor by $1/(\nu_1! \dots \nu_a!)$, where $\nu_j$ denotes the number of indistinguishable particles of kind $j$. Before the restrictions due to conservation laws are accounted for, the statistical weight factor $M_n$ is thus

$$M_n = \frac{\prod_{i=1}^{n} g_i}{\prod_{j=1}^{a} \nu_j!} . \tag{29}$$

The requirement that total angular momentum and total isospin are conserved restricts the phase space volume $M_n$. In the standard treatments of the SM in which angular momentum conservation is ignored, these restrictions on $M_n$ must of course also be neglected in the same spirit. But even when angular momentum is taken into account its effects on eq. (29) will be nearly negligible. This is because the intrinsic spins $\boldsymbol{s}_i$ are much smaller than the orbital angular momenta $\boldsymbol{l}_i$ with which they must couple to give the total angular momentum $\boldsymbol{I}$. The conservation of angular momentum will therefore mainly affect the orbital angular momenta (see Section 4), while the sum $\sum_i \boldsymbol{s}_i = \boldsymbol{S}$ will be permitted to take any value within its possible range nearly unrestricted. In other words: the orbital angular momentum of the system acts as a reservoir, which can accommodate the small angular momentum of the total spin $\boldsymbol{S}$ without difficulty.

The situation is very different for the isospins. The two initially colliding particles specify both the total isospin $T$ of the system and its projection $T_z$. The isospins of the emerging particles necessarily couple to these values. Out of the unrestricted statistical weight $M_n$ we have therefore to select exactly those combination of $\boldsymbol{t}_i$, which give $T$ and $T_z$. The correct statistical weight factor $L_n(T, T_z)$ is obtained from eq. (29) by multiplying with the *a priori* probability $P(T, T_z)$ that the $n$ isospin spin vectors $\boldsymbol{t}_i$ couple to $T$ and $T_z$,

$$L_n(T, T_z) = P(T, T_z) M_n = P(T, T_z) \frac{\prod_{i=1}^{n} g_i}{\prod_{j=1}^{a} \nu_j!} . \tag{30}$$

To obtain the *a priori* probability $P(T, T_z)$ we will consider the isospin vectors $\boldsymbol{t}_i$ to be semi-classical, so that they couple like ordinary vectors in space. The *a priori* probability can then be obtained considering the random

coupling of vectors in analogy with the case of momentum vectors in the preceding section. We will later compare our results in special cases to numerical quantal results, which show that this approximation is excellent.

We have to distinguish clearly between two different cases: *a*) no charges of the emitted particles are specified, so that there is no further condition on the $\boldsymbol{t}_i$; *b*) the charges of the particles are known, thus the projections $t_{iz}$ are given. We are then free to couple randomly only that part of $\boldsymbol{t}_i$ which is perpendicular to the $z$-axis. In addition to these two cases, one may occasionally deal with mixed cases, in which the charges of certain particles only are specified. For example, only the pion charges may be determined, and the rest left unspecified.

We will first treat case *a*) when the isospin vectors couple completely randomly in space. Eq. (9) and (10) for the asymptotic expression of the *a priori* probability of randomly coupled momentum vectors can be used immediately for the coupling of $n$ vectors $\boldsymbol{t}_i$ to a resultant $\boldsymbol{T}$,

$$P(\boldsymbol{T}) \simeq \frac{1}{(2\pi\sigma^2)^{\frac{3}{2}}} \exp\left[-\boldsymbol{T}^2/2\sigma^2\right], \tag{31}$$

with $\sigma^2 = \frac{1}{3}\sum_i \boldsymbol{t}_i^2$.

In the case of isospin we are not interested in the *a priori* probability of a $\boldsymbol{T}$ with specific direction, but in that for which the absolute value of the isospin is $T$ and its projection $T_z$. Consequently we integrate eq. (31) over $T_x$ and $T_y$ with the restriction $T_x^2 + T_y^2 = \boldsymbol{T}_\perp^2 = \boldsymbol{T}^2 - T_z^2 = \text{const.}$

$$P(T, T_z)\,\mathrm{d}T = 2\pi T_\perp \,\mathrm{d}T_\perp P(\boldsymbol{T}) = \pi \cdot 2T P(\boldsymbol{T})\,\mathrm{d}T \sim \pi^{-\frac{1}{2}} \frac{2T\,\mathrm{d}T}{(2\sigma^2)^{\frac{3}{2}}} \exp\left[-\boldsymbol{T}^2/2\sigma^2\right]. \tag{32}$$

We have made use of the relation $\mathrm{d}T_\perp^2 = \mathrm{d}T^2 = 2T\,\mathrm{d}T$.

This simple result, which we have obtained by purely classical reasoning, is generalized to a semi-classical expression by observing Kramers' rules of replacing $T$ by $T+\frac{1}{2}$ and $\boldsymbol{T}^2$ by $T(T+1)$. Correspondingly, we have to replace $\boldsymbol{t}_i^2$ by $t_i(t_i+1)$ for the individual isospin vectors in the expression for $\sigma^2$. This gives

$$P(T, T_z) \simeq \pi^{-\frac{1}{2}} \frac{2T+1}{(2\sigma^2)^{\frac{3}{2}}} \exp\left[-T(T+1)/2\sigma^2\right], \tag{33}$$

with $\sigma^2 = \frac{1}{3}\sum_i t_i(t_i+1)$.

In complete analogy with the results of Section 2 we expect this semi-classical expression to be correct to order $1/n$.

The *a priori* probability of eq. (33) is the one of greatest practical importance, as it corresponds to the case when the charge distribution among the emerging particles is left unspecified. It is sometimes of interest to study the charge distribution (case *b*)); for example, we may want to consider the emis-

sion of $n_+$, $n_0$ and $n_-$ pions of positive, neutral and negative charges. In this case the projection $t_{iz}$ of the isospin $\boldsymbol{t}_i$ is determined. The derivation of the *a priori* probability of a certain $T$ and $T_z$ is similar to the preceding, with the difference that the isospins are free to couple randomly only in the plane perpendicular to the $z$-axis, thus in two dimensions only. The length of a vector which couples in this plane is $t_{i\perp} = \sqrt{\boldsymbol{t}_i^2 - t_{iz}^2}$. Furthermore, we obviously must have

$$T_z = \sum_i t_{iz} . \tag{34}$$

The probability $P(T, T_z)$ is thus

$$P(T, T_z)\,\mathrm{d}T \simeq \iint\limits_{T_x^2+T_y^2=\boldsymbol{T}^2-T_z^2} \frac{1}{(2\pi\sigma^2)^{\frac{1}{2}}} \exp[-T_x^2/2\sigma^2] \cdot \frac{1}{(2\pi\sigma^2)^{\frac{1}{2}}} \exp[-T_y^2/2\sigma^2]\,\mathrm{d}T_x\,\mathrm{d}T_y = \tag{35}$$

$$= \frac{1}{2\pi\sigma^2} \iint\limits_{T^2=\boldsymbol{T}^2-T_z^2} \exp[-\boldsymbol{T}_\perp^2/2\sigma^2]\,\mathrm{d}T_x\,\mathrm{d}T_y =$$

$$= \frac{2T\,\mathrm{d}T}{2\sigma^2} \exp[-(\boldsymbol{T}^2 - T_z^2)/2\sigma^2] ,$$

valid for $T \geqslant |T_z|$ and with eq. (34) fulfilled. As in the derivation of eq. (32) we have made use of the relation $\mathrm{d}(T^2) = \mathrm{d}(T^2) = 2T\,\mathrm{d}T$. The quantity $\sigma^2$ applies this time to two dimensions and as none of the $x$- or $y$-directions are specified

$$\sigma^2 = \langle \sum_i t_{ix}^2 \rangle = \tfrac{1}{2} \langle \sum_i (t_{ix}^2 + t_{iy}^2) \rangle = \tfrac{1}{2} \sum_i (\boldsymbol{t}_i^2 - t_{iz}^2) . \tag{36}$$

The corresponding semi-classical result again follows immediately from Kramers' rules and is

$$P(T, T_z) \sim \frac{(2T+1)}{2\sigma^2} \exp[-\{T(T+1) - T_z^2\}/2\sigma^2] ; \qquad T \geqslant |T_z| ,$$

with

$$\sigma^2 = \tfrac{1}{2} \sum_i \{t_i(t_i+1) - t_{iz}^2\} . \tag{37}$$

This technique can also be applied to more complex cases. Consider for example the case when the charges of $n_1$ of the particles of isospin $\boldsymbol{t}_i$ are measured (*e.g.* the nucleon charges may be studied), while the charge distribution among the rest of the particles, $n_2$, is unspecified. The isospins of the latter

particles are denoted by $\boldsymbol{t}_k$. Thus

$$\text{(38)} \qquad \begin{cases} \boldsymbol{T} = \sum_i \boldsymbol{t}_i + \sum_k \boldsymbol{t}_k \,; \\ T_z = \sum_i t_{iz} + \sum_k t_{kz} = T_{1z} + T_{2z} \,. \end{cases}$$

Here $T$, $T_z$ and $T_{1z}$ are known quantities. We can regard the $\boldsymbol{t}_k$ as coupling randomly in space, while the $\boldsymbol{t}_i$ only couple their component perpendicular to the $z$-axis randomly. By reasoning in analogy with the preceding we find the semi-classical probability, valid asymptotically for $n_1$ and $n_2$ *both* large:

$$\text{(39)} \qquad P(T, T_z, T_{1z}) \simeq \frac{1}{2}\frac{(2T+1)}{(\sigma_1^2+\sigma_2^2)}\frac{1}{\sqrt{2\pi\sigma_2^2}} \exp\left[-(T_z - T_{1z})^2/2\sigma_2^2\right] \cdot \exp\left[-\frac{T(T+1)-T_z^2}{2(\sigma_1^2+\sigma_2^2)}\right]; \qquad T \geqslant |T_z|,$$

with

$$\sigma_1^2 = \tfrac{1}{2}\sum_i \{t_i(t_i+1) - t_{iz}^2\},$$

$$\sigma_2^2 = \tfrac{1}{3}\sum_k t_k(t_k+1)\,.$$

Eq. (39) is expected to be correct to order $1/n_1$ and $1/n_2$ (*).

The exact *a priori* probabilities can in principle be calculated by application of Racah techniques ([4-6]) or by the use of projection operators ([7]), but in most cases the expressions do not lend themselves to an easy comparison with our approximate values.

An exception is the statistical factor for the coupling of $n$ pions ($t_i = 1$), of which $n_+$, $n_0$ and $n_-$ have positive, neutral and negative charge. For $T=0$ CERULUS ([7]) obtains the exact *a priori* probability ($n_+ = n_-$)

$$\text{(40)} \qquad P^{T=0}_{n_+ n_0 n_-} = \begin{cases} 2^{-2n_+}\sum_{q=0}^{n_+}\binom{2n_+}{2q}\frac{1}{n_0+2q+1} \simeq \frac{1}{2n_0+n_++n_-+1}, & \text{for } n_0 \text{ even}, \\ 2^{-2n_+}\sum_{q=0}^{(n_+-1)}\binom{2n_+}{2q+1}\frac{1}{n_0+2q+2} \simeq \frac{1}{2n_0+n_++n_-+1}, & \text{for } n_0 \text{ odd}, \end{cases}$$

where the approximate value is correct to order $1/n$. Eq. (37) gives the approximate value for $T=0$ as $1/2\sigma^2$ with

$$\sigma^2 = \tfrac{1}{2}[n_+(1.2-1^2) + n_0(1.2-0^2) + n_-(1.2-1^2)] = \frac{n_+ + 2n_0 + n_-}{2}\,.$$

(*) In particular, eq. (39) does not apply to $n_1=0$ or $n_2=0$ as is evident from comparison to eq. (33) and (37).

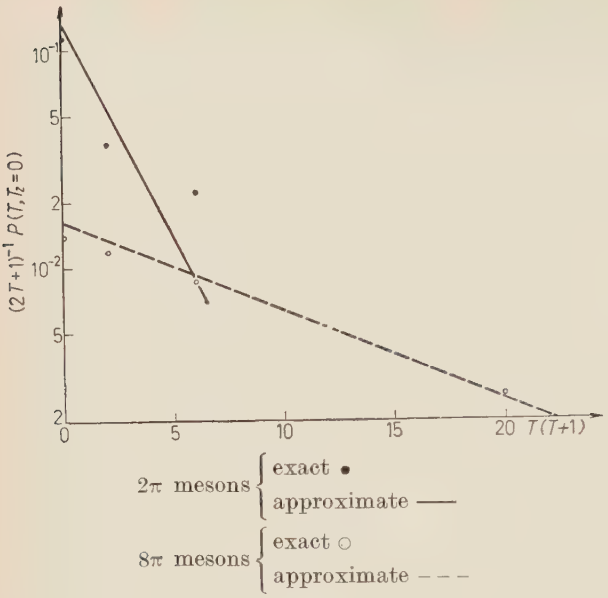


Fig. 1. – The exact and approximate *a priori* probabilities $P(T, T_z)$ of coupling the isospins of 2 and 8 pions to total isospin $T$ and projection $T_z=0$; the charges are unspecified.

Our approximation thus gives the result $1/(2n_0+n_++n_-)$, which is identical with the result of eq. (40) to order $1/n$.

Tabulated values for the *a priori* probability exist for special cases and small number of particles ([4-6]). They provide a further check on our approximation. In Fig. 1-2 we have studied the exact and approximate values of the *a priori* probability. All the comparisons have been been made after division by the trivial phase space factor $(2T+1)$. We have used $T(T+1)$ as variable and a logarithmic scale, so that the random coupling approximation yields a straight line. From the figures it is obvious that the variables used are the natural ones, as the exact solutions approximate a straight line very well. The quantitative agreement is surprisingly good even when the number of particles is very small.

The approximate formulae for statistical weights are not in any way intended to compete in accuracy with the exact expressions obtained by con-

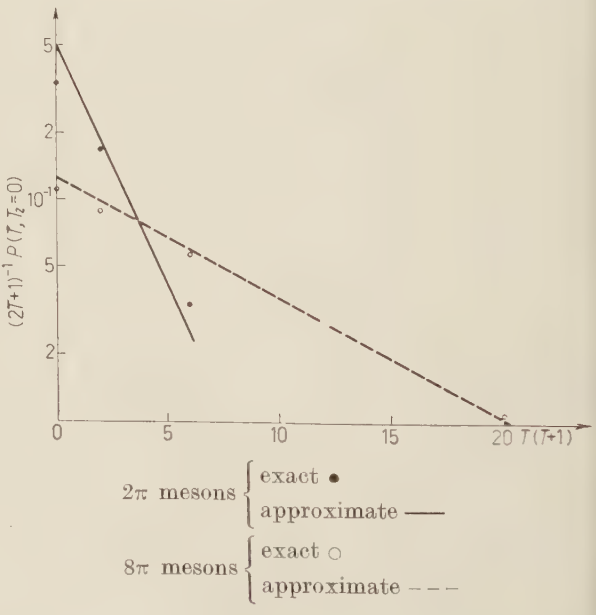


Fig. 2. – The exact and approximate *a priori* probabilities $P(T, T_z)$ of coupling the isospins of 2 and 8 charged pions to total isospin $T$ and projection $T_z=0$. The charges are specified to be $n_+=n_-$; $n_0=0$.

ventional techniques. They are intended to bring out the asymptotic limits for the *a priori* probabilities and to give a simple qualitative insight into their dependence on various quantities. In addition, they should be quite useful for orientation about the magnitude of the weight factors. We want finally to emphazise that our semi-classical approximation is most accurate for *low* values of $T$ and $T_z$, contrary to what might be thought of a classical approach.

## 4. – Angular momentum effects.

Since the SM makes the assumption that strong interaction reactions are governed by the phase space available to the reaction products, any calculation of the phase space must account for *all* restrictions imposed on it. In particular, in the CM system not only the total momentum, $\boldsymbol{P}=0$, is a good quantum number, but also the total angular momentum of the system. If we adopt a purely classical view, we have thus to impose the condition on the configuration-momentum phase space that the sum of the individual particle angular momenta, $\boldsymbol{l}_i=\boldsymbol{r}_i\times\boldsymbol{p}_i$, add to the total angular momentum $\boldsymbol{I}$. The accessible volume in the classical phase space including momentum and angular momentum conservation is simply

$$R_n(E,\boldsymbol{P}=0,\boldsymbol{I})=\int\!\!\dots\!\!\int \mathrm{d}\boldsymbol{p}_1\dots\mathrm{d}\boldsymbol{p}_n\,\mathrm{d}\boldsymbol{r}_1\dots\mathrm{d}\boldsymbol{r}_n f(p_1,\dots,p_n)\delta^{(3)}\Big(\sum_i \boldsymbol{p}_i\Big)\cdot \cdot\delta\Big(\sum_i \varepsilon_i - E\Big)\delta^{(3)}\Big(\sum_i \boldsymbol{r}_i\times\boldsymbol{p}_i-\boldsymbol{I}\Big)\,. \tag{41}$$

The integrals over the configuration space variables, $\boldsymbol{r}_i$, are over the interaction volume $\Omega$. It is obvious that the introduction of angular momentum conservation must effect branching ratios; it should, however, also be noticed that the classical expression (41) necessarily implies a unique angular distribution of the products, since the direction of a $\boldsymbol{p}_i$ is not independent of that of $\boldsymbol{I}$ because of the angular momentum conservation (*). There is therefore no ground whatsoever for the belief that statistical angular distributions have to be isotropic. Isotropy will only result if the total angular momentum $\boldsymbol{I}$ takes on any direction in space with equal probability. Since it is perpendicular to the beam, we do not have isotropy.

While the introduction of angular momentum conservation poses no problem of principle for the classical system, eq. (41) cannot be taken over identically

(*) Cook [2] and Koba [3] have considered some aspects of angular momentum conservation effects on branching ratios from a quantum mechanical viewpoint but neglecting momentum conservation. Their results are rather involved and the structure of their solutions is not evident.

to quantum mechanics since the particle momentum $\boldsymbol{p}_i$ does not commute with the particle angular momentum $\boldsymbol{l}_i$. We will therefore briefly analyse the approximations which go into eq. (41) and at the same time deduce general properties of angular distributions in statistical processes.

The total angular momentum $I$ of the CM system is a good quantum number. The two initially colliding particles are generally not in a state of definite total angular momentum, but we can easily analyse the process in terms of partial waves. The matrix element for any reaction will thus be a sum of coherent contributions from different $I$. Since the corresponding cross-section is proportional to the matrix element squared, there will occur interference terms between different partial waves (*). At this point, we invoke the basic assumption of the SM, namely that the formation process is unrelated to final products except through conservation of exact quantum numbers. Since phase relations between the matrix elements of different channels carry information about the formation process we are therefore forced to make the statistical assumption that the matrix elements of different channels have uncorrelated, random phases; this is the natural assumption of any SM and seems an implicit assumption in previous work (*e.g.* ([10])) since any systematic constructive or destructive interference destroys the possibility of considering branching ratios proportional to phase space on the average. While we here only need the randomness of phases, it should be observed that it is a further consequence of the statical assumption that the matrix elements have Gaussian probability distributions, if the assumption of randomness is to be invariant with respect to rotations in the Hilbert space of state vectors (**).

We now apply the random phase assumption to the partial waves. When we take the average over a large number of events the interference between different partial waves, $I$ and $I'$, will drop out since it is random; the contributions from different angular momenta are completely incoherent on the average. This has a most important consequence for the angular distribution of secondary particles: *the average angular distribution will have forward-backward symmetry in CM with respect to the beam direction even when the colliding particles are not identical.* This result is easily understood as follows: since only exact quantum numbers determine the final products and their properties it is in particular irrelevant how the total angular momentum $I$ and its projection $I_z$ have been achieved. These two quantum numbers will be the same, if the two colliding particles are interchanged and the reaction products must thus have a forward-backward symmetry in their distribution. This pre-

(*) There are some cases in which no interference between partial waves occurs, notably for the multiplicities. Interference is, however, important in the case of energy distributions and angular distributions.

(**) See ref. ([9]), Sect. **11**.

diction is very general and is independent of parameters of the model; it applies equally well if final state interactions are included, since it is, in a sense, a statement about the nature of the intermediate, strongly interacting, stage of the process, in which the formation process becomes independent of the emission process. The general nature of this property of the angular distribution makes it very suitable as a test for separating statistical from non-statistical reactions. Any process with an average non-symmetrical angular distribution must be non-statistical, while the reverse is not necessarily true (*). The occurrence of random phases in the SM has the further consequence that non-statistical and statistical processes become incoherent on the average and thus will be purely additive.

In order to obtain more precise statements about the influence of angular momentum conservation, we observe that the mean momentum of the emitted particles in most cases is fairly large. This suggests that we neglect the non-commutativity of $\boldsymbol{r}_i$ and $\boldsymbol{p}_i$ in calculating the phase space. Crude estimates indicate that $\langle r_i p_i \rangle \sim 3$ to 5, which implies that such an approximation hardly will affect any qualitative aspects of the problem. If we drop interference terms as before we are immediately led to eq. (41) for the description of the effects of angular momentum. We will for the moment treat $\boldsymbol{I}$ as having a specific direction and later take into account that only its magnitude and projection are known.

In the spirit of the classical approximation we account for the intrinsic spins of the particles only by their statistical weight factors, which is to say that the particle orbital angular momenta are large compared to their intrinsic spins. For simplicity we will first discuss the case of a spherically symmetric interaction volume $\Omega_0$; this brings out all the qualitative aspects of the problem. but since the interaction volume usually is taken to be Lorentz contracted, we will for completeness discuss the case of cylindrical symmetry around the beam direction later.

We start from the classical expression for the available phase space, eq. (41). In analogy with Section 2, we observe that the $\delta$-functions of momentum and angular momentum conservation just single out those combinations of $\boldsymbol{r}_i$ and $\boldsymbol{p}_i$ which happen to give the correct value of $\boldsymbol{P} = 0$ and $\boldsymbol{I}$. We therefore use the same technique as in Section 2 and consider eq. (41) for fixed absolute values of $\boldsymbol{r}_i$ and $\boldsymbol{p}_i$, but carry out the angular integrations over these variables. Without $\delta$-function restrictions the angular integration over the $2n$ solid angles gives $(4\pi)^{2n}$; the $\delta$-functions reduce this value be the *a priori* probability

(*) One expects naively that low multiplicity events tend to retain more memory of the formation process than high multiplicity events. As an example: $K^- + p \to \Sigma + \pi$ has an asymmetrical angular distribution which is unexplainable on the basis of the SM.

$P(p_1, ..., p_n; r_1, ..., r_n; \boldsymbol{P}=0; \boldsymbol{I})$ that the momenta and angular momenta of the particles add to $\boldsymbol{P}=0$ and $\boldsymbol{I}$. The phase space is thus identically

$$R_n(E, \boldsymbol{P}=0, \boldsymbol{I}) \quad (4\pi)^{2n} \int_0^\infty \dots \int_0^\infty p_1^2 \mathrm{d}p_1 \dots p_n^2 \mathrm{d}p_n \cdot r_1^2 \mathrm{d}r_1 \dots r_n^2 \mathrm{d}r_n \, f(p_1, \dots, p_n) \cdot \cdot \delta\Big(\sum_i \varepsilon_i - E\Big) P(p_1, \dots, p_n; r_1, \dots, r_n; \boldsymbol{P}=0; \boldsymbol{I}) , \tag{42}$$

where the *a priori* probability is given by

$$P(p_1, \dots, p_n; r_1, \dots, r_n; \boldsymbol{P}=0; \boldsymbol{I}) \equiv \equiv \frac{1}{(4\pi)^{2n}} \int \dots \int \mathrm{d}\boldsymbol{e}_1 \dots \mathrm{d}\boldsymbol{e}_n \, \mathrm{d}\boldsymbol{n}_1 \dots \mathrm{d}\boldsymbol{n}_n \cdot \delta^{(3)}\Big(\sum_i p_i \boldsymbol{n}_i\Big) \delta^{(3)}\Big(\sum_i p_i r_i \boldsymbol{e}_i \times \boldsymbol{n}_i - \boldsymbol{I}\Big) , \tag{43}$$

with $\boldsymbol{e}_i$ and $\boldsymbol{n}_i$ unit vectors.

To obtain a simple approximate expression for this *a priori* probability we apply the random coupling approximation to eq. (43) (cf. eq. (3) and following). The vectors $\boldsymbol{n}_i$ and $\boldsymbol{e}_i \times \boldsymbol{n}_i$ which occur in the $\delta$-functions do not have independent directions; their projections on any axis are, however, uncorrelated in sign. Hence we can regard $\boldsymbol{n}_i$ and $\boldsymbol{e}_i \times \boldsymbol{n}_i$ as effectively uncorrelated for the purpose of random coupling and we can regard the $\delta$-functions in eq. (43) as referring to independent variables. The error introduced in this way is only of the order of that of the RCA itself. Application of eq. (4)–(10) to $\sum_i p_i \boldsymbol{n}_i$ and $\sum_i p_i r_i \boldsymbol{e}_i \times \boldsymbol{n}_i$ yields immediately

$$P(p_1, \dots, p_n; r_1, \dots, r_n; \boldsymbol{P}=0; \boldsymbol{I}) \simeq \frac{1}{(2\pi\sigma_1^2)^{\frac{3}{2}}} \frac{\exp\left[-\boldsymbol{I}^2/2\sigma_2^2\right]}{(2\pi\sigma_2^2)^{\frac{3}{2}}} , \tag{44}$$

where

$$\sigma_1^2 = \sum_i p_i^2 \langle n_{ix}^2 \rangle = \tfrac{1}{3} \sum_i p_i^2 ,$$

and

$$\sigma_2^2 \quad \sum_i p_i^2 r_i^2 \, (\boldsymbol{e}_i \cdot \boldsymbol{n}_i)_x^2 \qquad \tfrac{1}{3} \sum_i p_i^2 r_i^2 \, \sin^2(\boldsymbol{n}_i, \boldsymbol{e}_i) \qquad \tfrac{2}{9} \sum_i p_i^2 r_i^2 .$$

The relations for $\sigma_1^2$ and $\sigma_2^2$ follow immediately from the fact that no direction in space is preferred by $\boldsymbol{e}_i$ and $\boldsymbol{n}_i$. In order to simplify eq. (44) even further we observe that the expression for $\sigma_2^2$ contains the sum over all particles of $p_i^2 r_i^2$. Obvsiouly such a sum will depend only weakly on any of the individual $r_i$; we therefore replace $r_i^2$ by its mean value $\langle r^2 \rangle$. This gives the approximate value of $\sigma_2^2$

$$\sigma_2^2 \simeq \tfrac{2}{9} \langle r^2 \rangle \sum_i p_i^2 . \tag{45}$$

The same statement applies equally well to the momentum variables of $\sigma_1^2$ and $\sigma_2^2$. We therefore replace $\sum_i p_i^2$ by its mean value as obtained from momentum phase space without momentum and angular momentum conservation in eq. (14). (This argument is the same as that leading from eq. (11) to eq. (13); the error introduced is discussed in Section 2.) The expression for the available phase space becomes approximately

$$(46)\qquad R_n(E, \boldsymbol{P}=0, \boldsymbol{I}) \simeq \frac{1}{((2\pi/3)\langle\sum_i p_i^2\rangle)^{\frac{3}{2}}} \frac{\exp\left[-\boldsymbol{I}^2/\frac{4}{9}\langle r^2\rangle\langle\sum_i p_i^2\rangle\right]}{((4\pi/9)\langle r^2\rangle\langle\sum_i p_i^2\rangle)^{\frac{3}{2}}}\ \Omega_0^n N_n^*(E)\,,$$

where $N_n^*(E)$ is the momentum phase space as defined by eq. (12), *i.e.* restricted by energy conservation only and $\Omega_0$ is the interaction volume.

When the interaction volume has cylindrical symmetry around the beam direction (taken as the $z$-axis), we divide $\boldsymbol{r}_i$ and $\boldsymbol{p}_i$ into parts parallel to the beam direction, $\boldsymbol{r}_{iz}$ and $\boldsymbol{p}_{iz}$, and transverse to the beam direction, $\boldsymbol{r}_{iT}$ and $\boldsymbol{p}_{iT}$. We also divide the total angular momentum into corresponding parts, $\boldsymbol{I}_z$ and $\boldsymbol{I}_T$,

$$(47)\qquad \boldsymbol{I}_z = \sum_i \boldsymbol{r}_{iT}\times\boldsymbol{p}_{iT}\,, \qquad \boldsymbol{I}_T = \sum_i (\boldsymbol{r}_{iT}\times\boldsymbol{p}_{iz} + \boldsymbol{r}_{iz}\times\boldsymbol{p}_{iT})\,.$$

We treat the effects of momentum conservation identically as before, while we let the angular momentum components couple randomly in the $z$-direction and in the transverse plane according to eq. (47). We have

$$(48)\qquad P(p_1, \ldots, p_n;\ r_{1T}, \ldots, r_{nT};\ r_{1z}, \ldots, r_{nz};\ \boldsymbol{P}=0;\ \boldsymbol{I}) \simeq$$

$$\simeq \frac{1}{((2\pi/3)\sum_i p_i^2)^{\frac{3}{2}}} \cdot \frac{1}{(2\pi\sigma_{2z}^2)^{\frac{1}{2}}} \cdot \frac{1}{(2\pi\sigma_{2T}^2)} \exp\left[-I_T^2/2\sigma_{2T}^2 - I_z^2/2\sigma_{2z}^2\right],$$

with

$$\sigma_{2z}^2 = \sum_i \langle(\boldsymbol{r}_{iT}\times\boldsymbol{p}_{iT})^2\rangle = \sum_i r_{iT}^2 p_{iT}^2 \langle\sin^2(\boldsymbol{r}_{iT}, \boldsymbol{p}_{iT})\rangle = \tfrac{1}{2}\sum_i r_{iT}^2 p_{iT}^2\,,$$

$$\sigma_{2T}^2 = \sum_i \left\{\langle(\boldsymbol{r}_{iT}\times\boldsymbol{p}_{iz})_x^2\rangle + \langle(\boldsymbol{r}_{iz}\times\boldsymbol{p}_{iT})_x^2\rangle\right\} = \tfrac{1}{2}\sum_i (r_{iT}^2 p_{iz}^2 + z_{iz}^2 p_{iT}^2)\,.$$

We express eq. (48) more conveniently by observing that only the linear dimensions of the volume in the $z$-direction should be changed. Denote by $\langle r_0^2\rangle$ the mean value of the uncontracted radius squared and let

$$\langle r_{iz}^2\rangle = \alpha^2\langle r_{0z}^2\rangle = \frac{\alpha^2}{3}\langle r_0^2\rangle\,,$$

where $\alpha$ is the linear contraction factor. As we have imposed no condition on the $p_i$ in the coupling, the momenta are isotropic in space. Thus

$$\begin{cases} \sigma_{zz}^2 = \frac{2}{9}\langle r_0^2\rangle \sum_i p_i^2 , \\ \sigma_{zT}^2 = \frac{1}{9}(1-\alpha^2)\, r_0^2 \sum_i p_i^2 . \end{cases} \tag{49}$$

We have used the same arguments as previously in replacing the square of position vectors by average values. In the same approximation as eq. (46) we have

$$R_n(E, \boldsymbol{P}=0, \boldsymbol{I}) \simeq \tag{50}$$

$$\simeq \frac{\exp\left[-(I_T^2/(1+\alpha^2) + I_z^2/2)(\frac{2}{9}\langle r_0^2\rangle \langle \sum_i p_i^2\rangle)^{-1}\right]}{((2\pi/3)\langle \sum_i p_i^2\rangle)^{\frac{3}{2}}\, ((4\pi/9)\, r_0^2 \sum_i p_i^2\rangle)^{\frac{1}{2}}((2\pi/9)(1-\alpha^2)\, r_0^2 \langle \sum_i p_i^2\rangle)} \alpha^n \Omega_0^n N_n^*(E) ,$$

where $\Omega_0$ is the uncontracted volume.

Eq. (46) and (50) give the branching ratios between different processes for given total angular momentum $\boldsymbol{I}$. The total angular momentum is entirely dominated by the orbital angular momentum of the initially colliding particles and is therefore perpendicular to the beam-direction: $I_z = 0$. The cross-section for different processes is obviously obtained by analysing the crosssection of the initially colliding particles into partial waves and corresponding branching ratios, which again can be made classically,

$$\sigma_n(E) \simeq \pi\lambda_i^2 \int_0^{I_m} 2I \, \frac{R_n(E, \boldsymbol{P}=0, I, I_z=0)}{\sum_{\text{all } n} R_n(E, \boldsymbol{P}=0, I, I_z=0)} \, \mathrm{d}I . \tag{51}$$

The maximum value of the total angular momentum is close to $I_m \simeq k_i R$, where $R$ is the radius of the interaction volume.

While we can obtain the influence of angular momentum conservation on branching ratios from eq. (46), (48) and (51), it is even simpler to see the structure of the angular distribution of the emitted particles (*). If the particle angular momenta were free to take any direction in space the angular distribution of the emitted particles would be isotropic. Because of angular momentum conservation the particle angular momenta $\boldsymbol{l}_i = \boldsymbol{r}_i \cdot \boldsymbol{p}_i$ are forced to align partially with the total angular momentum $\boldsymbol{I}$. We will therefore obtain

(*) We will use the technique of Ericson and Strutinski (8) for treating angular distributions in compound nucleus reactions. We refer also to the review article by Ericson (9).

the maximum anisotropy possible in the SM, if we consider the case when the particle angular momenta are completely aligned with $\boldsymbol{I}$; any decoupling of $\boldsymbol{l}_i$ from $\boldsymbol{I}$ will cause a smearing of the angular distribution. In case of complete alignment, the particle will be emitted entirely in the plane perpendicular to $\boldsymbol{I}$, so that the angular distribution may be described by the $\delta$-function $\delta(\boldsymbol{n}_i \cdot \boldsymbol{I})$. Here $\boldsymbol{n}_i$ is the direction of the particle. The total angular momentum is perpendicular to the beam direction. The actually measured angular distribution per unit solid angle $W_a(\boldsymbol{n}_i)$ is the average over the directions of $\boldsymbol{I}$ in the plane perpendicular to the beam. In terms of the azimuthal angle $\varphi$ of $\boldsymbol{I}$ and with $\theta_i$ the angle between $\boldsymbol{n}_i$ and the beam

$$(52) \qquad W_a(\boldsymbol{n}_i)\,\mathrm{d}\boldsymbol{n}_i \propto \frac{\mathrm{d}\boldsymbol{n}_i}{2\pi}\int_0^{2\pi}\delta(\boldsymbol{n}_i \cdot \boldsymbol{I})\,\mathrm{d}\varphi = \frac{\mathrm{d}\boldsymbol{n}_i}{2\pi}\int_0^{2\pi}\delta(I \sin\theta_i \cos\varphi)\,\mathrm{d}\varphi = \frac{\mathrm{d}\boldsymbol{n}_i}{\pi I \sin\theta_i}\,.$$

The aligned angular distribution $W_a(\boldsymbol{n}_i)$ is thus strongly peaked forward and backward with a minimum at $\theta_i = \pi/2$. The typical forward-backward peaking of the angular distribution is due to the fact that the beam direction is the only direction which is perpendicular to all the $\boldsymbol{I}$ over which we average. The contributions of particles emitted perpendicular to $\boldsymbol{I}$ will therefore pile up for $\sin\theta_i \simeq 0$. Any decoupling of $\boldsymbol{l}_i$ from the direction $\boldsymbol{I}$ will tend to smear the angular distribution in the neighbourhood of the beam direction inside the decoupling angle, while the angular distribution for other angles remains essentially that of the aligned one. Using eq. (44) we can easily estimate the extent to which $\boldsymbol{l}_i$ is decoupled from the direction of $\boldsymbol{I}$ in the case of a spherically symmetric interaction volume. If the length of $l_i$ is given as well as $\boldsymbol{I}$, the other particles must couple to an angular momentum $\boldsymbol{I} - \boldsymbol{l}_i$. The *a priori* probability of this is proportional to $\exp[-(\boldsymbol{I}-\boldsymbol{l}_i)^2/2\sigma_2^2]$, where $\sigma_2^2$ refers to the $(n-1)$ remaining particles. We study this as function of the angle $\psi_i$ between $\boldsymbol{I}$ and $\boldsymbol{l}_i$ and obtain

$$(53) \qquad \exp[-(\boldsymbol{I}-\boldsymbol{l}_i)^2/2\sigma_2^2] = \exp[-(I-l_i)^2/2\sigma_2^2] \cdot$$
$$\cdot \exp[-2Il_i(1-\cos\psi_i)/2\sigma_2^2] \simeq \exp[-(I-l_i)^2/2\sigma_2^2]\exp[-Il_i\psi_i^2/2\sigma_2^2]\,.$$

We thus see that $\boldsymbol{l}_i$ will be forced to align with $\boldsymbol{I}$ to within an angle $\psi_0 \approx$ $\approx (2\sigma_2^2/l_i I)^{\frac{1}{2}}$. The angular distribution will therefore deviate from the aligned distribution $1/\sin\theta_i$ within an angle $\psi_0$ around the beam direction, where it will be strongly smeared (see Fig. 3). It will be practically unchanged elsewhere. The cross-section will thus retain its typical feature of forward-backward peaking with a minimum at 90° to the beam. The angular distributions from a contracted volume will be very closely similar to those considered for a spherical volume.

It is also interesting to consider the features of the angular distributions in single events, even though interference effects will be important, since no averaging can be performed. For a purely classical individual event the total angular momentum $\boldsymbol{I}$ has a well defined direction perpendicular to the beam. Since the angular momenta of the emitted particles add up to the total angular momentum, there must be a tendency for the particles to come out in a plane perpendicular to $\boldsymbol{I}$; the angular distribution must therefore show azimuthal asymmetry in high multiplicity events. The angular distribution in the plane perpendicular to $\boldsymbol{I}$ is on the average isotropic for a statistical process, but will show strong fluctuations, since interference has not been averaged out. The statistical *azimuthal* distribution will be nearly independent of interference effects, however, and will have a half width of the order of $\psi_0$, since the uncertainty in azimuthal angle is due to the decoupling of the particle angular momentum $\boldsymbol{l}_i$ from $\boldsymbol{I}$, which smears the distribution by the decoupling angle (cf. preceding paragraph).

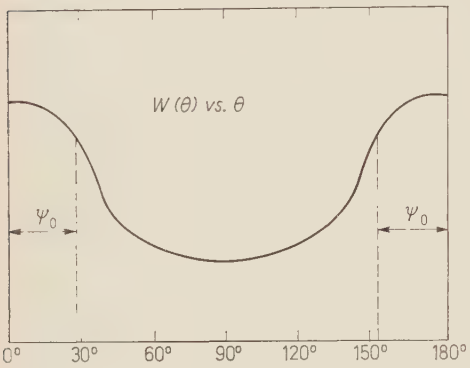


Fig. 3. – A characteristic statistical angular distribution $W(\theta)$. The angular distribution has forward-backward symmetry and shows forward-backward peaking with a minimum at 90° to the beam. It is smeared close to the beam direction within a decoupling angle $\psi_0$.

We will finally estimate the influence of angular momentum conservation on the shape of the energy spectra of the emitted particles and on the branching ratios between different processes.

We immediately notice that both momentum and angular momentum conservation must leave the shape of the energy spectra nearly unchanged, as soon as the multiplicity is not very low. The reason is that these conservation laws enter by the *a priori* probability $P(p_1, ..., p_n; r_1, ..., r_n; \boldsymbol{P}=0; \boldsymbol{I})$, which depends on the particle momenta only through the factor $\sum_i p_i^2$ in the random coupling approximation (eq. (44) and (45)). Since this factor is very insensitive to the momentum of an individual particle, it will have little effect on the energy distribution, which thus is easily obtained from the momentum phase space restricted only by energy conservation, as long as the high energy tail is excepted.

The multiplicities will be dramatically changed by inclusion of angular momentum. We assume in the following for the sake of argument that the particles are relativistic in order to easily expose the qualitative changes. Since the particles are relativistic $\langle \sum_i p_i^2 \rangle \simeq \frac{4}{3} E^2/n$ (see eq. (23)). From eq. (46)

we immediately conclude that the effect of angular momentum conservation is to multiply the phase space without angular momentum conservation by a factor proportional to $n^3 \exp[-naI^2/\langle r^2\rangle E^2]$, where $a$ is a constant of order unity. We have to distinguish between the limit of very low angular momentum (annihilation) with relatively small changes and that of high angular momentum with strong changes in multiplicity. For $I \simeq 0$ the above factor is proportional to $n^3$, which favours higher multiplicities. It is well known that the calculated average multiplicity in annihilation events comes out too small, if the natural interaction volume, the pion volume $(4\pi/3)(m_\pi)^{-3}$ is used; the interaction volume which reproduces the observed multiplicity is 10 times larger ([11]) (*). Since the inclusion of angular momentum favours higher multiplicity, it is no longer necessary to use quite as large an interaction volume as before. An estimate, which allows for the low multiplicity in annihilation indicates that the observed multiplicities are reproduced by an interaction volume 6 to 7 times larger than the natural volume. Thus while the inclusion of angular momentum reduces the size of the interaction volume needed, it still leaves us with a quite large volume to explain.

For large values of $I$ the angular momentum factor is dominated by its exponential part which is rapidly decreasing with $n$. In order to maintain the same multiplicities as have been previously calculated without angular momentum conservation which reproduce experiments with $\Omega_0$ equal the natural volume, it is thus necessary, to *increase* this volume. The increase is essentially by a factor $\exp[aI^2/\langle r^2\rangle E^2]$, which typically is of the order of 3 and possibly larger. The correct interaction volume is thus at least 3 times larger than the natural volume. A comparison with the interaction volume for annihilation shows that their difference has been reducduced to about a factor 2 or less. We therefore tentatively conclude that there is no significant difference between the interaction volumes needed to reproduce observed multiplicities in low and high angular momentum events. While the discrepancy in interaction volumes between these differents types of reactions thus seems to disappear, we are still left with the unexplained problem that the interaction volume is several times the natural volume (**).

([11]) F. CERULUS: *Nuovo Cimento*, **14**, 827 (1959).

(*) The large increase in the interaction needed to reproduce the experimental average multiplcity reflects the very slow variation of this quantity with $\Omega_0$. For relativistic particles it can easily be shown that the average multiplicity is proportional to $\Omega_0^{\frac{1}{4}}$.

(**) *Note added in proof.* – GRANOVSKIJ and KOPYLOV ([15]) have recently considered angular momentum effects in the SM and arrive to the opposite conclusion of ours, namely that angular momentum conservation has negligible influence on multiplicities. A study of their calculation shows that they start with the identical expression as we for the relative branching ratio of a particular $I$ eq. (41) ; they impose on this expression the condition $I_z = 0$, that the total angular momentum is perpendicular

These considerations on interaction volumes of course apply to the average angular momentum in the process. We may also ask how the multiplicity varies as a function of the partial waves. It is immediately evident that the multiplicity will be a decreasing function of angular momentum, *i.e.* high angular momenta (peripheral collisions) should have low multiplicities on phase space grounds only.

## 5. – Conclusion.

The great drawback of the SM in recent years is its ever increasing complexity, which is particularly regrettable, since the basic idea of the model is most simple: cross-sections proportional to the accessible phase space. The reasons for the increased complexity are two: 1) accelerator energies have increased and with them the average multiplicity per event and the number of energetically possible reactions; 2) various conservation laws, which were initially neglected in the theory, are now included and must be so unless shown to be unimportant. The methods developed up to now for treating problems of the SM assume that the number of emitted particles remains moderate. They consequently use techniques which are most suited for systems of a small number of particles. This is particularly evident when the isospin and angular momentum conservation are accounted for by Clebsch-Gordan techniques. It is therefore no surprise that these methods rapidly lead to excessive labour with increasing multiplicities. On the other hand it is obvious that systems of high multiplicities should asymptotically become simple and be describable by thermodynamical methods. The accuracy of thermodynamics is, however, not sufficient, since even high multiplicities still represent a small number of particles thermodynamically. The random coupling method developed in the preceding sections represents in a sense a compromise between these extremes. It has been chosen in such a way that the phase space is obtained exactly in the limit of high multiplicities and for a finite multiplicity $n$ is correct to order $1/n$. It is therefore a deliberate high multiplicity method and our philosophy in applying it is thus the opposite of that in the previous low multiplicity methods. There is, however, a large region of moderate multiplicities in which both approaches overlap, and they therefore complete each other.

to the beam. They omit, however, to observe that every partial wave has to be treated as a separate statistical system with a branching ratio which depends on *all* possible final products of this angular momentum channel; the correct total cross-section is obtained by multiplying every such branching ratio with the corresponding formation cross-section and summing over all partial waves, as we have outlined in eq. (51). It can easily be shown that their erroneous treatment is essentially equivalent to neglecting the conservation of the *length* of the total angular momentum $|\boldsymbol{I}|$, and the multiplicity change they find is consequently very small.

(15) Ya. I. Granowskij and G. I. Kopylov: *Soviet Physics, JETP*, **13**, 125 (1961).

One of the greatest advantages of the random coupling approximation is that it gives an excellent insight into the effects of the conservation laws on the phase space. Both for momentum and isospin conservation we have found that their net effect is to multiply the phase space without these conservation laws by the *a priori* probability that momentum and isospin vectors of the particles couple to correct total quantum numbers. We have derived simple analytical approximation formulas for these *a priori* probabilities. They show very clearly that energy spectra are nearly unaffected by momentum conservation, as might have been expected, since momentum conservation is a restriction on the system as a whole, rather than on any individual particle. We have furthermore shown by this approximation technique that the average angular correlation of two particles due to momentum conservation is proportional to $1/n$. The goodness of the asymptotic semi-classical expressions for statistical weight factors demonstrate that the corresponding quantum mechanical results rapidly turn to the semi-classical limit as the number of particles increases.

In Sections **2** and **3** we derived the results of the random coupling approximation for the usual versions of the SM, *i.e.* neglecting angular momentum conservation. In a complete description this conservation law must be inlcuded; this will not only influence the predicted multiplicities but leads to uniquely predicted angular distributions. The angular distributions are, however, considerably more sensitive than multiplicities and energy spectra to the validity of the basic statistical assumption: independence of formation and decay modes (but for exact quantum numbers). If the SM is applied outside its range of full validity, it is often useful as a rough guide for multiplicities and energy spectra, but angular distributions are then hardly expected to be well represented. On the other hand it is of considerable interest for the understanding of strong interaction mechanisms to know the extent of validity of the SM in different cases; it is therefore necessary to work out its exact predictions so that it can be subjected to stringent experimental tests. Consequently we have analysed the basic hypothesis of the SM in Section **4**. We found that the statistical description implicitly assumes that the matrix elements have random phases; there will thus be no interference effects on the average in the SM. This has the important consequence that the angular distribution of a particle emitted in the CM must have forward-backward symmetry on the average. Since this is a statistical prediction independent of any parameters of the model, it should be well suited as a simple test for separating statistical from non-statistical processes. It is of course to be expected that the high multiplicity events show more statistical features then others, since they imply a more complicated interaction. We have furthermore examined the qualitative features of the angular distributions in the CM system on the basis of a classical approximation. The particles are emitted preferentially in the

forward-backward direction with a minimum at 90° to the beam direction. The anisotropy of the particles is limited by a distribution $[\sin\theta_i]^{-1}$, where $\theta_i$ is the angle between the beam and the particle direction.

The influence of angular momentum conservation on the energy spectra of the emitted particles is weak, but the multiplicities are strongly affected. The qualitative effect is an increase of multiplicity for low total angular momentum and a decrease in multiplicity for large total angular momentum. This effect, reinterpreted in terms of interaction volumes, leads probably to the same interaction volume in annihilation events as for high energy nucleon-nucleon collisions. The large discrepancy between the interaction volumes needed for reproduction of observed multiplicities seems therefore to have been removed.

* * *

I have benefited from stimulating discussions with Dr. F. CERULUS and Dr. R. HAGEDORN on various aspects of the statistical model.

## RIASSUNTO (*)

Introduco un nuovo metodo per tener conto delle leggi di conservazione nel modello statistico della produzione di particelle. L'approssimazione diviene esatta nel limite delle alte molteplicità, e porta a semplici espressioni analitiche che permettono una valutazione immediata della influenza delle varie leggi di conservazione in differenti circostanze. Dimostro che la conservazione dell'impulso ha poca influenza sugli spettri d'energia delle particelle emesse; studio le sue conseguenze sulla correlazione angolare delle particelle. Mostro che i fattori statistici di peso, che risultano dall'accoppiamento dei vettori di isospin delle particelle emesse con l'imposta conservazione dell'isospin, sono ben rappresentati da espressioni semiclassiche; la dipendenza dei fattori di peso dall'isospin totale e dalla molteplicità diventa ovvia. Studio gli effetti generali della conservazione del momento angolare nel modello statistico; le distribuzioni angolari hanno simmetria antero-posteriore nel sistema del centro di massa, predizione specifica di questo modello e prova attendibile della sua validità. Nella approssimazione classica la distribuzione angolare ha un picco antero-posteriore, però non superiore alla distribuzione limite $1/\sin\theta$, in cui $\theta$ è l'angolo della particella con la direzione del fascio. La conservazione del momento angolare lascia gli spettri di energia quasi invariati, mentre le molteplicità ne sono fortemente influenzate; dimostro che i volumi effettivi di interazione nella annichilazione nucleone-antinucleone e nelle collisioni nucleone-nucleone sono approssimativamente uguali, se si tien conto di questo effetto.

(*) *Traduzione a cura della Redazione.*

IL NUOVO CIMENTO Vol. XXI, N. 4 16 Agosto 1961

# Phenomenological Analysis of Photon-Proton Elastic Scattering.

K. Berkelman (*)

*Laboratori di Fisica, Istituto Superiore di Sanità - Roma*

(ricevuto il 14 Giugno 1961)

**Summary.** — Recent experimental data on Compton scattering by the proton at energies above 300 MeV suggest an extension of previous phenomenological calculations. The present model takes into account the Thompson and magnetic moment scattering, the electric dipole scattering from the virtual charged pion current, and the « Low diagram » dependent on the $\pi^0$ mean life. The resulting differential cross-section is in qualitative agreement with the available data. The polarization of the recoil proton and the dependence on incident photon polarization are also calculated. Above 500 MeV the cross-sections for unpolarized and polarized photons and the recoil proton polarization are all quite sensitive to the $\pi^0$ mean life.

## 1. – Introduction.

In the low-energy limit the scattering of light by protons can be treated in the same way as the Compton scattering of light by electrons; and indeed the cross-section at zero energy is obtained merely by substituting the proton mass for the electron mass in the classical Thompson scattering formula. At higher energies photon-proton scattering becomes a much more complicated process, because of the excitation of intermediate pion-nucleon states. In the present work we shall use the phenomenological approach, determining separately the contributions of the various interfering processes in the scattering.

(*) On leave from Cornell University, visiting at the Istituto Superiore di Sanità with a grant from the National Science Foundation.

This approach has been taken before by many authors [1-5] with various degrees of sophistication, but in each case the maximum photon lab energy considered was about 300 MeV. Recent experiments at the Cornell and Frascati synchrotrons [6,7] in the energy region 300 to 800 MeV prompt one to extend the theoretical analysis to higher energies. In addition, the success of recent experiments [8-10] on the recoil proton polarization in $\pi^0$ photoproduction, and the demonstrated availability of polarized high-energy photon beams [11] suggest a phenomenological analysis of the polarization properties of the proton Compton scattering in anticipation of eventual experimental investigation.

## 2. – Multipole analysis.

We shall express the differential cross-section for scattering of unpolarized photons in terms of matrix elements $T_\alpha$ for the scattering in state $\alpha$ as follows (*):

$$\mathrm{d}\sigma/\mathrm{d}\Omega = 2\langle \sum T_\alpha|^2\rangle_{e,e',\sigma}\,, \tag{1}$$

where $T_\alpha$ is expressible in the form $a_\alpha(k) f_\alpha(\boldsymbol{k}, \boldsymbol{k}', \boldsymbol{e}, \boldsymbol{e}', \sigma)$, a product of a complex function $a_\alpha$ of the photon energy $k$ and a scalar function $f_\alpha$ of the unit vectors $\boldsymbol{k}$, $\boldsymbol{k}'$, $\boldsymbol{e}$, $\boldsymbol{e}'$, and $\sigma$, that is, the photon initial and final momentum, initial and final polarization, and the proton spin. The brackets denote an average over spin and polarization states. Eq. (1) can be re-expressed in terms of $a_\alpha$ and $f_\alpha$:

$$\mathrm{d}\sigma/\mathrm{d}\Omega = \sum_{\alpha\leq\beta} \mathrm{Re}\, a_\alpha(k)\, a^*_\beta(k) F_{\alpha\beta}(x)\,, \tag{2}$$

(1) N. Austern: *Phys. Rev.*, **100**, 1522 (1955).

(2) Y. Yamaguchi: (unpublished, quoted by T. Yamagata in Ph. D. Thesis, University of Illinois, 1956).

(3) B. T. Feld: *Ann. Phys.*, **4**, 189 (1958).

(4) W. J. Karzas, W. K. R. Watson and F. Zachariasen: *Phys. Rev.*, **110**, 253 (1958).

(5) L. G. Hyman, R. Ely, D. H. Frisch and M. A. Wahlig: *Phys. Rev. Lett.*, **3**, 93 (1959).

(6) J. W. Dawire, M. Feldman, V. L. Highland and R. Littauer: (to be published).

(7) G. Cortellessa, A. Reale and P. Salvadori: *Rend. Ist. Sup. Sanità* (to be published).

(8) P. C. Stein: *Phys. Rev., Lett.*, **2**, 473 (1959).

(9) R. Querzoli, G. Salvini and A. Silvestrini: *Nuovo Cimento*, **19**, 53 (1961).

(10) L. Bertanza, P. Franzini, I. Mannelli, G. V. Silvestrini and V. Z. Peterson: *Nuovo Cimento*, **19**, 953 (1961).

(11) G. Barbiellini, G. Bologna, G. Diambrini and G. P. Murtas: (unpublished); see also R. C. Smith and R. F. Mozley: *Proc. of Rochester Conf.* (1960), p. 22.

(*) Unless otherwise noted, all quantities are measured in the center-of-mass system.

where $x = \cos\theta$ and

$$(3) \qquad \begin{cases} F_{\alpha\alpha}(x) = 2\langle |f_\alpha|^2 \rangle_{e,e',\sigma}, \\ F_{\alpha\beta}(x) = 4\langle \mathrm{Re}\, f_\alpha f_\beta^* \rangle_{e,e',\sigma}. \end{cases}$$

From symmetry requirements [12] one can show that the $f_\alpha$ for the various dipole states $\alpha$ are as follows:

$$(4) \qquad \begin{cases} f_{E1} = \boldsymbol{e}'\cdot\boldsymbol{e}, \\ f_{E1^*} = i\boldsymbol{\sigma}\cdot\boldsymbol{e}'\times\boldsymbol{e}, \\ f_{M1} = \boldsymbol{m}'\cdot\boldsymbol{m}, \\ f_{M1^*} = i\boldsymbol{\sigma}\cdot\boldsymbol{m}'\times\boldsymbol{m}, \end{cases}$$

where the asterisk denotes the spin-flip amplitude and $\boldsymbol{m} = \boldsymbol{k}\times\boldsymbol{e}$. Using the same formalism we can write the polarization of the recoil proton as

$$(5) \qquad \boldsymbol{P}\,\mathrm{d}\sigma/\mathrm{d}\Omega = \sum_{\alpha>\beta} \mathrm{Im}\, a_\alpha(k)\, a_\beta^*(k) F_{\alpha\beta}(x)\boldsymbol{n},$$

where $\boldsymbol{n} = (\boldsymbol{k}\times\boldsymbol{k}')/\sin\theta$ is the unit vector normal to the scattering plane and

$$(6) \qquad F_{\alpha\beta}(x) = -4\langle \mathrm{Im}\,\boldsymbol{\sigma}\cdot\boldsymbol{n} f_\alpha f_\beta^* \rangle_{e,e',\sigma}.$$

In Table I are listed the $F_{\alpha\beta}$ factors corresponding to all pairs of dipole states. On the main diagonal and in the upper right ($\alpha \leqslant \beta$) are the angular

TABLE I. – *Angular distribution functions $F_{\alpha\beta}$ for differential cross-section and recoil polarization with unpolarized incident photons.*

| $\alpha$ \ $\beta$ | $E1$ | $E1^*$ | $M1$ | $M1^*$ |
|---|---|---|---|---|
| $E1$ | $\frac{1}{2}(1+x^2)$ | 0 | $2x$ | 0 |
| $E1^*$ | $x(1-x^2)^{\frac{1}{2}}$ | $\frac{1}{2}(3-x^2)$ | 0 | $2x$ |
| $M1$ | 0 | $(1-x^2)^{\frac{1}{2}}$ | $\frac{1}{2}(1+x^2)$ | 0 |
| $M1^*$ | $(1-x^2)^{\frac{1}{2}}$ | 0 | $x(1-x^2)^{\frac{1}{2}}$ | $\frac{1}{2}(3-x^2)$ |

[12] M. J. MORAVSCIK: *Internal report BNL* 459, (1957) (unpublished).

distribution terms computed from eq. (3), and in the lower left ($\alpha > \beta$) are the angular-distribution terms for the recoil polarization computed from eq. (6). As one should expect from general symmetry arguments, there is no interference in the differential cross-section between spin-flip and non-spin-flip states, and the interference between terms of opposite parity gives rise to angular-distribution terms asymmetric about 90° in the center of mass. The recoil-polarization angular dependence always contains the factor $\sin\theta$: that is, the polarization vanishes for scattering at 0° and 180°, as it should, since the vector $\boldsymbol{n}$ cannot be defined in such cases. Furthermore, the polarization is non-zero only in the case of spin-flip, non-spin-flip interference: and the interference between states of the same parity produces a recoil polarization which vanishes at 90° in the center of mass.

The above results for the scattering of unpolarized photons were obtained by averaging over the various directions of the incident linear polarization $\boldsymbol{e}$ or equivalently, averaging over the angle $\varphi$ between $\boldsymbol{e}$ and the scattering plane. Simply by omitting this averaging step, we obtain instead the differential cross-section as a function of $\varphi$, as well as $\theta$. The recoil polarization for polarized photons can of course also be obtained if desired. Since this experiment probably cannot be done in the foreseeable future, we shall not concern ourselves with it here. Table II shows the angular distribution factors $F_{\alpha\beta}(x, y)$, where $x = \cos\theta$ and $y = \cos\varphi$. As expected, the azimuthal angular

TABLE II. – *Angular distribution functions $F_{\alpha\beta}$ for differential cross-section with linearly polarized incident photons.*

| $\alpha$ \ $\beta$ | $E1$ | $E1^*$ | $M1$ | $M1^*$ |
|---|---|---|---|---|
| $E1$ | $1 - x^2y^2 - y^2$ | 0 | $2x$ | 0 |
| $E1^*$ | | $1 - x^2y^2 + y^2$ | 0 | $2x$ |
| $M1$ | | | $x^2 - x^2y^2 + y^2$ | 0 |
| $M1^*$ | | | | $2 - x^2 + x^2y^2 - y^2$ |

distribution is symmetric about the planes of both the electric and magnetic vectors of the incident photon wave. Furthermore, the angular distribution in $\theta$ for a magnetic multipole state is the same as that in the corresponding electric state rotated through 90° in azimuth, the terms coming from the interference between electric and magnetic multipoles being independent of azimuth.

## 3. – Phenomenological model.

In our model of the photon-proton scattering below 1 GeV five processes are assumed to contribute: 1) the direct electromagnetic scattering, which we shall separate for convenience into the charge (Thompson) scattering and the Dirac magnetic moment scattering, denoted by subscripts $T$ and $M$; 2) the electric dipole $J=\frac{1}{2}$ scattering via the virtual charged meson current, denoted by $E$; 3) the resonance scattering associated with the $T=\frac{3}{2}$, $J=\frac{3}{2}$ pion-nucleon resonance, denoted by 33; 4) the scattering associated with the $T=\frac{1}{2}$, $J=\frac{3}{2}$ second pion-nucleon resonance, denoted by 13; and 5) the scattering due to the so-called Low diagram ([13]) in which the photon and proton exchange a $\pi^0$ which couples to the photon by means of the decay interaction $\pi^0 \to \gamma+\gamma$. Other states can certainly be expected to contribute, for example the retardation terms associated with the virtual charged meson contribution and other terms corresponding to excitation of virtual pions in non-resonant states; but in the absence of reliable estimates of these effects, we shall neglect them in the hope that they are small.

The Thompson scattering formula can be extended using very general arguments of gauge and relativistic invariance ([13,14]) to the following expression for the amplitude, to first order in $k$:

$$T_{\text{Th}} = -(e^2/M)\boldsymbol{e}'\cdot\boldsymbol{e} - 2i\mu_p^2 k\,\boldsymbol{\sigma}\cdot\boldsymbol{m}'\times\boldsymbol{m} - (ie\mu_p k/2M)\cdot$$

$$\cdot[\boldsymbol{\sigma}\cdot\boldsymbol{k}\,\boldsymbol{m}\cdot\boldsymbol{e}' + \boldsymbol{\sigma}\cdot\boldsymbol{m}\,\boldsymbol{k}\cdot\boldsymbol{e}' - \boldsymbol{\sigma}\cdot\boldsymbol{k}'\,\boldsymbol{m}'\cdot\boldsymbol{e} - \boldsymbol{\sigma}\cdot\boldsymbol{m}'\,\boldsymbol{k}'\cdot\boldsymbol{e}] - (ie\mu_{\text{anom}}k/M)\boldsymbol{\sigma}\cdot\boldsymbol{e}\times\boldsymbol{e}',$$

(using center-of-mass co-ordinates, $\hbar=c=1$, $e^2=1/137$). The first term is the classical Thompson scattering; the second is a magnetic dipole transition corresponding classically to a precession of $\boldsymbol{\mu}_p$ around $\boldsymbol{\mu}_p\times\boldsymbol{H}$, while the last two are small recoil terms in $1/M$. Besides neglecting the recoil terms, we shall make two other modifications; we multiply the Thompson term by $k/k_L$, the ratio of center of mass to lab photon energy, to account for the higher order dependence on $k$ (see for example Powell ([15])); and we replace the total proton magnetic moment $\mu_p$ by the Dirac moment $e/2M$, since in our model the anomalous moment is interpreted as a pion cloud effect, which is treated

([13]) F. E. Low: *Phys. Rev.*, **96**, 1428 (1954); *Proc. CERN Conf.*, (1958), p. 98.

([14]) M. Gell-Mann, M. L. Goldberger and W. E. Thirring: *Phys. Rev.*, **95**. 1612 (1954).

([15]) J. L. Powell: *Phys. Rev.*, **74**, 1258 (1948); **75**, 32 (1949).

separately. We then have

$$a_T = -(e^2/M)(k/k_L)\,,$$
$$a_M = -\tfrac{1}{2}(e^2/M)(k/M)\,.$$
$$f_T = \boldsymbol{e}'\cdot\boldsymbol{e} = f_{E1}\,,$$
$$f_M = i\boldsymbol{\sigma}\cdot\boldsymbol{m}'\times\boldsymbol{m} = f_{M1^*}\,.$$

At low energies the process in which the photon scatters electromagnetically from the virtual charged pion takes place through the $J=\frac{1}{2}$ total angular momentum and parity state, as does the corresponding direct photoelectric production of the $\pi^+$. This state is a combination of electric dipole spin-flip and non-spin-flip given by

$$f_E = \tfrac{1}{2}f_{E1} + \tfrac{1}{2}f_{E1^*} = \tfrac{1}{2}(\boldsymbol{e}'\cdot\boldsymbol{e} + i\boldsymbol{\sigma}\cdot\boldsymbol{e}'\times\boldsymbol{e})\,.$$

The energy dependence $a_E(k)$ has been calculated from perturbation theory with some success in the low energy photoproduction and photon scattering ([4]), but one cannot expect this to have any meaning at the higher energies of interest here. Dispersion relations have been used to derive the amplitudes for somewhat different sets of states which include the $J=\frac{1}{2}$-state in linear combination with $J=\frac{3}{2}$ — ([16,17]). This makes the phenomenological analysis at high energy where the second resonance ($J=\frac{3}{2}$—) dominates somewhat ambiguous just where the evaluation of the dispersion integrals becomes less certain. This complication occurs only in the evaluation of the real part of $a_E$ instead, the imaginary part is given simply in terms of the total absorption (*i.e.*, photoproduction) in this state ([17]):

$$\operatorname{Im} a_E = 2k|E_1|^2\,,$$

where $E_1$ is the $J=\frac{1}{2}$— electric dipole photoproduction amplitude as defined by WATSON *et al.* ([18]). Assuming that the non-isospin-dependent part of the photoproduction amplitude between threshold and 500 MeV is entirely accounted for by the $E_1$ amplitude, we can use the experimental data to eva-

([16]) M. JACOB and J. MATHEWS: *Phys. Rev.*, **117**, 854 (1960).

([17]) L. I. LAPIDUS and CHOU KUANG-CHAO: *Žurn. Èksp. Theor. Fiz.*, **37**, 1714 (1959) (trans. *Sov. Phys. JEPT*, **10**, 1213 (1960)); *Žurn. Èksp. Theor. Fiz.*, **38**, 201 (1960) (trans. *Sov. Phys. JETP*, **11**, 147 (1960)).

([18]) K. M. WATSON, J. C. KECK, A. V. TOLLESTRUP and R. L. WALKER: *Phys. Rev.*, **101**, 1159 (1956).

luate $E_1$:

$$|E_1|^2 = \mathrm{d}\sigma_{\gamma\pi^+}/\mathrm{d}\Omega\,(90°) - \tfrac{1}{2}\,\mathrm{d}\sigma_{\gamma\pi^0}/\mathrm{d}\Omega\,(90°)\,.$$

In the vicinity of the photopion threshold we have estimated the real part of the amplitude $a_E$ by comparing the differential cross-section at 0° calculated from the present model setting $\mathrm{Re}\,a_E = 0$, with the prediction of the dispersion relation

$$\frac{\mathrm{d}\sigma}{\mathrm{d}\Omega}\,(k_L,\,0°) = \left| -\frac{e^2}{M} + \frac{k_L^2}{2\pi^2}\int_0^\infty \frac{\sigma_{\mathrm{tot}}(k_L')\,\mathrm{d}k_L'}{k_L'^2 - k_L^2} + i\,\frac{k_L}{4\pi}\,\sigma_{\mathrm{tot}}(k_L)\right|^2 (*),$$

and using the discrepancy to solve for $\mathrm{Re}\,a_E$. The resulting behavior of the amplitude is in qualitative agreement with previous estimates [15,18] and shows the expected cusp at the meson threshold. At the higher energies the neglected retardation terms will contribute significantly to the forward cross-section and any such calculation of $\mathrm{Re}\,a_E$ will have little meaning. Consequently, we have arbitrarily set $\mathrm{Re}\,a_E = 0$ above 350 MeV. This should be borne in mind in assessing the reliability of predictions of the model at high energies. It is also possible that the steep rise in the double charged-meson photoproduction cross-section [19] around 500 MeV is caused by a direct photon-meson current interaction associated with a strong $J = \frac{1}{2}$ — electric dipole effect, analogous to that occurring at the single-meson threshold. If this is the case, our guess at the energy dependence of $\mathrm{Im}\,a_E$ is also in error.

Following AUSTERN [1] and FELD [2] we interpret the scattering through the $T = \frac{1}{2}$, $J = \frac{3}{2}$— intermediate pion-nucleon state in terms of a simple isobar model. The total resonant scattering cross-section $\sigma_{\gamma\gamma}$ is just the cross-section $\sigma_{\gamma^*}$ for producing the isobar multiplied by the relative width for decay of the isobar into the photon-nucleon channel:

$$\sigma_{\gamma\gamma} = \sigma_{\gamma^*}\,\Gamma_\gamma/\Gamma\,.$$

Since the pion-nucleon mode accounts for virtually all of the isobar decays, we can replace $\sigma_{\gamma^*}$ by $\sigma_{\gamma\pi}$ and $\Gamma_\gamma/\Gamma$ by $\sigma_{\pi\gamma}/\sigma_{\pi\pi}$, the ratio of the resonance cross-sections for $\pi + \mathcal{N} \to \mathcal{N} + \gamma$ and pion-nucleon scattering. Finally, $\sigma_{\pi\gamma}$ can be

(*) Actually, this is only approximate. We have neglected the term involving the integral over the difference between the total cross-sections for photons circularly polarized parallel and anti-parallel to the proton spin. The $\pi^0$ lifetime contribution is identically zero in the forward direction, and hence no error is introduced by uncertainty in $\tau$.

[19] B. M. CHASAN, G. COCCONI, V. T. COCCONI, R. M. SCHECTMAN and D. H. WHITE: *Phys. Rev.*, **119**, 811 (1960).

replaced by $\sigma_{\gamma\pi}$, the cross-section for the inverse process, by detailed balancing:

$$\sigma_{\gamma\pi}/q^2 = \sigma_{\pi\gamma}/2k^2 ,$$

where $q$ is the center-of-mass pion momentum. Thus we have

$$\sigma_{\gamma\gamma} = (2k^2/q^2)(\sigma^2_{\gamma\pi}/\sigma_{\pi\pi}) . \tag{7}$$

Equating the $T=\frac{3}{2}$ resonant photoproduction cross-section $\sigma_{\gamma\pi}$ to $\frac{3}{2}\sigma_{\gamma\pi^0}$ and using $\sigma_{\pi^+\pi^+}$ for $\sigma_{\pi\pi}$ where the resonance dominates,

$$\sigma^{33}_{\gamma\gamma} = (9k^2/2q^2)(\sigma^2_{\gamma\pi^0}/\sigma_{\pi^+\pi^+}) \tag{8}$$

in which each of the cross-sections is to be interpreted as only the 33 resonance contribution. The $J=\frac{3}{2}+$ photon-plus-proton total angular momentum and parity state is actually a superposition of spin-flip and non-spin-flip amplitudes. The angular part of the magnetic dipole $J=\frac{3}{2}$ amplitude is given by

$$f_{33} = f_{M1} - \tfrac{1}{2} f_{M1^*} = \boldsymbol{m}'\cdot\boldsymbol{m} - \tfrac{1}{2} i\,\boldsymbol{\sigma}\cdot\boldsymbol{m}'\times\boldsymbol{m} ,$$

which one can verify by using projection operators ([12]). Calculating $F_{33\text{-}33}(x)$ from the $F_{\lambda,\beta}(x)$ terms in Table I, and integrating over solid angle, one obtains

$$\sigma^{33}_{\gamma\gamma} = 4\pi\,|\,a_{33}\,|^2 ,$$

and hence

$$|\,a_{33}\,| = (\sigma^{33}_{\gamma\gamma}/4\pi)^{\frac{1}{2}} ,$$

where $\sigma^{33}_{\gamma\gamma}$ is given by eq. (8). The phase of the resonant photon scattering is the same as for the corresponding pion scattering; that is

$$a_{33}(k) = (\sigma^{33}_{\gamma\gamma}/4\pi)^{\frac{1}{2}} \exp[\,i\delta_{33}] .$$

The requirement that the imaginary part of the forward amplitude be given by $(k/4\pi)\sigma_{tot}$ determines that $\delta_{33}(k)$ runs between $0^\circ$ and $180^\circ$. For the numerical calculations the photoproduction cross-section and scattering cross-section and phase are taken from experimental data given in references ([20-22]).

The second pion-nucleon resonance, which we assume to take place in the

([20]) K. Berkelman and J. A. Waggoner: *Phys. Rev.*, **117**, 1364 (1960).
([21]) S. J. Lindenbaum: *Ann. Rev. Nucl. Sci.*, **7**, 317 (1957).
([22]) K. Dietz and G. Höhler: *Zeits. Naturforsch.*, **14**a, 994 (1959).

$T=\frac{1}{2}$, $J=\frac{3}{2}-$ state ([23]), can be treated in much the same way. Reinterpreting eq. (7) in terms of the $T=\frac{1}{2}$ resonance we obtain

$$\sigma_{\gamma\gamma}^{13} = (12k^2/q^2)(\sigma_{\gamma\pi^0}^2/\sigma_{\pi^-\pi}) , \tag{9}$$

in which each of the cross-sections represents just the 13 resonance contribution. Actually, it is not quite that simple. The 13 isobar can also decay in the double-pion mode, and judging from the photoproduction cross-sections ([19]), does so about half the time. Thus $\Gamma_\gamma/\Gamma$ becomes about $\frac{1}{2}\sigma_{\pi\gamma}/\sigma_{\pi\pi}$, and $\sigma_{\gamma^*}$ becomes about $2\sigma_{\gamma\pi}$. Note, however, that the effect cancels out to first order and eq. (9) is still approximately correct. The uncertainties in the photoproduction data in this energy region do not justify a more sophisticated treatment than this.

The $J=\frac{3}{2}-$ state is given in terms of our dipole states by

$$f_{12} = f_{E1} - \tfrac{1}{2} f_{E1^*} = \boldsymbol{e}'\cdot\boldsymbol{e} - \tfrac{1}{2} i\,\boldsymbol{\sigma}\cdot\boldsymbol{e}'\times\boldsymbol{e} .$$

Calculating $F_{13\text{-}13}(x)$ and integrating over solid angle again, we obtain

$$\sigma_{\gamma\gamma}^{13} = 4\pi\,|a_{13}|^2 ,$$

and hence

$$a_{13}(k) = (\sigma_{\gamma\gamma}^{13}/4\pi)^{\frac{1}{2}} \exp[\delta i_{13}],$$

where $\sigma_{\gamma\gamma}^{13}$ is given by eq. (9). As in the case of the first resonance, $\delta_{13}(k)$ runs between 0° and 180°. For the numerical calculations we have taken $\sigma_{\gamma\pi^0}$ and $\sigma_{\pi^-\pi}$ from a crude Breit-Wigner fit to the photoproduction ([20]) and pion scattering ([24]) data (after subtracting the extrapolated 33-resonance contribution) using a resonance lab photon energy of 750 MeV and a width $\Gamma$ of 96 MeV in the center of mass. The corresponding phase $\delta_{13}(k)$ is given by

$$\operatorname{tg}\delta_{13} = \tfrac{1}{2}\Gamma/(E_r - E) .$$

It is probably true that the single-level resonance formula does not give an accurate picture of the 13 amplitude and phase, but in the absence of any experimental or theoretical knowledge it is perhaps the best one can do.

A straightforward calculation of the amplitude for the Low diagram (pho-

([23]) R. F. PEIERLS: *Phys. Rev.*, **118**, 325 (1960).
([24]) P. FALK-VAIRANT and G. VALLADAS: *Proc. Rochester Conf.* (1960), p. 38.

ton and proton exchanging a neutral pion) yields [16,25]

$$T_L = -(e^2/M)(g/\alpha)(2/\mu\tau)^{\frac{1}{2}}(kM/E\mu)[(k-k')^2-\mu^2]^{-1} i\boldsymbol{\sigma}\cdot(\boldsymbol{k}-\boldsymbol{k}')(\boldsymbol{k}-\boldsymbol{k}')\cdot(\boldsymbol{e}\times\boldsymbol{e}'),$$

where $g^2 = 14$, $E$ is the total center-of-mass energy, and $\tau$ is the mean life of the $\pi^0$. One assumes unity form factor at the $\pi\gamma\gamma$ vertex; that is, the pion decay interaction strength is negligibly affected by the fact that the interaction takes place off the energy shell. In our notation we then have

$$T_L = a_L(k)\big(x - x_p(k)\big)^{-1} f_L,$$

where

$$x_p(k) = 1 + \mu^2/2k^2;$$

$$a_L = -(e^2/M)(g/\alpha)(2/\mu\tau)^{\frac{1}{2}}(kM/E\mu),$$

$$f_L = i\boldsymbol{\sigma}\cdot(\boldsymbol{k}-\boldsymbol{k}')(\boldsymbol{k}-\boldsymbol{k}')\cdot(\boldsymbol{e}\times\boldsymbol{e}').$$

For simplicity in the angular distribution calculations we have separated the pole denominator $x - x_p$ from the angular dependence function $f_L$. From the form of $f_L$ it is clear that the scattering contribution from the Low process does not occur in a single multipole state but is rather a superposition of many.

## 4. – Results.

For the particular set of six states in terms of which we have chosen to express the various contributions to the photon-proton scattering, we can again construct the matrix of angular distribution factors $F_{\alpha\beta}$ in analogy with Table I and II. Table III gives the differential cross-section and polarization terms for unpolarized incident photons, and Table IV gives the values of $[F_{\alpha\beta}(x, 0) - F_{\alpha\beta}(x, 1)]/\sin^2\theta$, the difference in the $\theta$ angular distribution between scattering in the planes perpendicular and parallel to the incident photon polarization, divided by $\sin^2\theta$ (taking advantage of the fact that for dipole transitions this is the only allowed angular dependence symmetric about 90° and vanishing at 0° and 180°). Note from Tables III and IV that the $\pi^0$ mean life produces no polarization effects; that is, for unpolarized incident photons all terms involving the Low process vanish identically in the recoil polarization distribution $P\,d\sigma/d\Omega$, and the Low terms in the differential cross-section are independent of incident photon polarization.

[25] G. Bernardini, A. O. Hanson, A. C. Odian, T. Yamagata, L. B. Auerbach and I. Filosofo: *Nuovo Cimento*, **18**, 1203 (1960).

TABLE III. – *Angular distribution functions $F_{\alpha\beta}$ for the differential cross-section and recoil polarization with unpolarized incident photons.*

| $\alpha$ \ $\beta$ | $T$ | $M$ | $E$ | 33 | 13 | $L$ |
|---|---|---|---|---|---|---|
| $T$ | $\frac{1}{2}(1+x^2)$ | 0 | $\frac{1}{2}(1+x^2)$ | $2x$ | $1+x^2$ | 0 |
| $M$ | $x(1-x^2)^{\frac{1}{2}}$ | $\frac{1}{2}(3-x^2)$ | $x$ | $-\frac{1}{2}(3-x^2)$ | $-x$ | $2(1-x)^2$ |
| $E$ | $\frac{1}{2}x(1-x^2)^{\frac{1}{2}}$ | $\frac{1}{2}(1-x^2)^{\frac{1}{2}}$ | $\frac{1}{2}$ | $\frac{1}{2}x$ | $-\frac{1}{4}(1-3x^2)$ | $-(1-x)^2$ |
| 33 | $-\frac{1}{2}(1-x^2)^{\frac{1}{2}}$ | $x(1-x^2)^{\frac{1}{2}}$ | $\frac{1}{4}(1-x^2)^{\frac{1}{2}}$ | $\frac{1}{8}(7+3x^2)$ | $\frac{5}{2}x$ | $-(1-x)^2$ |
| 13 | $-\frac{1}{2}x(1-x^2)^{\frac{1}{2}}$ | $(1-x^2)^{\frac{1}{2}}$ | $\frac{1}{4}x(1-x^2)^{\frac{1}{2}}$ | $-(1-x^2)^{\frac{1}{2}}$ | $\frac{1}{8}(7+3x^2)$ | $(1-x)^2$ |
| $L$ | 0 | 0 | 0 | 0 | 0 | $2(1-x)^3$ |

The predictions of our phenomenological model can now be obtained explicitly by substituting the $F_{\alpha\beta}$ factors from the tables and the $a_\alpha(k)$ factors discussed in the previous section into eqs. (2) and (5) to obtain $(\mathrm{d}\sigma/\mathrm{d}\Omega)(k,\theta)$ and $P(k,\theta)\,(\mathrm{d}\sigma/\mathrm{d}\Omega)(k,\theta)$. Fig. 1 and 2 show the center-of-mass differential cross-section for scattering of unpolarized photons, as a function of photon lab energy $k_L$ at 90° in the center of mass, and as a function of center-of-mass angle for a number of photon energies, taking several values of the $\pi^0$ mean life. Also plotted in Fig. 1 are the available experimental data above the meson threshold ([6,25]) showing for the most part, satisfactory agreement with the present theory. The effect of the 33 pion-nucleon resonant state on the

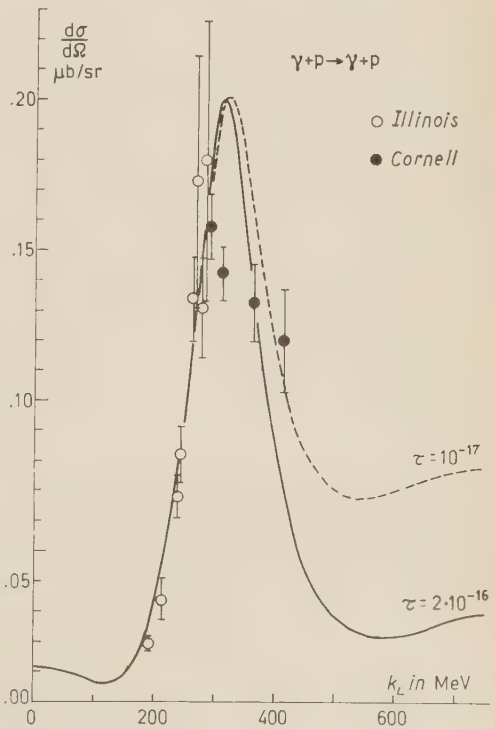


Fig. 1. – Calculated center-of-mass differential scattering cross-section at 90°, as a function of laboratory photon energy and for two values of the $\pi^0$ mean life. Experimental data from references ([6]) and ([25]).

proton Compton scattering is evident in the strong peak at 320 MeV. In fact the scattering cross-section above the meson threshold seems to parallel the photoproduction cross-section, although of course with a different angular

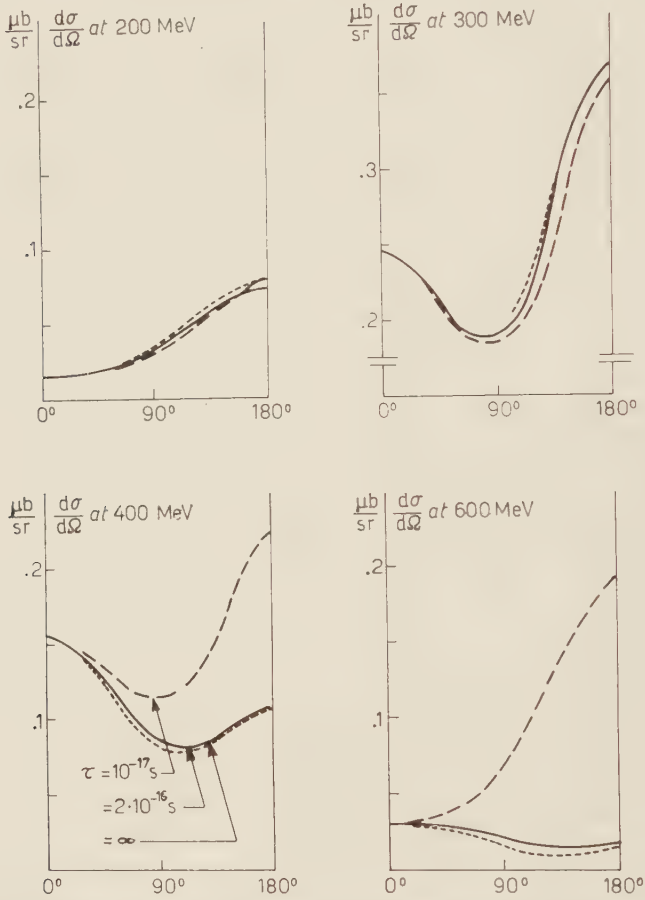


Fig. 2. Calculated center-of-mass differential cross-section as a function of center-of-mass angle, plotted for four laboratory photon energies and three values of the $\pi^0$ lifetime.

distribution. The angular distribution has a minimum at 90° characteristic of both the electric dipole Thompson scattering and the magnetic dipole first resonance scattering. The interference terms produce an asymmetry about 90° which changes sign going through the first resonance. Above 400 MeV the theoretical predictions are not very well established because of the various simplifying assumptions and naive guesses we have had to use. It is quite clear, however, that the $\pi^0$ lifetime effect, already pointed out by JACOB and

TABLE IV. – $[F_{\alpha\beta}(\Phi = 90°) - F_{\alpha\beta}(\Phi = 0°)]/\sin^2\theta$, *the difference in the* $\theta$ *angular distribution between scattering in the planes perpendicular and parallel to the incident photon polarization, divided by* $\sin^2\theta$.

| $\alpha$ \ $\beta$ | $T$ | $M$ | $E$ | 33 | 13 | $L$ |
|---|---|---|---|---|---|---|
| $T$ | 1 | 0 | 1 | 0 | 2 | 0 |
| $M$ | | 1 | 0 | $-1$ | 0 | 0 |
| $E$ | | | 0 | 0 | 3 | 0 |
| 33 | | | | $-\frac{3}{4}$ | 0 | 0 |
| 13 | | | | | $\frac{3}{4}$ | 0 |
| $L$ | | | | | | 0 |

MATHEWS [16] below the resonance, becomes quite appreciable above the resonance especially at backward angles and for $\tau < 10^{-16}$ s (*). The analysis of the experimental data below 300 MeV [25] has indicated a mean life around $10^{-17}$ s, while the emulsion data [26] on the process $K^+_{\pi 2} \to \pi^+ + \pi^0$, $\pi^0 \to \gamma + e^+$ indicate a value $\tau = (1.9 \pm .5)\cdot 10^{-16}$ s. A measurement of the Compton cross-section above 400 MeV and at a large angle should be crucial for the measurement of $\tau$. A preliminary measurement at 770 MeV and 90° has given a rather high value for the cross-section $((.13 \pm .06)\ \mu b/sr)$, which is an indication of a short lifetime more in accord with the low energy Compton analysis than with the emulsion value.

It should be pointed out, especially if the $\pi^0$ mean life is short, that there may well be a significant contamination in the $\pi^0$ photoproduction differential cross-section measurements (typically 1 to 3 $\mu$b/sr above 500 MeV) from the Compton scattering (up to .2 $\mu$b/sr), particularly in cases where the $\pi^0$ de-

(*) In an unpublished report LAPIDUS and CHOU have recently suggested that the sign of the Low amplitude usually assumed is in error. If this is true, regardless of the $\pi^0$ lifetime assumed, the addition of the Low amplitude to the scattering in the region of the first resonance does not improve the agreement between theory and experiment. However, at photon energies above 400 MeV, where the contribution comes mainly from the amplitude-squared term rather than the interference, the sign of the Low amplitude has little observable effect and the predictions of the present analysis are not altered.

[26] R. G. GLASSER, N. SEEMAN and B. STILLER: *Bull. Am. Phys. Soc.*, **6**, 39 (1961); *Phys. Rev.* (to be published).

tection efficiency is very low relative to the scattered photon efficiency. This may help to explain some of the inconsistencies in the $\pi^0$ photoproduction data.

Fig. 3 shows the recoil proton polarization in the direction $\boldsymbol{k}\times\boldsymbol{k}'$ at 90° in the center of mass, as a function of photon energy. The curve should not be regarded as a firm prediction of the polarization, especially at the higher energies where inaccuracies in our estimates of the energy dependence of the amplitudes and phases as well as the presence of other scattering states not

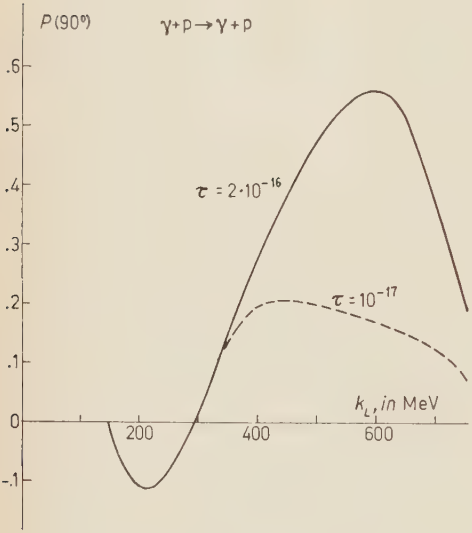


Fig. 3. – Calculated recoil proton polarization at 90° in the center of mass as a function of photon energy and for two values of the $\pi^0$ mean life.

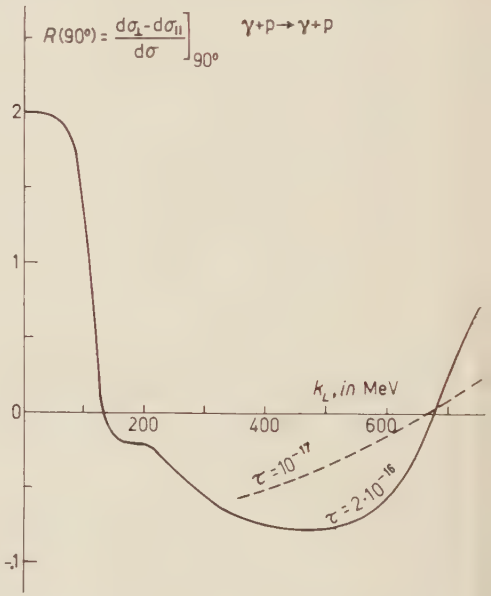


Fig. 4. – Calculated azimuthal asymmetry as a function of energy, for linearly polarized photons scattered through 90° in the center of mass.

included in the model can influence the polarization considerably. The negative polarization between the meson threshold and 300 MeV is due to the interference between the electric dipole virtual charged pion contribution and the magnetic dipole scattering through the 33 resonance. The large positive polarization centered around 600 MeV comes mostly from the interference between the first and second pion-nucleon resonances, in a way quite reminiscent of the recoil proton polarization in $\pi^0$ photoproduction ([27]). As in the photoproduction case, if our assignment of negative parity to the second resonance is in error, the polarization should be much smaller. Since the life-

([27]) J. J. SAKURAI: *Phys. Rev. Lett.*, **1**. 258 (1958).

time contribution to the recoil protons is unpolarized, the recoil polarization becomes considerably diluted if the lifetime is short, especially at high energies.

Fig. 4 shows the energy dependence of the quantity $R(k, \theta) = (d\sigma_{\perp} - d\sigma_{\parallel})/d\sigma$ at 90° in the center of mass; that is, the difference between the differential cross-sections for scattering perpendicular and parallel to the incident photon polarization plane, divided by their mean. Since for dipole transitions the angular distribution has to be $\sin^2\theta$, unless one is looking for contributions from higher multipoles, nothing new can be learned from the angular distribution in the scattering of polarized photons. Here again, because of the simplifying assumptions implicit in the model, one should not attach undue significance to the quantitative predictions of Fig. 4, particularly at high energy. The qualitative features, however, should be observable; that is, $R = 2$ where the Thompson scattering dominates, $R < 0$ where the 33 pion-nucleon resonance dominates, and $R > 0$ where the 13 second resonance dominates, and the second resonance has positive parity, excited through magnetic dipole absorption instead of electric dipole as assumed, then $R$ will be negative in the energy region dominated by the second resonance. The fact that the Low process is independent of incident photon polarization has a diluting effect on $R$, most easily observable around 500 MeV.

* * *

The author is deeply indebted to Prof. Marc Ross and Dr. Ronald F. Peierls for helpful criticisms and suggestions. He also wishes to thank Prof. Giorgio Cortellessa, Dr. Armando Reale, Dr. Paolo Salvadori Prof. John DeWire, and Prof. Raphael Littauer for informing him of their experimental results prior to publication, and Prof. Mario Ageno and the Istituto Superiore di Sanità for their gracious hospitality. Finally, a post-doctoral fellowship from the National Science Foundation is gratefully acknowledged.

## RIASSUNTO

I risultati sperimentali più recenti sullo scattering Compton sul protone a energie superiori a 300 MeV suggeriscono una estensione del calcolo fenomenologico. Il modello qui proposto prende in considerazione lo scattering Thompson e lo scattering dovuto al momento magnetico, lo scattering di dipolo elettrico dalla corrente pionica virtuale e il « diagramma di Low » che dipende dalla vita media del mesone $\pi^0$. La sezione d'urto differenziale così calcolata è in accordo qualitativo con i dati sperimentali. Sono state anche calcolate la polarizzazione del protone di rinculo e la dipendenza dalla polarizzazione dei fotoni incidenti. La sezione d'urto al disopra di 500 MeV, sia per fotoni polarizzati che non polarizzati, dipende sensibilmente dal valore scelto per la vita media del $\pi^0$.

# Cosmic Ray and Geomagnetic Disturbances from July 1957 to July 1958.

## Part III. – The Correlation with Solar Radio Bursts.

F. Bachelet, P. Balata, A. M. Conforto and G. Marini

*Istituto di Fisica dell'Università - Roma*
*Istituto Nazionale di Fisica Nucleare - Sezione di Roma*
*Commissione Italiana Anno Geofisico Internazionale - Roma*

(ricevuto il 17 Giugno 1961)

**Summary.** — A statistical approach is discussed to the comparison of the time correlation of solar radio bursts of spectral types II and IV with the geomagnetic and cosmic ray storms. The analysis is carried out for the events of the period July 1957-July 1958. The solar radio bursts best correlated to the geophysical perturbations under study turn out to be type IV radio events, although the correlation is far from being of the « one to one » character. The comparison with other authors' results makes it clear that a better definition of type IV emission is fundamental in this respect.

## 1. – Introduction.

The spectral analysis of the solar radio emission has recently provided a valuable means of investigating the perturbations occurring in the solar corona in connection with chromospheric eruptions.

Several authors [1-6] examined those solar radio bursts (spectral types II

[1] J. A. Roberts: *Austral. Journ. Phys.*, **12**, 327 (1959).
[2] D. J. McLean: *Austral. Journ. Phys.*, **12**, 404 (1959).
[3] A. Maxwell, A. R. Thompson and G. Garmire: *Planet. Space Sc.*, **1**, 325 (1959).
[4] Y. Kamiya and M. Wada: *Rep. Ion. Space Res. Jap.*, **13**, 105 (1959).
[5] Y. Hakura and T. Goh: *Journ. Radio Res. Lab.*, **6**, 635 (1959).
[6] P. Simon: *Ann. Astrophys.*, **23**, 102 (1960).

and IV) which display the closest association with optical flares (7) as a possible indication of the emission of the corpuscular clouds responsible for geomagnetic and cosmic ray storms: but the results seem partly contradictory and not completely conclusive.

In the present work we shall discuss one approach to a systematic study of the correlations of type II and IV radio bursts (RB) with magnetic storms (MS) and the cosmic ray storms having the character of a Forbush decrease (CRS). This analysis covers the period July 1957-July 1958 for which a careful selection of MS and CRS was available (8). Its distinctive features, with regard to the previous studies, are meant to be *a*) the use of as complete lists of solar events as possible, *b*) a comparative procedure for both types II and IV applied step by step, and *c*) the distribution analysis of the times required by the hypothetic corpuscular beams for their transit from the Sun to the Earth.

## 2. – Solar radio emission data.

For the radio events of type II (slow drift bursts) we used lists published by the Observatories of Harvard (Fort Davis, Texas, (100÷580) MHz) and Sydney (Dapto, Australia, (40÷240) MHz) in the *I.A.U. Quarterly Bulletin on Solar Activity*, to which we refer the reader. We do not know of any other systematic recordings of type II bursts, which, as generally accepted, can be unmistakably identified only from radio spectrograms.

In the period under study (July 1957-July 1958) the observation time covered by at least one of the two stations turned out to be of $\sim 59\%$ altogether. In counting these bursts we considered as a single event any pair of them (7 cases, out of a total of 67 events) which occurred within half an hour's distance from each other.

A more complex situation is found for the observation data relative to type IV bursts (broad-band, high-intensity continuum). In this case the lists presented by various authors are largely different in number of events because of the different characteristics taken as essential for their identification. On one hand, for example, there is a wide selection only based upon a criterion of energy flux as derived from single-frequency recordings at the decimetre and centimetre wavelengths (9); on the other hand, there is a narrow list obtained from spectrographic recordings at the metre lengths with the restriction that a type II burst be present right before type IV (2).

Nevertheless, the various authors generally seem to agree in considering

(7) See for example: G. Swarup, P. H. Stone and A. Maxwell: *Astrophys. Journ.*, **131**, 725 (1960).

(8) F. Bachelet, P. Balata, A. M. Conforto and G. Marini: *Nuovo Cimento*, **16**, 292 and 320 (1960) Part I and II.

(9) J. F. Denisse: private communication.

TABLE I.

| A) Solar events | | | | | | | B) Geophysical events | | | | |
|---|---|---|---|---|---|---|---|---|---|---|---|
| Date | Optical flare | | | Type IV radio burst | | | Date | Magnetic storm | | C.R. storm | |
| | Onset time U.T. | Position | Importance | Onset time U.T. | Importance | Observatories (*) | | Onset time U.T. | Type (**) | Onset time U.T. | Type (**) |
| 1957 | | | | | | | 1957 | | | | |
| June 28 | 0658 | 09 N; 27 E | 2 | 0707 | 3 | N | June 30 | 0528 | $\bar{A}$ | C6 ± 2 | I |
| July 3 | 0830 | 09 N; 42 W | 3 | 0832 | 3+ | N | July 5 | 0042 | $\bar{A}$ | | |
| July 16 | 1742 | 33 S; 29 W | 1+ | 1751 | 3+ | N H | July 19 | 1344 | $\bar{B}$ | 10 - 8 | III |
| July 21 | 1320 | 29 N; 11 E | 2 | 1336 | 3 | N** H | July 22 | 0419 | $\bar{B}$ | | |
| July 24 | 1816 | 24 S; 22 W | 3 | 1801 | 3+ | N H | July 27 | 1959 | $\bar{B}$ | | |
| Aug. 28 | 0913 | 30 S; 35 E | 3- | 0920 | 3+ | N | Aug. 29 | 1920 | $\bar{A}$ | 19 - 1 | I |
| Aug. 30 | 2215 | SID | | 2212 | 3+ | N* H | Aug. 31 | 1812 | $\bar{B}$ | | |
| Aug. 31 | 1257 | 25 N; 02 W | 3 | 1259 | 3+ | N H | Sept. 2 | 0314 | $\bar{A}$ | C5 ± 3 | X |
| Sept. 2 | 1257 | 11 N; 26 W | 2 | 1255 | 3+ | N | Sept. 4 | 1300 | $\bar{A}$ | | |
| Sept. 11 | 0243 | 11 N; 03 W | 3 | 0255 | 3 | N S | Sept. 13 | 0046 | $\bar{A}$ | 03 ± 6 | X |
| Sept. 12 | 1510 | 11 N; 18 W | 2 | 1515 | 3+ | N H | | | | | |
| Sept. 18 | 1818 | 21 N; 03 E | 3+ | 1808 | 3 | N* H | Sept. 21 | 1005 | $\bar{A}$ | 16 + 4 | I |
| Sept. 21 | 1330 | 11 N; 07 W | 3 | 1334 | 3 | N* H | Sept. 22 | 1345 | $\bar{A}$ | | |
| | | | | | | | Sept. 23 | 0235 | $\bar{A}$ | | |
| Sept. 26 | 1907 | 25 N; 15 E | 3 | 1916 | 3 | N** H | Sept. 29 | 0016 | $\bar{A}$ | 00 ± 4 | II |
| Oct. 20 | 1637 | 27 S; 38 W | 3+ | 1646 | 3+ | N H | Oct. 21 | 1530 | $\bar{A}$ | | |
| | | | | | | | Oct. 21 | 2241 | $\bar{B}$ | 23 ± 1 | I |
| Nov. 24 | 0848 | 14 S; 36 E | 3 | 0960 | 3+ | N | Nov. 25 | 0430 | $\bar{A}$ | | |
| | | | | | | | Nov. 26 | 0155 | $\bar{A}$ | 03 ± 2 | I |

| | | | | | | | | | | | |
|---|---|---|---|---|---|---|---|---|---|---|---|
| 1958 Feb. 9 | 2108 | 12 S; 14 W | 2+ | 2111 | 3+ | N H | 1958 Feb. 11 | 0125 | $\bar{A}$ | 02±1 | I |
| 3219 March 3 | 1005 | 17 S; 60 E | 3 | 1002 | 3+ | N* H | | | — | — | |
| March 23 | 0947 | 14 S; 80 E | 3+ | 1002 | 3+ | N | March 25 | 1540 | $\bar{B}$ | 17±1 | I |
| Apr. 2 | 1951 | 16 S; 23 E | 1+ | 1951 | 3 | N** H | — | — | — | — | — |
| Apr. 6 | 1939 | 16 S; 28 W | 1 | 1935 | 3 | N H | — | | — | | |
| June 4 | 2147 | 15 N; 58 W | 2 | 2140 | 3+ | N** H | | | | | |
| June 5 | 1656 | 21 S; 67 E | 2+ | 1703 | 3+ | N | June 7 | 0046 | $\bar{A}$ | 06±12 | X |
| June 6 | 0436 | 16 N; 78 W | 2 | 0433 | 3+ | N | June 8 | 1728 | $\bar{C}$ | — | — |
| July 7 | 0020 | 25 N; 08 W | 3+ | 0027 | 3+ | N H S | July 8 | 0748 | $\bar{A}$ | 07±5 | II |
| July 19 | 1905 | 23 N; 13 E | 2+ | 1905 | 3 | N* S | July 21 | 1637 | $\bar{B}$ | 17±2 | I |
| | | | | | | | July 22 | 1207 | $\bar{B}$ | — | — |
| July 29 | 0259 | 14 S; 44 W | 3 | 0303 | 3+ | N S | July 31 | 1529 | $\bar{B}$ | | |
| July 29 | 0458 | 14 S; 38 W | 1 | 0520 | 3 | N | Aug. 1 | | | 02±10 | X |

Case of « probable » type IV

| | | | | | | | | | | | |
|---|---|---|---|---|---|---|---|---|---|---|---|
| 1957 June 28 | 1223 | 12 N; 21 E | 2 | 1222 | 3 | N* | 1957 (June 30 | 0528 | $\bar{A}$ | 06±2 | I) |
| Aug. 31 | 0544 | 13 N; 03 E | 1+ | 0550 | 3 | N* | (Aug. 31 | 1812 | $\bar{B}$ | — | —) |
| | | | | | | | (Sept. 2 | 0314 | $\bar{A}$ | 05±3 | X) |
| Nov. 5 | 1205 | 24 S; 53 W | 2 | 1205 | 3 | N* | Nov. 6 | 1821 | $\bar{A}$ | — | — |
| | | | | | | | Nov. 8 | 0730 | $\bar{C}$ | — | — |
| Dec. 19 | 0757 | 20 N; 14 E | 2+ | 0803 | $\geqslant 3-$ | N* | | — | — | — | |
| 1958 July 11 | 0740 | 25 S; 29 E | 2+ | 0752 | 3 | N* | 1958 July 13 | 2208 | $\bar{B}$ | — | |

(*) N, N*, N** = « certain », « uncertain », « different from » type IV according to Nera; H = type IV according to Harvard; S = type IV according to Sydney.

(**) See ref. (8), part I and II.

as a distinctive feature of type IV radio bursts the very large bandwidth of their spectra and their smooth appearence, differently from the « noise storm » continuum, which would only occur at the metre wavelengths and is accompanied by short and narrow bursts of type I.

In accordance with all that, it seemed here justified to follow the viewpoint of FOKKER ([10]), *i.e.* that a radio burst be taken as type IV only if it consists of a steady and very strong enhancement of the solar radio emission ranging from the metre to centimetre wavelengths. For the requirement of the presence and intensity at widely separated wavelengths it was needed to rely upon single-frequency recordings for the period under study. In particular we used the data collected by the Nera Observatory (IRA Section of the Netherland PTT) ([11]). This institution, in co-operation with other world-wide stations, has established a 24-hour continuous patrol of solar radio emission at 200, 545 and 3 000 MHz ([12]); this enabled them to prepare an IGY catalogue of all flare-associated radio bursts, with the assignment of a radio importance index which takes into account the total energy flux of a burst at each of the three frequencies. On the other hand for the formal identification we thought it useful to consider both the single-frequency data and, even more, the spectrographic data as given by the Harvard ([13]) and Sydney ([2]) Observatories.

According to this criterion, we took from the Nera IGY catalogue all the bursts of the highest radio importance (*i.e.* —3—) and from them we selected only those for which a definite assignment as type IV was given by at least one of the Observatories of Harvard, Sydney, and Nera.

The list of the selected type IV bursts is reported in Section A of Table I along with: *a*) their onset time (for convenience taken at 500 MHz); *b*) their radio importance according to the Nera IGY catalogue; and *c*) a symbol specifying the judgment of quality given by Nera or the presence of the radio burst in the type IV lists given by Harvard and Sydney. In the same Section A of the Table I the associated optical flares are reported, along with their main characteristics.

The five radio bursts reported at the end of the list should be considered, according to our selection rule, as probable, but still dubious type IV bursts. They were included in the list only for the sake of completeness, but they were not taken into account in any of the subsequent analyses; however we can anticipate, once and for all, that all the preliminary analyses in which such « probable » events were included did give practically the same results.

([10]) A. D. FOKKER: *Information Bullettin of Solar Radio Observatories in Europe*, n. 5 (Nov., 1960), p. 5.

([11]) A. D. FOKKER: private communication.

([12]) L. D. DE FEITER, A. D. FOKKER, H. P. T. VAN LOHUIZEN and J. ROOSEN: *Planet. Space Sc.*, **2**, 223 (1960).

([13]) A. MAXWELL: private communication.

### 3. – Statistical analysis.

To compare the different degree of association of the spectral type II and IV radio bursts with the geophysical perturbations under study, the superposed epoch method was firstly used, assuming as zero time the onset of the solar radio event.

The daily planetary index $A_p$ was chosen as a measure of geomagnetic activity and the pressure-corrected nucleonic intensity recorded in Rome was used to examine the behaviour of cosmic rays.

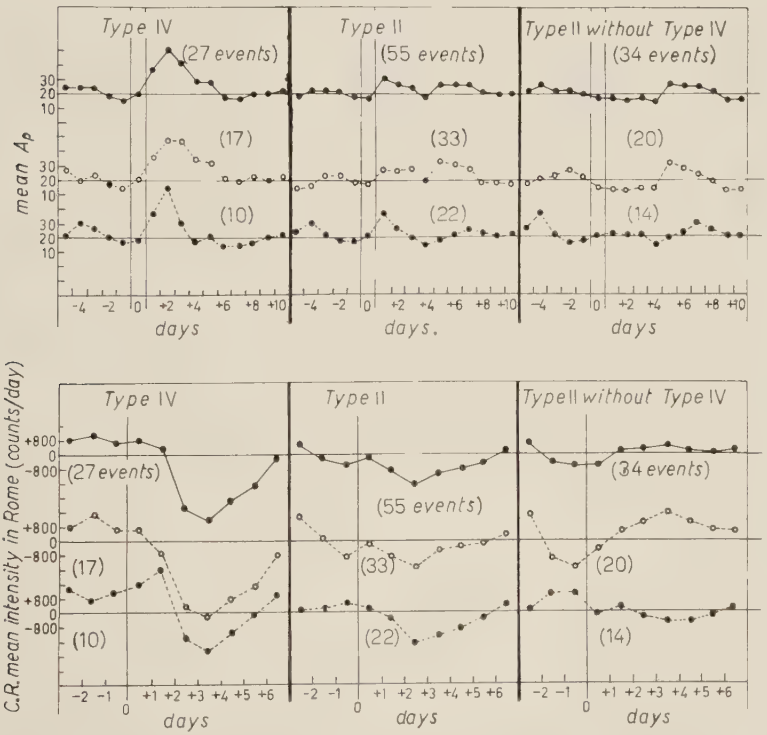


Fig. 1. – Superposed epoch diagrams of geomagnetic planetary index $A_p$ and of cosmic ray neutron intensity in Rome, using the solar radio bursts of type IV and II as epochs. For $A_p$ values, *zero interval* is the U.T. day in which the burst starts. For cosmic ray intensity, *zero time* is the beginning of the U.T. bihourly interval in which the onset time of the burst occurs, and zero level is the daily mean counting rate, *i.e.* ~376 000 counts per day.

●——— Events of the whole period July 1957-July 1958;

○– – – First group events, of July-December 1957;

●– – – Second group events, of January-July 1958.

It should be remarked that in this particular study we considered as a single event (for both types II and IV), each group of bursts which happened to occur at a time distance $< 24$ hours; in such cases the zero time is fictitious, corresponding to the mean of the individual onset times. It should be added, however, that exactly the same results were obtained in the parallel analyses, here not reported, where all the solar radio events of one type were instead taken individually.

Fig. 1 shows the superposed epoch diagrams of the $A_p$ index and of the cosmic ray intensity relative to the following groups of solar events:

1) All the selected type IV RB (*).

2) All the available type II RB.

3) Those particular type II RB, which did not happen to occur within $\pm 48$ hours of a type IV (« type II without type IV »).

The graphs relative to type IV bursts display a well defined geophysical

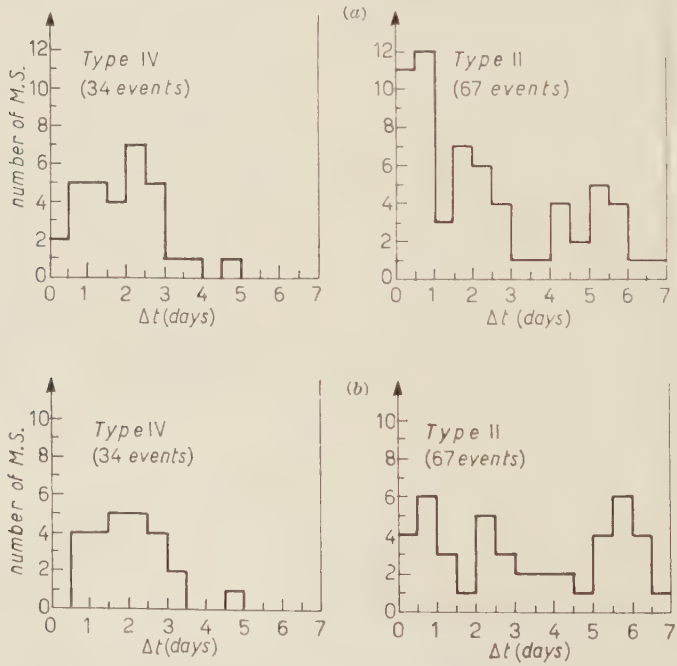


Fig. 2. – The distribution of the *first* magnetic storm following a solar radio burst. In part (*a*) the same MS may have been counted up several times, corresponding to different radio bursts; in part (*b*) each MS is computed only once.

(*) The two first type IV bursts of Table I were omitted in this analysis because of the incompleteness of cosmic ray data in Rome in the corresponding period.

effect within the first 3 days following the solar event: *i.e.* enhancement of $A_p$ values and sharp variation in cosmic ray intensity with the character of a typical Forbush decrease. Similar effects are hardly perceptible in the graphs relative to type II, and completely disappear in those relative to « type II without type IV » bursts.

All these features are confirmed if each group of solar events is broken into two subgroups pertaining to the first and second part of the considered interval of time, *i.e.* relative to two periods, which were considerably different as to the intensity of solar activity.

It seems consequential to interpret these results in the sense that type IV bursts are the solar radio events far best correlated with geomagnetic and cosmic ray perturbations. As for type II RB, instead, it should be inferred that all geophysical effects, if any, apparently connected to them in a minority of cases, are nothing but accidental coincidences.

Another argument in favour of this interpretation is given by the study of the time distribution of the geophysical events with respect to both types of bursts. This study was carried out only for the MS (ref. [8]), because for them the available statistics are larger than for the CRS; on the other hand the latter are generally time-associated with the former.

In Fig. 2 such a time distribution is shown for the MS respectively following type IV and II bursts within a time interval ($\Delta t_{max}$) of 7 days. For each solar event what is reported in part *a*) is the very first MS which happens to follow the burst itself, and in part *b*) the first MS which is found to follow it after the exclusion of those MS already taken into account for a previous solar event of the same type. In the first case, a spurious repetition of geomagnetic events may sometimes take place; while in the second case it may obviously occur that the results are not independent from the $\Delta t_{max}$ adopted.

By both methods, however, the delay times of the MS with respect to type IV bursts turn out to be confined within the first 4 days; *i.e.* they correspond to transit times in agreement with the values generally accepted for the auroral corpuscular streams. On the contrary the delay times relative to type II radio bursts do not show any particular concentration so that again indication is obtained that any connection of the geophysical events with this type of bursts is probably a casual one, only due to their high rate of occurrence.

## 4. – Associations of individual geophysical and solar events.

A direct time association of the individual solar radio bursts to the geophysical events under consideration was also attempted, with the understanding that by this procedure all the events would contribute with equal weight to

the general degree of correlation; while in the former case of the Chree analysis, maximum contribution to the resulting average effect might possibly derive from the fewest large events, to the disfavour of the majority of those less eminent.

On suggestion of the time distributions as obtained in Fig. 2 for type IV RB, a delay $\Delta t$ such that

$$\tfrac{1}{2} \text{ day} \leqslant \Delta t \leqslant 3\tfrac{1}{2} \text{ days},$$

was taken as the criterion for associating in time a MS or a CRS to a solar radio event in general.

The complete list, classification and characteristics of those geophysical events may be found in ref. ([8]) (*).

In Section B of Table I, along with type IV RB, the geophysical events satisfying the above mentioned criterion are also reported. The counterpart for type II RB is not included for the sake of brevity.

The percentages of MS and CRS respectively associated to either types of solar radio events can be then obtained by the rule that a particular geophysical event may be related to one radio burst only. In particular as concerns the MS, we limit ourselves to taking into consideration only those classified as types $\bar{A}$ and $\bar{B}$, *i.e.* the MS which are distinguished for displaying a SSC and being typical of the maximum solar activity as well as being indicative of the arrival on the Earth of a plasma beam emitted from active regions at the Sun.

The figures we get for the association cases are thus as follows:

Out of 34 type IV RB: 22 with MS (65%), 16 with CRS (47%);
Out of 67 type II RB: 22 with MS (33%), 13 with CRS (19%).

It seems then confirmed, from this viewpoint too, that the geophysical correlation is definitely higher for type IV than for type II bursts.

It should be remarked in this connection that, while associating solar radio to geophysical events one by one individually might require in some cases a rather subjective choice, the above reported figures are largely free from a bias of that kind.

When looking at the situation the other way round, *i.e.* when starting from the totals of MS (46) and CRS (25), the association cases with type IV are found to be 48% and 64% respectively; while a comparison with type II is not possible because of the limited coverage (about 59%) of observation time available for these RB. On the other hand, they seem to occur at such

(*) It should be remarked that in this reference the CRS of August 1, 1958 did not appear.

a high rate that a straight computation as above of the association percentages would not make sense in this case, as the accidental « coincidences » should be accounted for.

Restricting ourselves to type IV bursts only, a comparison with the data of different authors was also assayed:

1) In the case of a list reported by DENISSE (9) the definition of type IV seems rather dishomogeneous with respect to the present one and the total number of radio bursts is larger by about a factor 2, in the same period of time. So that relating these solar events to the same CRS and MS of ref. (8) leads to practically the same number of association cases, *i.e.* to much lower percentages.

2) The definition of type IV seems instead quite homogeneous and the number of radio bursts slightly lower, in the case of a list reported by HAKURA *et al.* (5). When correlating these solar events either with the authors' classification of geomagnetic storms or with the MS and CRS of ref. (8) again, the resulting percentages of association cases are this time comparable to ours.

3) In consideration of the extremely high correlation found by MCLEAN (2), for his own classification, between type IV bursts and geomagnetic storms, it was interesting for us to apply his criterion of definition of type IV to our lists. Thus we also selected those particular type IV events which were immediately preceded by a type II and again found high correlation percentages. Nevertheless, we wonder how significant these results can be considered, when taking into account that the available statistics are very low, in neither case including more than ten events.

4) Finally in the case of a list reported by KAMIYA *et al.* (4) a direct comparison seems quite arduous because of the ambiguity of all the criteria of classification and association used therein; so that actually any conclusion seems rather artificial and questionable.

## 5. – Concluding remarks.

From all that precedes there seems to have emerged a definite indication that the considered geophysical association is prevalent with type IV against type II RB, but that even with type IV such a correlation depends considerably on the definition of the radio burst itself and in no case turns out to be of « one to one » character.

In other words it appears that, in order to identify those solar flares best associated with geomagnetic and cosmic ray storms, the presence of type IV radio emission is an important but not a determinant factor, just as it had

already been found to be by many authors for the high optical importance of the flare itself. In this respect it seems essential to investigate more carefully the very character and definition of this kind of radio emission.

In lack of a complete and biunivocal correlation it would seem reasonable to also take into account the influence of solar, interplanetary and terrestrial conditions which might influence either the radio-wave or corpuscular beams simultaneously emitted by the Sun in such a way that in some cases only one of them is detectable at the Earth. Actually when looking at possible parameters indicative of these conditions, neither the heliographic longitude of the associated flare, nor the Earth's position on the ecliptic nor the presence of a previously emitted solar cloud was found, at least within our limited statistics, to play an essential role in the association.

It seem then necessary to conclude that the question is still open not only to which physical processes are to be implied, but also to which phenomenological aspects of the solar events are determinant to forecast the arrival on the Earth of ionized matter capable of inducing geomagnetic storms and the Forbush type decreases of cosmic ray intensity.

* * *

We are very grateful to Prof. J. F. DENISSE, Dr. A. MAXWELL and Dr. D. J. MCLEAN for their lists of solar radio events and useful comments. We are particularly indebted to Dr. A. D. FOKKER for the large amount of material he has put at our disposal and for his stimulating discussion and encouragement.

## RIASSUNTO

Si riporta un'analisi statistica della correlazione temporale fra i « bursts » di radioemissione solare meglio associati ai brillamenti e le tempeste geomagnetiche e di raggi cosmici nel periodo luglio 1957-luglio 1958. Nel corso di tutta l'analisi si fa il confronto fra i « bursts » di tipo spettrale II e IV. Gli eventi radiosolari meglio correlati con gli eventi geofisici studiati risultano i tipi IV, ma anche in questo caso la correlazione è ben lontana da una corrispondenza biunivoca. Il confronto coi risultati ottenuti da altri autori mette in evidenza che una più approfondita indagine e una migliore definizione della radioemissione di tipo IV sarebbe essenziale per ottenere conclusioni definitive a questo riguardo.

IL NUOVO CIMENTO Vol. XXI, N. 4 16 Agosto 1961

# On the Triple Angular Correlation.

V. De Sabbata

*Istituto Nazionale di Fisica Nucleare - Sezione di Bologna*

(ricevuto il 28 Giugno 1961)

**Summary.** - A general formulation of triple angular correlations is given in order to examine the β-γ-γ correlation in particular and its implications on the symmetry properties of the weak and strong interactions. The invariance for time reversal is especially considered.

## 1. – Introduction.

We have analysed, in some details, the implications obtained by studying the triple angular correlations and particularly the β-γ-γ cascade for not oriented nuclei, and we have given great attention to the possibility of putting in evidence a probable non-invariance for time reversal in the weak and strong interactions. In fact, the study of the angular correlation of three radiations in coincidence, could be looked at as a source of more information than the measurements of double correlation.

The lack of a convenient tabulation of the parameters entering the correlation, has, perhaps, limited the application of this problem.

The β-γ-γ process is a little more complicated than the similar problem of electromagnetic radiations, as it happens in the case of γ-γ-γ correlation, because the interaction constants are not known and there is a mixing of various multipoles deriving from different interactions and also because it is necessary to deal with the additional detailed relationship between two radiations, *i.e.* the combined β-particle and neutrino field or better, the antineutrino.

The Coulomb interaction must also be taken into account, and that, as

is well known, makes things more complicated for what concerns the symmetry properties [1].

In fact, if there is an interaction in the final states, as is the case in the Coulomb interactions for the electrons in β-decay, the terms proving the time reversal change.

The effect is that in the terms which, in absence of interaction, would be tests for time reversal, there are corrections present also when the time reversal is not violated, whereas the terms which in absence of interaction are not tests for the time reversal, present modifications only if there is no invariance for time reversal. However, in β-decay, such terms are of the order of $Z\alpha$, where $Z$ is the atomic number of the emitting nucleus and $\alpha$ the fine structure constant.

Several studies and formulations have been done [2-15] and a review of β-γ correlation is given by ROSENFELD [11] and by DEVONS and GOLDFARB [12]. In this work Rosenfeld's notations [11] are mostly used.

First of all, we deal with the formulas of the angular correlations and give them in such a general form to comprehend the orientation of the nucleus and the polarization of the emitted radiations. Afterwards we consider them in different specified cases, and put them in a convenient and suitable form for calculations relative to possible experiments and tests on the time reversal invariance.

## 2. – The general formalism of the correlation function.

Let us consider from a general point of view, the β-decay from oriented nuclei, followed by γ-radiations. The neutrino or the antineutrino in the case of $\beta^-$-decay will be considered as a particle emitted in a successive step, although actually this separation does not occur.

(1) See for istance: T. D. LEE and C. N. YANG: *Elementary Particles and weak Interactions* (Brookhaven, 1957).
(2) M. MORITA: *Prog. Theor. Phys.*, **14**, 127 (1955).
(3) M. MORITA: *Progr. Theor. Phys.*, **15**, 445 (1956).
(4) K. ALDER, B. STECH and A. WINTHER: *Phys. Rev.*, **107**, 728 (1957).
(5) R. B. CURTIS and R. R. LEWIS: *Phys. Rev.*, **107**, 1381 (1957).
(6) M. MORITA and R. S. MORITA: *Phys. Rev.*, **107**, 1316 (1957).
(7) M. MORITA: *Phys. Rev.*, **107**, 1729 (1957).
(8) M. MORITA and R. S. MORITA: *Phys. Rev.*, **110**, 461 (1958).
(9) B. A. JACOBSON and E. M. HENLEY: *Phys. Rev.*, **113**, 225, 234 (1959).
(10) P. STICHEL: *Zeits. f. Phys.*, **150**, 264 (1958).
(11) L. ROSENFELD: *Oriented Nuclei* (Copenhagen, 1959).
(12) S. DEVONS and L. J. B. GOLDFARB: *Handb. d. Phys.*, **42**, 362 (1957).

We shall consider therefore the intermediate states between the $\beta$ and neutrino emission, as states referring to virtual transitions.

The fact that we regard the electron and the neutrino as two particles successively emitted, does not imply any modification because the way the correlation is obtained is only a question of angular momentum conservation, holding for both the virtual and the actual transitions.

As is well known, the principal feature of the angular correlation function is the factorization property that holds also for mixed radiations, each separated link corresponding to various radiations.

Let $\boldsymbol{\eta}$ be the direction of orientation of the nucleus, $\boldsymbol{p}$ the direction of emission of the electron, $\boldsymbol{q}$ of the neutrino, $\boldsymbol{r}$ of the first $\gamma$ and $\boldsymbol{s}$ of the second $\gamma$; we have:

$$(1)\qquad W(\omega_{\eta p}, \omega_{pq}, \omega_{qr}, \omega_{rs}) = \sum_{\substack{kk_1k_2k_4 \\ k_3k_6k_5}} \sum_{x_1x_4x_6x_5} f_k\, q^{kk_1k_2k_4k_3k_6k_5}_{x_1x_4x_6x_5}\, \mathcal{Q}^{kk_1k_2k_4k_3k_6k_5}_{0x_1x_4x_6x_5}(\omega_{\eta p}, \omega_{pq}, \omega_{qr}, \omega_{rs})\,.$$

$f_k$ is the orientation factor as given for instance by ROSENFELD ([11]); $q^{kk_1k_2k_4k_3k_6k_5}_{x_1x_4x_6x_5}$ is the emission factor that, as is well known, can be factorized for the various successive emissions as:

$$(2)\qquad q^{kk_1k_2k_4k_3k_6k_5}_{x_1x_4x_6x_5} =$$

$$= \sum_{J_1J_1'} \sum_{ll'\lambda\lambda'} \hat{J}\hat{J}_1'\hat{l}\hat{k}\hat{k}_1\hat{k}_2 \quad X\begin{pmatrix} l & J_1 & J \\ l' & J_1' & J \\ k_1 & k_2 & k \end{pmatrix} (-)^{l'-\lambda'}\hat{l}'(ll'\lambda - \lambda' \mid k_1x_1)\alpha^{(J_1)}_{l\lambda}\alpha^{(J_1')*}_{l'\lambda'}\cdot$$

$$\cdot \sum_{J_2J_2'} \sum_{l_1l_1'\lambda_1\lambda_1'} \hat{J}_1\hat{J}_2'\hat{l}_1\hat{k}_2\hat{k}_4\hat{k}_2 X\begin{pmatrix} l_1 & J_2 & J_1 \\ l_1' & J_2' & J_1' \\ k_4 & k_3 & k_2 \end{pmatrix} (-)^{l_1'-\lambda_1'}\hat{l}_1'(l_1l_1'\lambda_1 - \lambda_1' \mid k_4x_4)\beta^{(J_1)}_{l_1\lambda_1}\beta^{(J_1')*}_{l_1'\lambda_1'}\cdot$$

$$\cdot \sum_{J_3J_3'} \sum_{l_2l_2'\lambda_2\lambda_2'} \hat{J}_2\hat{J}_3'\hat{l}_2\hat{k}_3\hat{k}_6\hat{k}_5 X\begin{pmatrix} l_2 & J_3 & J_2 \\ l_2' & J_3' & J_2' \\ k_6 & k_5 & k_2 \end{pmatrix} (-)^{l_2'-\lambda_2'}\hat{l}_2'(l_2l_2'\lambda_2 - \lambda_2' \mid k_6x_6)\gamma^{(J_2)}_{l_2\lambda_2}\gamma^{(J_2')*}_{l_2'\lambda_2'}\cdot$$

$$\cdot \sum_{l_3l_3'\lambda_3\lambda_3'} \hat{J}_3\hat{l}_3(-)^{J_3'+J_5+k_5+l_5}\ \overline{W}\begin{pmatrix} l_3 & k_5 & l_3' \\ J_3 & J_5 & J_3 \end{pmatrix} (-)^{l_3'-\lambda_3'}\hat{l}_3'(l_3l_3'\lambda_3 - \lambda_3' \mid k_5x_5)\gamma^{(J_3)}_{l_3\lambda_3}\gamma^{(J_3')*}_{l_3'\lambda_3'}\,,$$

where the first line is the emitting factor of the first particle with angular momentum $\boldsymbol{l}$; the second line refers to the second particle with angular momentum $\boldsymbol{l}_1$; the third one to the third particle with angular momentum $\boldsymbol{l}_2$ and the last one to the last emitted particle with angular momentum $\boldsymbol{l}_3$.

$\alpha_{l\lambda}$, $\beta_{l_1\lambda_1}$, $\gamma_{l_2\lambda_2}$, $\gamma_{l_3\lambda_3}$, are coefficients that depend on the interaction and that

characterize the state of polarization of the emitted particle by their dependence on the projection $\lambda$ of $l$ on the direction of emission. The symbol $\hat{a}$ is used for $(2a+1)^{\frac{1}{2}}$, the $(abcde|ef)$ are the usual Clebsh-Gordan (C.G.) coefficients, the $\overline{W}$ are related to the usual Racah coefficients by $W(abcd|ef)=(-)^{a+b+c+d}\overline{W}\begin{pmatrix} a & b & e \\ d & c & f \end{pmatrix}$ more convenient for the symmetry properties (*).

The $X$ are the usual Fano coefficients. $\boldsymbol{J}$ and $\boldsymbol{J}_5$ are the spins of the initial and final nucleus and the other $\boldsymbol{J}$ are the spins of the intermediate states.

The $\boldsymbol{k}$ are obviously the resultant of the vectors $\boldsymbol{l}$ and $\boldsymbol{l}'$, *i.e.* the vectors that satisfy the triangular relation $\boldsymbol{l}+\boldsymbol{l}'-\boldsymbol{k}=0$. At last:

$$(3)\qquad \mathscr{D}^{k k_1 k_2 k_3 k_4 k_5}_{0 x_1 x_4 x_6 x_5}(\omega_{\eta p}, \omega_{pq}, \omega_{qr}, \omega_{rs}) = \sum_{x x_2' x_2 x_3 x_3' x_5'} D^{k}_{0x}(\omega_{\eta p}) \cdot$$

$$\cdot (-)^{k-x}\,\overline{V}\begin{pmatrix} k & k_1 & k_2 \\ -x & x_1 & x_2' \end{pmatrix} \cdot D^{k_2}_{x_2' x_2}(\omega_{1q})(-)^{k_2-x_2}\,\overline{V}\begin{pmatrix} k_2 & k_4 & k_3 \\ -x_2 & x_4 & x_3' \end{pmatrix} \cdot$$

$$\cdot D^{k_3}_{x_3' x_3}(\omega_{qr})(-)^{k_3-x_3}\,\overline{V}\begin{pmatrix} k_3 & k_6 & k_5 \\ -x_3 & x_6 & x_5' \end{pmatrix} D^{k_5}_{x_5' x_5}(\omega_{rs})\,,$$

where the $\overline{V}$ symbols are related to the C.G. coefficients by

$$\overline{V}\begin{pmatrix} a & b & c \\ \alpha & \beta & \gamma \end{pmatrix} = \frac{1}{\hat{c}}\,(-)^{2b+c+\gamma}(ab\alpha\beta\,|\,c-\gamma)\,,$$

and are more useful for the symmetry properties (**).

The $D^{a}_{\alpha_1\alpha_2}(\omega_{pq})$ are the rotation matrices that satisfy the addition theorem and have the group properties, as given, for instance, by ROSENFELD [11].

In the case of $\beta^-$-decay we may regard the first particle emitted as the electron and the second one as the antineutrino; the intermediate states of angular momentum $\boldsymbol{J}_1$, $\boldsymbol{J}_1'$, refer to virtual transitions. The formula is still valid because, as already pointed out, the factorization is based on the conservation of angular momentum and it does not matter whether it is a virtual or actual transition.

The $\omega_{ab}$ are the Eulerian angles which define the mutual orientation of the two polar systems of axes $\boldsymbol{a}$ and $\boldsymbol{b}$.

If the neutrino is not observed, we must average over the direction of emission of the neutrino and, thus, we have for the emission factor (after some

(*) The symbol $\overline{W}$ is in fact invariant for any permutation of the columns and for the simultaneous exchange of the upper and lower letter in two columns.

(**) In the $\overline{V}$ symbols the columns may be arbitrarily permuted; for each odd permutation it occurs to multiply by $(-)^{a+b+c}$ and also a simultaneous exchange of sign of $\alpha, \beta, \gamma$ leads to the value of $\overline{V}$ multiplied by $(-)^{a+b+c}$.

rearrangement of the indices):

$$(4)\qquad q^{kk_1k_2k_3k_4}_{x_1x_3x_4} =$$

$$= \sum_{J_1J_1'} \sum_{ll'\lambda\lambda'} \sum_{l_1\lambda_1'} A^{(J_1)}_{ll_1\lambda\lambda_1} A^{(J_1')*}_{l'l_1\lambda'\lambda_1} (-)^{l'-\lambda'} \hat{l}'(ll'\lambda - \lambda' \; k_1x_1) \hat{J}\hat{J}_1'\hat{l}\hat{k}\hat{k}_1\hat{k}_2 X \begin{pmatrix} l & J_1 & J \\ l' & J_1' & J \\ k_1 & k_2 & k \end{pmatrix} \cdot$$

$$\cdot \hat{J}_1'\hat{J}_2(-)^{J_1+J_3+l_1+k_2} \overline{W} \begin{pmatrix} J_2 & J_1 & l_1 \\ J_1' & J_2 & k_2 \end{pmatrix} \cdot$$

$$\cdot \sum_{l_2l_2'\lambda_2\lambda_2'} \hat{J}_2\hat{J}_3\hat{l}_2\hat{k}_2\hat{k}_3\hat{k}_4 X \begin{pmatrix} l_2 & J_3 & J_2 \\ l_1' & J_3 & J_2 \\ k_3 & k_4 & k_2 \end{pmatrix} (-)^{l_2'-\lambda_2'} \hat{l}_2'(l_2l_2'\lambda_2 - \lambda_2' \,|\, k_3x_3)\gamma_{l_2\lambda_2}\gamma^*_{l_2'\lambda_2'} \cdot$$

$$\cdot \sum_{l_3l_3'\lambda_3\lambda_3'} \hat{J}_3\hat{l}_3(-)^{J_3+J_5+k_4+l_5} \overline{W} \begin{pmatrix} l_3 & k_4 & l_3' \\ J_3 & J_5 & J_3 \end{pmatrix} (-)^{l_3'-\lambda_3'} \hat{l}_3'(l_3l_3'\lambda_3 - \lambda_3' \,|\, k_4x_4)\lambda_{l_3\lambda_3}\lambda^*_{l_3'\lambda_3'} \,,$$

where there is no summation $\sum_{J_2J_2'}$, and $\sum_{J_3J_3'}$ since the states $J_2$ and $J_3$ are not virtual but actually reached by the nucleus, and the $J_2$, $J_2'$ on one part and $J_3$, $J_3'$ on the other take the same single value; furthermore, we have conglobed in the $A^{(J)}_{ll_1\lambda\lambda_1}$ coefficients, the interaction factors $\alpha_{l\lambda}$ and $\beta_{l_1\lambda_1}$.

We have also for the $\mathscr{D}$ function:

$$(5)\qquad \mathscr{D}^{kk_1k_2k_3k_4}_{0x_1x_3x_4}(\omega_{\eta p}, \omega_{xr}, \omega_{rs}) = \sum_{xx_2x_3x_4'} D^k_{0x}(\omega_{\eta p})(-)^{k-x} \overline{V} \begin{pmatrix} k & k_1 & k_2 \\ -x & x_1 & x_2' \end{pmatrix} \cdot$$

$$\cdot D^{k_2}_{x_2'x_3}(\omega_{xr})(-)^{k_2-x_3} \overline{V} \begin{pmatrix} k_2 & k_3 & k_4 \\ -x_2 & x_3 & x_4' \end{pmatrix} D^{k_4}_{x_4'x_4}(\omega_{rs}) \,,$$

If in addition the nuclei are not oriented, we must put $k = 0$; then the orientation factor may be normalized to unity ($f_0 = 1$). In this case, taking into account the properties of C.G., Racah and $X$ coefficients, we have for the emission factor (rearranging the indices from $k_3$, $k_4$ to $k_2$, $k_3$):

$$(6)\qquad q^{k_1k_2k_3}_{x_1x_2x_3} = \sum_{J_1J_1'} \sum_{ll'\lambda\lambda'} \sum_{l_1\lambda_1} A^{(J_1)}_{ll_1\lambda\lambda_1} A^{(J_1')*}_{l'l_1\lambda'\lambda_1} (-)^{l'-\lambda'} \hat{l}'(ll'\lambda - \lambda' \,|\, k_1x_1) \cdot$$

$$\cdot \hat{J}_1'\hat{l}(-)^{k_1}(-)^{2J_1+J+J_2+l'+l_1} \hat{J}_1\hat{J}_2 \overline{W} \begin{pmatrix} l & J_1 & J \\ J_1' & l' & k_1 \end{pmatrix} \overline{W} \begin{pmatrix} J_2 & J_1 & l_1 \\ J_1' & J_2 & k_1 \end{pmatrix} \cdot$$

$$\cdot \sum_{l_2l_2'\lambda_2\lambda_2'} \hat{J}_2\hat{J}_3\hat{l}_2\hat{k}_1\hat{k}_2\hat{k}_3 X \begin{pmatrix} l_2 & J_3 & J_2 \\ l_2' & J_3 & J_2 \\ k_2 & k_3 & k_1 \end{pmatrix} (-)^{l_2'-\lambda_2'} \hat{l}_2'(l_2l_2'\lambda_2 - \lambda_2' \,|\, k_2x_2)\gamma_{l_2\lambda_2}\gamma^*_{l_2'\lambda_2'} \cdot$$

$$\cdot \sum_{l_3l_3'\lambda_3\lambda_3'} \hat{J}_3\hat{l}_3(-)^{J_3+J_5+l_3+k_3} \overline{W} \begin{pmatrix} l_3 & k_3 & l_3' \\ J_3 & J_5 & J_3 \end{pmatrix} (-)^{l_3'-\lambda_3'} \hat{l}_3'(l_3l_3'\lambda_3 - \lambda_3' \,|\, k_3x_3)\gamma_{l_3\lambda_3}\gamma^*_{l_3'\lambda_3'} \,,$$

and for the angular function

$$\mathscr{D}^{k_1k_2k_3}_{x_1x_2x_3}(\omega_{qr},\omega_{rs}) = \sum_{x_1'x_3'} D^{k_1}_{x_1x_1'}(\omega_{qr})(-)^{k_1-x_1'}\overline{V}\begin{pmatrix} k_1 & k_2 & k_3 \\ -x_1' & x_2 & x_3' \end{pmatrix} D^{k_3}_{x_3'x_3}(\omega_{rs}) \,. \tag{7}$$

Now we note that for processes in which the state of polarization of the electron is not determined, we have $\lambda' = \lambda$ and $x_1 = 0$. If furthermore the radiation is circularly polarized or unpolarized we still have $\lambda_2 = \lambda_2' = \lambda_3 = \lambda_3' = 1$ and $x_2 = x_3 = 0$. In the case of definite circular polarization and if we deal with pure radiation, there will be, in the « link », factors of C.G. such as $(l\ l\ 1\ -1\ |\ k\ 0)$ whereas for opposed polarization we have the same expression multiplied by $(-)^k$. If the radiation is unpolarized, there will be only even powers of $k$, as on the other hand is well known.

To have for instance some odd $k_2$, it is necessary to select $\gamma$-rays of defined circular polarization, in the experiment.

## 3. – Allowed transitions.

For allowed transitions the values of $k_1$ are restricted to be 0 or 1.

The evaluation of the partial amplitudes $A^{(J_1)}_{l_1'\lambda_1'l_1\lambda_1}$ and the $\sum$ on $J_1$, $J_1'$ gives the following result, apart from some constant factors (see Appendix):

$$\varphi_{k_1k_2k_3} = \sum_{rr'} a^{k_2}_{rr'}\Omega^{k_1k_2k_3}_{rr'} \,, \tag{8}$$

where $a^{k_1}_{rr'}$ are related to the coefficients for the Fermi and Gamow-Teller interactions and

$$\Omega^{k_1k_2k_3}_{rr'} = \omega^{k_1}_{rr'}\Phi^{J_2}_{l_2}(k_2)\,\Phi^{J_3}_{l_3}(k_3) \,, \tag{9}$$

with

$$\omega^{k_1}_{rr'} = (-)^{J+J_2+k_1+r+r'+1}\overline{W}\begin{pmatrix} r & k_1 & r' \\ l & l & l \end{pmatrix}\overline{W}\begin{pmatrix} r' & k_1 & r \\ J_2 & J & J_2 \end{pmatrix}\hat{l}\,\hat{J}_2\,\hat{r}\,\hat{r}' \,. \tag{10}$$

Then the angular correlation, apart from some constant factors, is:

$$W(\omega_{qr},\omega_{rs}) = \sum_{k_1k_2k_3}\varphi_{k_1k_2k_3}\mathscr{D}^{k_1k_2k_3}_{000}(\omega_{qr},\omega_{rs}) \,, \tag{11}$$

where

$$(12)\qquad \varphi_{k_1k_2k_3} = |M_F|^2\left\{|C_V|^2+|C_V'|^2+|C_S|^2+|C_S'|^2+\frac{2m}{E}\,\mathrm{Re}\,(C_V^*C_S+C_V'^*C_S')\right\}\cdot$$

$$\cdot\omega_{00}^0\Phi_{l_2}^{J_2}(k_2)\Phi_{l_3}^{J_3}(k_3)+|M_{GT}|^2\left\{|C_A|^2+|C_A'|^2+|C_T|^2+|C_T'|^2+\frac{2m}{E}\,\mathrm{Re}\,(C_A^*C_T+C_A'^*C_T')\right\}\cdot$$

$$\cdot\omega_{11}^0\Phi_{l_2}^{J_2}(k_2)\Phi_{l_3}^{J_3}(k_3)+M_FM_{GT}\frac{v}{c}\left\{2\,\mathrm{Re}\,(C_S^*C_T'+C_S'^*C_T-C_V^*C_A'-C_V'^*C_A)+\right.$$

$$+2\eta\,\mathrm{Im}\,(C_S^*C_A'+C_S'^*C_A-C_V^*C_T'-C_V'^*C_T)\Big\}\omega_{01}^1\Phi_{l_2}^{J_2}(k_2)\Phi_{l_3}^{J_3}(k_3)+$$

$$+|M_{GT}|^2\frac{v}{c}\left\{2\,\mathrm{Re}\,(C_T^*C_T'-C_A^*C_A')-2\eta\,\mathrm{Im}\,(C_A^*C_T'+C_A'^*C_T)\right\}\omega_{11}^1\Phi_{l_2}^{J_2}(k_2)\Phi_{l_3}^{J_3}(k_3)\,,$$

where explicitly:

$$\omega_{00}^0=\omega_{11}^0=1;\qquad \omega_{01}^1=\frac{1}{\sqrt{3}}\,\delta_{JJ_3};\qquad \omega_{11}^1=-\frac{1}{\sqrt{3}}\,\frac{J_2(J_2+1)-J(J+1)+2}{2\sqrt{J_2(J_2+1)}},$$

and

$$(13)\quad \Phi_{l_2}^{J_2}(k_2)=\sum_{l_2l_2'\lambda_2\lambda_2'}\hat{J}_2\hat{J}_3\hat{l}_2\hat{k}_1\hat{k}_2\hat{k}_3X\begin{pmatrix}l_2 & J_3 & J_2\\ l_2' & J_3 & J_2\\ k_2 & k_3 & k_1\end{pmatrix}(-)^{l_2-\lambda_2}\hat{l}_2'(l_2l_2'\lambda_2-\lambda_2'|k_20)\gamma_{l_2\lambda_2}\gamma_{l_2'\lambda_2'}^*,$$

$$(14)\quad \Phi_{l_3}^{J_3}(k_3)=\sum_{l_3l_3'\lambda_3\lambda_3'}\hat{J}_3\hat{l}_3(-)^{J_3+J_4+l_3+k_3}\overline{W}\begin{pmatrix}l_3 & k_3 & l_3'\\ J_3 & J_5 & J_3\end{pmatrix}(-)^{l_3'-\lambda_3'}\hat{l}_3'(l_3l_3'\lambda_3-\lambda_3'|k_30)\gamma_{l_3\lambda_3}\gamma_{l_3'\lambda_3'}^*.$$

These two last factors are simplified if the radiation is pure. Then we have $l_2=l_2'$ and $l_3=l_3'$. In addition, if the radiation is polarized, there is not even the $\sum$ on $\lambda$, *i.e.*

$$(15)\quad \Phi_{l_2}^{J_2}(k_2)=\hat{J}_2\hat{J}_3\hat{l}_2\hat{k}_1\hat{k}_2\hat{k}_3\quad X\begin{pmatrix}l_2 & J_3 & J_2\\ l_2 & J_3 & J_2\\ k_2 & k_3 & k_1\end{pmatrix}(-)^{l_2-1}\hat{l}_2(l_2l_21-1|k_20)|\gamma_1|^2\,,$$

$$(16)\quad \Phi_{l_3}^{J_3}(k_3)=\hat{J}_3\hat{l}_3(-)^{J_3+J_5+l_3+k_3}\overline{W}\begin{pmatrix}l_3 & k_3 & l_3\\ J_3 & J_5 & J_3\end{pmatrix}(-)^{l_3-1}(l_3l_31-1|k_30)|\gamma_2|^2\,.$$

We have the same quantities multiplied respectively by $(-)^{k_2}$ and $(-)^{k_3}$ for the opposed polarization.

Of course, if the radiation is not polarized, there are only the even powers of $k_2$ and $k_3$. Now, it would appear that an experiment on triple correlation should define terms with odd $k_1+k_2+k_3$.

It should however be noted, that, as is well known, the polarization-direction correlation experiments, such as β-γ correlation from oriented nuclei, if in a formal sense are triple correlation experiments, they are really different from three-direction correlation. The main difference is the occurrence of odd parity terms.

We have seen that in a given link of the correlation the odd $k$ are present only if a measure of circular polarization is done; however in the triple correlation, terms with $\boldsymbol{p}\cdot\boldsymbol{r}\wedge\boldsymbol{s}$, proportional to $\mathscr{Q}^{111}_{000}(\omega_{pr},\omega_{rs})$, would seem to exist. Which does not happen in the case of a measure of triple coincidence γ-γ-γ because in such case all the $k$ are even if the polarization is not observed, but it does not even happen in the case of β-γ-γ correlation where $k_1=1$ obtained in the case of allowed transitions, would appear to lead to terms of the type of $\mathscr{Q}^{1kk}_{000}$ with even $k$; but here too, such terms are not present because of the symmetry properties of

$$X\begin{pmatrix} l_2 & J_3 & J_2 \\ l_2' & J_3' & J_2' \\ k_2 & k_3 & k_1 \end{pmatrix},$$

coefficients which in the case of sharp states ($J_3=J_3'$ and $J_2=J_2'$) andpure radiation ($l_2=l_2'$) are different from 0 only if $k_1+k_2+k_3$ is even.

Therefore, measurements of the direction of the second radiation for a possible test of time-reversal invariance in weak interaction do not present anything new in respect of a simple β-γ correlation. Explicitly, when the γ's polarization is not observed, the angular correlation is:

$$W(\omega_{rs}) = (a^0_{00}\,\delta_{JJ_2} + a^0_{11}) \sum_{k=\text{even}} \Phi^{J_2}_{l_2}(k)\,\Phi^{J_3}_{l_3}(k)\,\mathscr{Q}^{0kk}_{000}(\omega_{rs})\,, \tag{17}$$

with

$$\begin{cases} a^0_{00} = |M_F|^2 \left\{ |C_V|^2 + |C_V'|^2 + |C_S|^2 + |C_S'|^2 + \dfrac{2m}{E}\,\mathrm{Re}\,[C_V^* C_T + C_V'^* C_S'] \right\}, \\ a^0_{11} = |M_{GT}|^2 \left\{ |C_A|^2 + |C_A'|^2 + |C_T|^2 + |C_T'|^2 + \dfrac{2m}{E}\,\mathrm{Re}\,[C_T^* C_T + C_A'^* C_T'] \right\}. \end{cases} \tag{18}$$

The function $\mathscr{D}$ is reduced to Legendre polynomials:

$$\mathscr{D}^{0kk}_{000}(\omega_{rs}) = \frac{(-)^k}{\hat{k}}\,P_k(\cos\theta_{rs})\,, \tag{19}$$

If $J_2\neq J$ (*i.e.* $J_2=J\pm1$) we have pure Gamow-Teller transition.

When we measure the polarization of the first γ we have also terms with

$\mathscr{D}_{000}^{1k_2k_3}$ with odd $k_2$, and $k_3 = k_2 \pm 1$. It is:

$$\mathscr{D}_{000}^{1kk+1}(\omega_{pr}, \omega_{rs}) = \tag{20}$$

$$= \frac{(-)^k}{\sqrt{(2k+1)(2k+3)(k+1)}} [P'_{k+1}(\cos\vartheta_{rs}) \cos\vartheta_{ps} - P'_k(\cos\vartheta_{rs}) \cos\vartheta_{pr}],$$

where $P'$ is the derivative of the Legendre polynomials with respect to $\cos\vartheta$. A similar expression is for $\mathscr{D}_{000}^{1k_2k_2-1}$.

Then the angular correlation gives:

$$W(\omega_{pr}, \omega_{rs}) = (a_{00}^0 \delta_{JJ_2} + a_{11}^0) \sum_{k=\text{even}} \Phi_{l_2}^{J_2}(k) \Phi_{l_3}^{J_3}(k) \frac{P_k(\cos\vartheta_{rs})}{\hat{k}} + \tag{21}$$

$$+ \frac{v}{c} \frac{1}{\sqrt{3}} \left[ b_{01}^1 \delta_{JJ_2} - a_{11}^1 \frac{J_2(J_2+1) - J(J+1) + 2}{2\sqrt{J_2(J_2+1)}} \right] \sum_{k_2k_3} \Phi_{l_2}^{J_2}(k_2) \Phi_{l_3}^{J_3}(k_3) \mathscr{D}_{000}^{1k_2k_3},$$

where $k_2$ is odd and $k_3 = k_2 \pm 1$.

$a_{00}^0$ and $a_{11}^0$ are given by (18) and

$$b_{01}^1 = a_{01}^1 + a_{10}^1 = M_F M_{GT} \{2 \text{ Re } (C_S^* C'_T + C'^*_S C_T - C_V^* C'_A - C'^*_V C_A) + \tag{22}$$

$$+ 2\eta \text{ Im } (C_S^* C'_A + C'^*_S C_A - C_V^* C'_T - C'^*_V C_T)\},$$

$$a_{11}^1 = |M_{GT}|^2 \{2 \text{ Re } (C_T^* C'_T - C_A^* C'_A) - 2\eta \text{ Im } (C_A^* C'_T + C'^*_A C_T)\}. \tag{23}$$

We understand therefore that the observation of the direction of a second $\gamma$ does not add anything new to our knowledge of the symmetry properties of weak interaction obtained by studying the $\beta$-$\gamma$ circular-polarization correlation from not oriented nuclei. However, if the first $\gamma$ radiation is mixed, then the

$$X \begin{pmatrix} l_2 & J_3 & J_2 \\ l'_2 & J_3 & J_2 \\ k_2 & k_3 & k_1 \end{pmatrix},$$

coefficient is different from zero also for $k_1 + k_2 + k_3$ odd. In this case, in in the triple angular correlation $\beta$-$\gamma$-$\gamma$ also without measuring the polarization, odd parity term $\mathscr{D}_{000}^{1kk}$ (with $k$ even), related to products of the type $\boldsymbol{p} \cdot \boldsymbol{s} \wedge \boldsymbol{r}$, can be present. These terms will give some information on the time reversal invariance in the strong interaction.

## Appendix

Here are the calculations of the interaction coefficients for the allowed $\beta$ transitions.

We put

$$\text{(A-1)} \qquad \begin{cases} p = (-)^{l'-\lambda}(ll'\lambda - \lambda | k_1 0)\,, \\ p_1 = (-)^{l_1'-\lambda_1}(l_1 l_1' \lambda_1 - \lambda_1 | 00) = 1\,. \end{cases}$$

These are the polarization coefficients expressing the influence of the states of polarisation of the electron and neutrino on the emission factor $q_{l_1 l_2 l_3}$.

For the partial amplitudes we have:

$$\text{(A-2)} \qquad A^{(J_1)}_{l l_1 \lambda \lambda_1} \to A^{(J_1)}_{p p_1} = \sum_r a^{(r)}_{p p_1} \omega^{(J_1)}_r\,,$$

with

$$\text{(A-3)} \qquad a^{(r)}_{p p_1} = (F^{(r)}_{p p_1} + \tfrac{1}{2} i\eta C^{(r)}_{p p_1})(J_2 \| \bar{O}^r \| J)\,,$$

and

$$\text{(A-4)} \qquad \omega^{(J_1)}_r = (-)^{2J_1 + J_2 - J + r + 1} \hat{J}_2 \hat{r} \overline{W} \begin{pmatrix} l & r & l_1 \\ J_2 & J_1 & J \end{pmatrix},$$

where $F^{(r)}_{p p_1}$ are the coefficients for the Fermi and Gamow-Teller interactions (see for instance (11)) and $C^{(r)}_{p p_1}$ are the coefficients of the correction term that take account for the Coulomb effects to a first approximation.

$(J_r \| \bar{O}^r \| J)$ are the reduced matrix elements of the nuclear operator $\bar{O}^r$ where the bar denotes a sum of the operators acting on the single nucleons.

$\eta = Z\alpha m/p$ ($Z$ is the charge of the emitting nucleus, $\alpha$ the fine structure constant and $m, p$ respectively the mass and momentum of the electron).

Then we can write:

$$\text{(A-5)} \qquad \varphi_{k_1 k_2 k_3} = \sum_{r r'} a^{k_1}_{r r'} \Omega^{l_1 l_2 l_3 k_2 k_3}_{r r'}\,,$$

with

$$\text{(A-6)} \qquad a^{k_1}_{r r'} = \sum_{p p_1} p^{k_1} a^{(r)}_{p p_1} a^{(r')*}_{p p_1}\,,$$

and

$$\text{(A-7)} \qquad \Omega^{l_1 l_2 l_3 k_2 k_3}_{r r'} = \sum_{J_1'} (-)^{l' + \lambda_1 + r' + 2J_1 + J + J_2 + l' + 1} \cdot$$

$$\cdot \hat{l}\hat{r}\hat{r}' \begin{pmatrix} J_2 & J_1 & l_1 \\ J_1' & l' & k_1 \end{pmatrix} \overline{W} \begin{pmatrix} J_2 & J_1 & l_1 \\ J_1' & J_2 & k_1 \end{pmatrix} \Phi^{J_2}_{l_2}(k_2) \Phi^{J_3}_{l_3}(k_3)\,,$$

or

$$\Omega^{k_1 k_2 k_3}_{r r'} = \omega^{k_1}_{r r'} \Phi^{J_2}_{l_2}(k_2) \Phi^{J_3}_{l_3}(k_3)\,,$$

where

$$\text{(A-8)}\qquad \omega^{k_1}_{rr'} = \sum_{J_1 J_1'} (-)^{k_1+J_1+J_2+l_1+r+r'} \hat{J}_1 \hat{r}_1 \hat{J} \hat{r}' \hat{J}_1' \hat{l} \hat{J}_1 \hat{J}_2 \overline{W} \begin{pmatrix} l & J_1 & J \\ J_1' & l_1 & k_1 \end{pmatrix} \cdot$$

$$\cdot \overline{W} \begin{pmatrix} J_2 & J_1 & l_1 \\ J_1' & J_2 & k_1 \end{pmatrix} \overline{W} \begin{pmatrix} l & r & l_1 \\ J_2 & J_1 & J \end{pmatrix} \overline{W} \begin{pmatrix} l & r' & l_1 \\ J_2 & J_1' & J \end{pmatrix},$$

$$\text{(A-9)}\qquad \begin{cases} \Phi^{J_2}_{l_2}(k_2) = \hat{J}_2 \hat{J}_3 \hat{l}_2 \hat{k}_1 \hat{k}_2 \hat{k}_3 \Lambda \begin{pmatrix} l_2 & J_3 & J_2 \\ l_2 & J_3 & J_2 \\ k_2 & k_3 & k_1 \end{pmatrix} (-)^{l_2-1} \hat{l}_2 (l_2 l_2 1 - 1 \,|\, k_2 0) \\ \Phi^{J_3}_{l_3}(k_3) = \hat{J}_3 \hat{l}_3 (-)^{J_3+J_3+l_3+k_3} \overline{W} \begin{pmatrix} l_3 & k_3 & l_3 \\ J_3 & J_5 & J_3 \end{pmatrix} (-)^{l_3-1} \hat{l}_3 (l_3 l_3 1 - 1 \,|\, k_3 0)\,. \end{cases}$$

We sum on $J_1'$ and $J_1$ taking into account the:

$$\text{(A-10)}\qquad \overline{W} \begin{pmatrix} J_2 & J_1 & l_1 \\ J_1' & J_2 & k_1 \end{pmatrix} \overline{W} \begin{pmatrix} l & r' & l_1 \\ J_2 & J_1' & J \end{pmatrix} =$$

$$= \sum_j (-)^a \hat{j}^2 \overline{W} \begin{pmatrix} j & r' & J_2 \\ l_1 & J_1 & l \end{pmatrix} \overline{W} \begin{pmatrix} j & l & J_1 \\ J_1' & k_1 & J \end{pmatrix} \overline{W} \begin{pmatrix} j & J & k_1 \\ J_2 & J_2 & r' \end{pmatrix}$$

$$a = j + J_1' + J_2 + l_1 + J_2 + J_1 + k_1 + l + r' + J\,.$$

The right-hand side of the expression (A-10) is put in (A-8) where, then, we do the $\sum$ on $J_1'$, $J_1$ and $j$:

$$\text{(A-11)}\qquad \sum_{J_1'} (-)^{J_1'+j+l} \hat{J}_1^2 \overline{W} \begin{pmatrix} l & J & J_1' \\ k_1 & J_1 & j \end{pmatrix} \overline{W} \begin{pmatrix} l & J & J_1' \\ J_1 & k_1 & l \end{pmatrix} = \overline{W} \begin{pmatrix} l & J_1 & j \\ J & k_1 & l \end{pmatrix},$$

$$\text{(A-12)}\qquad \sum_{J_1} \hat{J}_1^2 (-)^b \overline{W} \begin{pmatrix} J_1 & l & J_2 \\ r & J & l \end{pmatrix} \overline{W} \begin{pmatrix} J_1 & l & J \\ k_1 & j & l \end{pmatrix} \overline{W} \begin{pmatrix} J_1 & l & j \\ r' & J_2 & l \end{pmatrix} =$$

$$= \overline{W} \begin{pmatrix} r & k_1 & r' \\ l & l & l \end{pmatrix} \overline{W} \begin{pmatrix} r & k_1 & r' \\ j & J_2 & J \end{pmatrix}$$

$$b = J_1 + r + k_1 + r' + l + l + l + j + J_2 + J\,.$$

At last:

$$\text{(A-13)}\qquad \sum_j \hat{j}^2 (-)^{j+J_2+r} \overline{W} \begin{pmatrix} r' & J_2 & j \\ k_1 & J & J_2 \end{pmatrix} \overline{W} \begin{pmatrix} r' & J_2 & j \\ J & k_1 & r \end{pmatrix} = \overline{W} \begin{pmatrix} r' & J & J_2 \\ J_2 & k_1 & r \end{pmatrix}.$$

It remains:

$$\text{(A-14)} \qquad \omega_{rr'}^{k_1} = (-)^{J+J_2+k_1+r+r'+1} \overline{W} \begin{pmatrix} r & k_1 & r' \\ l & l & l \end{pmatrix} \overline{W} \begin{pmatrix} r' & J & J_2 \\ J_2 & k_1 & r \end{pmatrix} \hat{l}\, \hat{J}_2\, \hat{r}\, \hat{r}' \,.$$

We have:

$$\text{(A-15)} \qquad \omega_{rr'}^{k_1} = \omega_{r'r}^{k_1} \,.$$

It is:

$$\text{(A-16)} \quad \begin{cases} \omega_{00}^{0} = \delta_{JJ_2}; \qquad \omega_{11}^{0} = 1 \ \text{(with } J_2 = J \,, \quad J \pm 1) \,, \\ \omega_{01}^{1} = \omega_{10}^{1} = \dfrac{1}{\sqrt{3}}\, \delta_{JJ_2} \,, \\ \omega_{11}^{1} = -\dfrac{1}{\sqrt{3}} \dfrac{J_2(J_2+1) - J(J+1) + 2}{2\sqrt{J_2(J_2+1)}} = \begin{cases} -\dfrac{1}{\sqrt{3}} \dfrac{1}{\sqrt{J(J+1)}} & \text{for} \quad J_2 = J \,, \\ \dfrac{1}{\sqrt{3}} \sqrt{\dfrac{J-1}{J}} & \text{for} \quad J_2 = J - \\ -\dfrac{1}{\sqrt{3}} \sqrt{\dfrac{J+2}{J+1}} & \text{for} \quad J_2 = J + \end{cases} \end{cases}$$

---

## RIASSUNTO

Viene data una formulazione generale delle correlazioni angolari triple per esaminare in particolare la correlazione $\beta$-$\gamma$-$\gamma$ e le sue implicazioni sulle proprietà di simmetria delle interazioni deboli e forti con speciale riguardo alla invarianza per inversione del tempo.

# LETTERE ALLA REDAZIONE

*(La responsabilità scientifica degli scritti inseriti in questa rubrica è completamente lasciata dalla Direzione del periodico ai singoli autori)*

## The Linear $K\pi$ Interaction and the Relative $\Sigma$-$\Lambda$ Parity.

S. Barshay (*)

*Physics Department, Brandeis University - Waltham, Mass.*

(ricevuto il 22 Maggio 1961)

The strong forward peak in the center-of-mass differential cross-section for $K^0$ production in the process

$$\pi^- + p \to K^0 + \Lambda \,, \tag{1}$$

led to the remark of Goldhaber [1] that this might be understood in terms of the «stripping» of a virtual $K^+$ via absorption of the high-energy incident pion

$$\pi^- + K^+ \to K^0 \,. \tag{2}$$

Barshay [2] and Schwinger [3] suggested the linear $K\pi$ interaction of the charge-independent form $K^\dagger \boldsymbol{\tau} K \cdot \boldsymbol{\pi}$ as a means of achieving the process (2). Here the particle symbol denotes the corresponding field operator, the symbol $\dagger$ denotes the hermitian adjoint and $\boldsymbol{\tau}$ is the vector operator composed of the Pauli matrices. This strong interaction is invariant under $P$, the parity operation, only if the two K-mesons appearing in the coupling have opposite parity (more generally, it is invariant under $CP$ only if the two K-mesons behave in an opposite manner under this operation). At the time of its proposal it was thought that the $\theta$ and the $\tau$ might be two such K-mesons [2-4]. A recent experiment [5] indicates the existence of an excited K-meson, the K*, which decays via

$$K^* \to K + \pi \,. \tag{3}$$

It appears that the K* has isotopic spin $\frac{1}{2}$ [5]. Tiomno *et al.* [6] have revived the linear $K\pi$ interaction in the form

$$K^\dagger \boldsymbol{\tau} K^* \cdot \boldsymbol{\pi} + \text{hermitian conjugate} \,, \tag{4}$$

as an explanation for the peaking in process (1) via the mechanism (2) with $K^+$ changed to $K^{*+}$. Reasonable agreement

(*) This work was partially supported by National Science Foundation Grant G-14688.

(1) M. Goldhaber: *Phys. Rev.*, **101**, 433 (1956).

(2) S. Barshay: *Phys. Rev.*, **104**, 853 (1956).

(3) J. Schwinger: *Phys. Rev.*, **104**, 1164 (1956). See also P. Budini and L. Fonda: *Nuovo Cimento*, **5**, 306 (1957).

(4) T. D. Lee and C. N. Yang: *Phys. Rev.*, **102**, 290 (1956).

(5) M. Alston, L. Alvarez, P. Eberhard, M. Good, W. Graziano, H. Ticho and S. Wojcicki: *Phys. Rev. Lett.*, **6**, 300 (1961).

(6) J. Tiomno, A. L. L. Videira and N. Zagury: *Phys. Rev. Lett.*, **6**, 120 (1961).

with experiment is obtained if the K* is a scalar particle in its coupling with the $\Lambda$-nucleon system [6]. A vector K* would also give agreement since the effective part of a vector coupling of K* to $\Lambda\mathcal{N}$ in process (1) would be essentially the same as the scalar coupling. This implies that the K-$\Lambda$ relative parity is odd [7] (*).

From this phenomenological explanation of the marked forward peaking of $K^0$ in process (1) several questions arise: (1) Why is a similar forward peaking absent for the $K^+$ from the process $\pi^+ + p \to K^+ + \Sigma^+$ at moderate incident pion energies $\sim 1.1$ GeV [8]? (2) Why are the process $\pi^+ + p \to K^+ + \Sigma^+$ and $\pi^- + p \to K^+ + \Sigma^-$ similar in appearence at moderate incident pion energies [8] when the latter does not involve the « stripping » process [2] (a K-meson cannot absorb a $\pi^-$ and turn into a $K^+$)? (3) Why at very high energies $\sim 16$ GeV does there appear to be a marked backward peaking of the $\Sigma^+$ and $\Sigma^-$ produced in $\pi^-$-nucleus collisions [9]?

We would like to sugge t that these questions can be answered [10] in a qualitatively consistent manner under the hypothesis [11] that the relative $\Sigma$-$\Lambda$ parity is odd. This hypothesis was advanced in 1958 on the basis of an analysis of the experimental data on K-nucleon scattering, and has been given a theoretical basis in the model of the $\Sigma$-hyperon as a bound $S$-state of a pion and a $\Lambda$ [12,13]. Under this hypothesis, the K* parity relative to the $\Sigma$-nucleon system will be odd, but the K-$\Sigma\mathcal{N}$ relative parity will be even [11]. If the K*$\Sigma\mathcal{N}$ coupling is pseudoscalar the calculations of CHAN [14] indicate (*a*) that the forward peaking of $K^+$ (or the backward peaking of $\Sigma^+$) in the process $\pi^+ + p \to K^+ + \Sigma^+$ will be absent and (*b*) that, unless the effective pseudoscalar coupling constant is extremely large, the « stripping » process will make only a small contribution to the cross-section for this process. Therefore at moderate incident pion energies the processes $\pi^+ + p \to K^+ + \Sigma^+$ and $\pi^- + p \to K^+ + \Sigma^-$ may well be similar, *neither* one receiving a large contribution from the « stripping » mechanism. However, at higher energies we may expect the processes $\pi^+ + p \to \Sigma^+ + K_0^+ + \pi^+$ to proceed via the steps

$$(5) \qquad p \to \Sigma^+ + K^0 ,$$

$$\pi^+ + K^0 \to K^{*+} ,$$

$$K^{*+} \to K^+ + \pi^0 \text{ or } K^0 + \pi^+ .$$

Since the K$\Sigma\mathcal{N}$ coupling is scalar, the $\Sigma^+$ should be markedly peaked backward, similar to the $\Lambda$-hyperons in process (1). The similarity should be most marked for $\Sigma^+$ produced at recoil laboratory kinetic energies corresponding

---

(*) M. M. BLOCK *et al.*: *Phys. Rev. Lett.*, **3**, 291 (1959).

(*) The simple « stripping » mechanism, in Born approximation, does not explain the sizable polarization of $\Lambda$ particles produced in reaction (1). However it is not unreasonable that, among other things, multiple scattering effects in initial and final states superimposed upon this basic mechanism will produce parts of the amplitude out of phase with the Born approximation.

(8) F. EISLER *et al.*: *Nuovo Cimento*, **10**, 468 (1958); private communication from J. SANDWEISS.

(9) J. BARTKE *et al.*: *Phys. Rev. Lett.*, **6**, 303 (1961).

(10) A discussion of question (1) is contained in a Brookhaven National Laboratory internal report by M. A. B. BÈG, J. BERNSTEIN and P. C. DE CELLES, as quoted by Y. NAMBU and J. J. SAKURAI: *Phys. Rev. Lett.*, **6**, 377 (1961).

(11) S. BARSHAY: *Phys. Rev. Lett.*, **1**, 97 (1958).

(12) S. BARSHAY and M. SCHWARTZ: *Phys. Rev. Lett.*, **4**, 618 (1960).

(13) S. BARSHAY and H. PENDLETON III: *Phys. Rev. Lett.*, **6**, 421 (1961). In the concluding paragraph of this Letter, the second reference to reference (7) should be to reference (3).

(14) C. H. CHAN: *Phys. Rev. Lett.*, **6**, 383 (1961).

to the preferred energies of the scalar K-exchange diagram, namely those obtained by equating the square of the baryon four-momentum transfer to $\sim 0$ to $-m_K^2$, where $m_K$ is the K-meson mass. Further, we would expect $\Sigma^+$ production via (5) to predominate over $\Sigma^-$ production in $\pi^-$p collisions at similar high energies where production of an additional pion is important.

These points should be subject to experimental test. Indeed an attempt to observe a strong similarity between the backward peaking of Λ-hyperons from process (1) and of $\Sigma^+$ from process (5) would be a useful experiment on the question of the relative Σ-Λ parity, as well as a test of the above model for process (1).

At extremely high energies we might expect a $\pi^-$-nucleus collision to involve two stages: (1) the production in a $\pi^-$-nucleon collision of a pair of high energy pions at small angles to the incident $\pi^-$ ([15]) with this followed by (2) production via the « stripping » reaction on the same (or another nucleon) of a Σ-hyperon. Such a sequence might be

$$
\begin{aligned}
(6)\qquad \pi^- + p &\to \begin{cases} \pi^- + \pi^+ + n\,, \\ \pi^- + \pi^0 + p\,, \end{cases} \\
\pi^- + n &\to K^{*0} + \Sigma^-\,, \\
\pi^0 + p &\to K^{*0} + \Sigma^+\,, \\
K^{*0} &\to \begin{cases} K^+ + \pi^-\,, \\ K^0 + \pi^0\,. \end{cases}
\end{aligned}
$$

Both $\Sigma^+$ and $\Sigma^-$ so produced should exhibit the backward peak in the center-of-mass angular distribution characteristic of the « stripping » process. This is in qualitative agreement with experiment ([9]).

It would seem that there is now real hope of reconciling the long-standing nice features of the phenomenological linear Kπ interaction with both *CP* invariance and with the observed difference between Σ and Λ production at moderate energies, under the hypothesis of odd relative Σ-Λ parity.

* * *

The author has enjoyed a number of conversations with Dr. H. Pendleton III.

([15]) S. D. Drell: *Phys. Rev. Lett.*, 5, 342 (1960).

# Two-Pion Exchange Contribution in Proton Compton Scattering (*).

A. P. Contogouris

*Laboratory of Nuclear Studies - Cornell University - Ithaca, N. Y.*

(ricevuto il 19 Giugno 1961)

It has been recently claimed (1) that the sign of the one-pion exchange contribution (Low amplitude) in the scattering of photons by protons differs from that used in the work of Jacob and Mathews (2); consequently this process cannot account for the disagreement between the dispersion theoretical calculations and the experimental results in the range of $(150 \div 230)$ MeV photon lab. energy. The purpose of the present note is to show that inclusion of two-pion exchange effects (Fig. 1) with appropriate phase and strength significantly improves the theoretical predictions in this range.

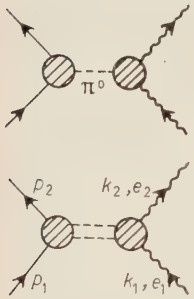


Fig. 1. – One-pion (Low process) and two-pion exchange diagrams in scattering of photons by protons.

From the point of view of Mandelstam representation for nucleon Compton scattering, two-pion exchange contributes a branch cut $(2\mu)^2 \leqslant t < \infty$ in the momentum transfer variable, the square of which is denoted by $t$. Provided that the Compton effect is treated to the lowest order in the fine-structure constant, this gives the nearest singularity, after the pole at $t = \mu^2$ that is introduced by the Low amplitude. Since, now, we are interested in a relatively short range at low photon energies, we may replace, in a first approximation, this two-pion cut by a pole of appropriate position and strength; for scattering at higher energies a more-than-one-pole approximation is expected to be necessary.

In the channel $\gamma + \gamma \to \pi + \pi \to \mathcal{N}' + \mathcal{N}'$ only even angular-momentum states of the system are permitted (3). Moreover, since the lowest of them is expected to play the dominant role, we shall henceforth consider the state $J = 0$ only. Then, the effect of the two-pion intermediate state might be approximated by simply

(*) Supported by the joint program of the Office of Naval Research and the U. S. Atomic Energy Commission.

(1) L. I. Lapidus and Chou Kuang-chao: *On the role of the one-pion pole diagram in γ-rays scattering by protons* (preprint).

(2) M. Jacob and J. Mathews: *Phys. Rev.*, **117**, 854 (1960).

(3) M. Gourdin and A. Martin: *Nuovo Cimento*, **17**, 224 (1960).

adding to the Compton scattering amplitude a contribution in the form of a lowest order perturbation term with exchange of a «particle» of spin 0, isospin $T=0$ and mass determined from the position of the pole [4]. This procedure will be fully justified if an $S$-wave $\pi$-$\pi$ resonance, speculated by some authors [5,6] in the state $T=0$, is confirmed.

The amplitude for the scattering of photons by particles with spin $\frac{1}{2}$ can be written in the center-of-momentum (c.m.) system as follows [7]:

$$(1)\quad A_{\gamma\to\gamma} = R_1(\hat{e}_1,\hat{e}_2) + R_2(\hat{k}_1\times\hat{e}_1,\hat{k}_2\times\hat{e}_2) + iR_3(\boldsymbol{\sigma}\cdot\hat{e}_1\times\hat{e}_2) + iR_4(\boldsymbol{\sigma}\cdot[\hat{k}_2\times\hat{e}_2]\times[\hat{k}_1\times\hat{e}_1]) + \\ + iR_5((\boldsymbol{\sigma}\hat{k}_1)(k_2\cdot\hat{e}_2\times\hat{e}_1) - (\boldsymbol{\sigma}\hat{k}_2)(\hat{k}_1\cdot\hat{e}_1\times\hat{e}_2)) + iR_6(\boldsymbol{\sigma}\hat{k}_2)\,((\hat{k}_2\cdot\hat{e}_2\times\hat{e}_1) - (\boldsymbol{\sigma}\hat{k}_1)(\hat{k}_1\cdot\hat{e}_1\times e_2))\,,$$

where $\hat{e}_1$, $\hat{e}_2$ are the polarization vectors and $\hat{k}_1$, $\hat{k}_2$ the directions of the initial and final photon respectively; the scalar amplitudes $R_i$ $(i=1,\ldots,6)$ are functions of the photon energy and of the scattering angle. For the contribution under investigation, since the intermediate «particle» is now scalar, the coupling in the two-photon vertex has to be expressed in terms of the invariant combination

$$(2)\qquad \tfrac{1}{2}F_{\mu\nu}F^{\mu\nu} = \boldsymbol{H}^2 - \boldsymbol{E}^2\,,$$

of the electromagnetic field tensor (instead of $e_{\varkappa\lambda\mu\nu}F^{\varkappa\lambda}F^{\mu\nu} = \boldsymbol{E}\cdot\boldsymbol{H}$ used for intermediate pseudoscalar); also, the coupling in the nucleon vertex is now proportional to $\bar{u}(p_2)u(p_1)$ (instead of $\bar{u}(p_2)\gamma_5 u(p_1)$), where $u(p)$ is the Dirac spinor of the proton. The form of the two-pion exhange amplitude is, then, in the c.m. system:

$$(3)\qquad A_{\pi\pi} = L\left(\frac{E_k+M}{2M} - \frac{E_k-M}{2M}(\boldsymbol{\sigma}\hat{k}_2)(\boldsymbol{\sigma}\hat{k}_1)\right)((\hat{k}_1\times\hat{e}_1,\hat{k}_2\times\hat{e}_2) - (\hat{e}_1,\hat{e}_2)),$$

where

$$(4)\qquad L = -G\,\frac{e^2}{M}\cdot\frac{M}{E_k+k}\cdot\frac{k^2}{k^2(1-x)+t_p/2}\,.$$

Here $E_k$ is the proton energy, $k$ the photon momentum, $x$ the cosine of the c.m. scattering angle, $t_p$ the position of the pole and $G$ a constant expressing the pole-strength. Simple vector algebra gives the following contributions to the amplitudes of (1)

$$(5)\qquad \begin{cases} R_1 = -R_2 = L\left(\dfrac{E_k+M}{2M} - \dfrac{E_k-M}{2M}\,x\right) & R_3 = -R_4 = L\,\dfrac{E_k-M}{2M}\,(1-x) \\ & R_5 = -R_6 = L\,\dfrac{E_k-M}{2M}\,. \end{cases}$$

---

[4] For a similar procedure in charged pion photoproduction see B. De Tollis, E. Ferrari and H. Munczek: *Nuovo Cimento*, **18**, 198 (1960).

[5] P. Carruthers and H. Bethe: *Phys. Rev. Lett.*, **4**, 536 (1960).

[6] J. G. Taylor: *Phys. Rev. Lett.*, **6**, 237 (1961).

[7] L. I. Lapidus and Chou Kuang-chao: *Žurn. Éksp. Teor. Fiz.*, **37**, 1714 (1959), [transl. *Sov. Phys. JETP*, **10**, 1213 (1960)].

In view of the predictions about possible resonances in ref. ([6]) and of a possible large $T = 0$ $S$-wave amplitude at very low energy in the pion-pion interaction ([8]), the position of the pole is expected to be in the range $(2\mu)^2 < t \lesssim (3\mu)^2$. In the present calculation we adopt $t_p = (2.5\mu)^2$ and adjust the pole strength $G$ by trying to fit the experimental data at a certain energy and angle. We want to stress that as far as we are interested in a relatively short interval of photon energies ($< 230$ MeV) a different choice of $t_p$ is quite possible; with $G$ treated as adjustable parameter the conclusions are essentially the same.

Under the assumption that pion photoproduction below 500 MeV proceeds through charged $E1(\frac{1}{2})$ amplitude and $M1(\frac{3}{2})$ amplitude in the $T = \frac{3}{2}$ state, while above 500 MeV through $E1(\frac{3}{2})$ alone, the differential cross-sections for proton Compton scattering at $\theta_{c.m.} = 90°$ and 135° have been calculated ([1]). In these calculations the Low amplitude was introduced with $\pi^0$ life-time $\tau = 2 \cdot 10^{-16}$ s ([9]) and with two choices of the sign (curves D.R. $+A$ and D.R. $-A$ of Figs. 2 and 3). For

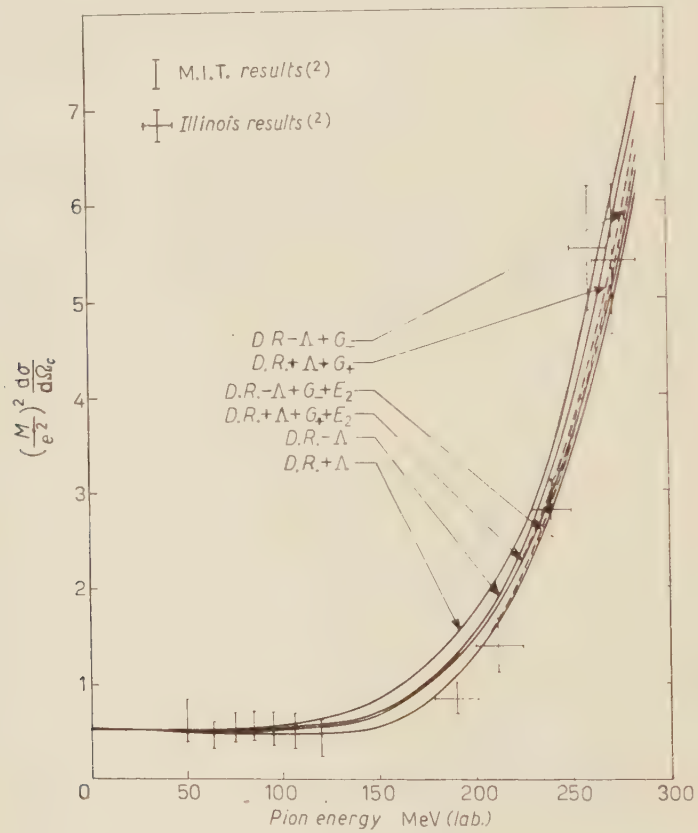


Fig. 2. – Differential cross-sections at $\theta_{c.m.} = 90°$.

([8]) B. Desai: *Phys. Rev. Lett.* **6**, 497 (1961).

([9]) G. Harris, J. Orear and S. Taylor: *Phys. Rev.*, **106**, 327 (1957); R. Blackie, A. Engler and T. Mulvey: *Phys. Rev. Lett.*, **5**, 384 (1960); R. Glasser, N. Seeman and B. Stiller: *Proc. of the 1960 Annual Intern. Conf. on High Energy Physics at Rochester* (New York, 1960), p. 30; A. Tollestrup, S. Berman, R. Gomez and H. Ruderman: *Proc. of the 1960 Annual Intern. Conf. on High Energy Physics at Rochester* (New York, 1960), p. 27.

the first choice, corresponding to that of ref. ([1]), the two-pion exchange contribution has been subsequently added with $G = G_+ = 1.58$ (curve D.R.$+A+G_+$); for the second choice, corresponding to that of ref. ([2]), $G = G_- = 0.95$ has been used (curve D.R. $-A+G_-$). For this value of $G$ the contribution of the amplitude $A_{\pi\pi}$ is nearly equal to that of the Low-process for $\tau = 10^{-17}$ s. Greater values of $G_+$ do not improve the predictions.

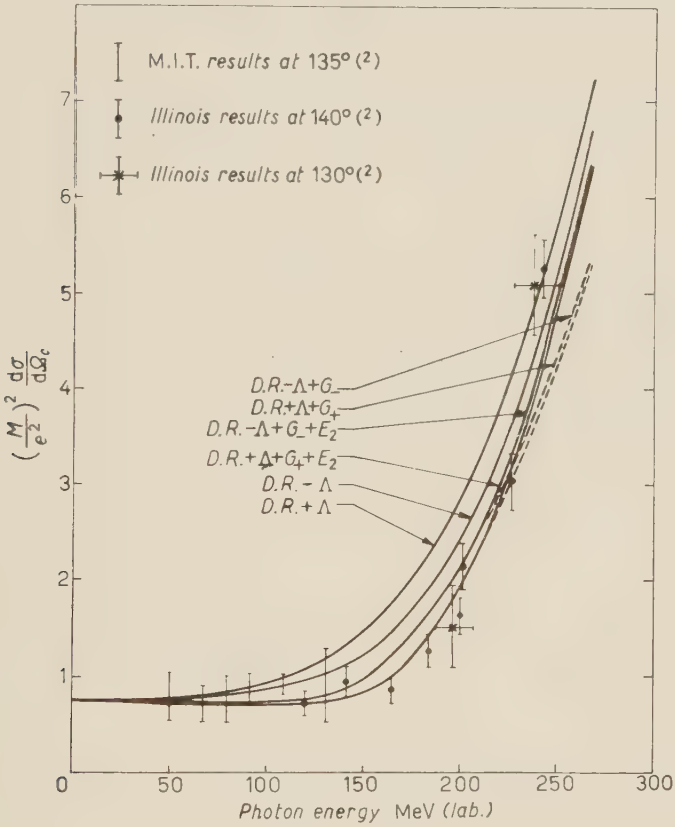


Fig. 3. – Differential cross-sections at $\theta_{c.m.} = 135°$.

Especially for the second choice the agreement with the experimental data is good up to 270 MeV, apart from the points at $\approx 240$ MeV, $\theta_{c.m.} = 135°$. At this energy, however, the effect of a small $E2(\frac{3}{2})$ amplitude in the radiation that produces the first photopion resonance, is not negligible; moreover, it is supported from the existing data at higher energies ([10]). With an electric quadrupole admixture of $\approx 1\%$ at the total photoproduction cross-section ([11]), the whole set of data up to

([10]) A. P. Contogouris: *Bull. Am. Phys. Soc.*, **6**, 256 (1961) and to be published.

([11]) In the notation of ref. ([7]) this corresponds to a ratio $E_2/M_1 \approx 0.3$. For a set of approximate dispersion relations including electric quadrupole contribution see either of ref. ([7]) or ([10]).

270 MeV is fairly well accounted for (curves D.R.$+A+G_-+E_2$ and D.R. $A+G_-+E_2$, especially the second) ([12]).

At higher energies a more trustworthy calculation within the framework of Mandelstam representation is under consideration; in this way some information about the magnitude of the pole-strength $G$ is also expected to be accessible. If a significantly smaller value of $G$ is predicted, the two-pion exchange contribution, although it may improve the agreement with the experimental results, will not be sufficient. One might, then, have to examine the contribution of a three-pion intermediate state.

* * *

It is a pleasure to thank Professor T. Kinoshita and Mr. T. Truong for helpful discussions.

([12]) The arguments of ref. ([1]) are based on Goldberger and Treiman's analysis of neutral pion decay [*Nuovo Cimento*, **9**, 451 (1958)]. We have considered the second choice ($DR-A+...$) in order to show that, even if this choice is proven by further analysis to be correct, inclusion of two-pion exchange may give very good agreement with the experimental data without having to use $\pi^0$ lifetime smaller than $2\cdot10^{-16}$ s [see ref. ([2])].

IL NUOVO CIMENTO Vol. XXI, N. 4 16 Agosto 1961

# Hyperon Photon-Decay.

G. Calucci and G. Furlan

*Istituto di Fisica dell'Università - Trieste*
*Istituto Nazionale di Fisica Nucleare - Sezione di Trieste*

(ricevuto il 26 Giugno 1961)

Recent experimental evidence has been found about the decay mode $Y \to \mathcal{N}+\gamma$ ([1,2]). In this short note we want to discuss a « pole » approximation in order to evaluate the decay rate and the other characteristic parameters of the process. A similar type of evaluation has been already applied to the pionic decay $Y \to \mathcal{N}+\pi$ by Feldman, Salam and Matthews ([3]), who suggested the same method for photon decays.

From invariance grounds, the more general matrix element for the process

$$Y(q) \to \mathcal{N}(p)+\gamma(k) ,$$

can be written, at the first order in the weak and electrical coupling constants $G$ and $e$, and neglecting usual constants, as

$$M = ieG\bar{u}_{\mathcal{N}}(p)\{[a_1(k^2)\gamma_\lambda + a_2(k^2)\sigma_{\lambda\mu}k_\mu + a_3(k^2)k_\lambda] + \\ + \gamma_5[b_1(k^2)\gamma_\lambda + b_2(k^2)\sigma_{\lambda\mu}k_\mu + b_3(k^2)k_\lambda]\} u_Y(q)e_\lambda^{(r)}(\bar{k}) \equiv M^{(r)}(e, k, p) ,$$

moreover $k^2=0$ (real photon) and $k_\lambda \cdot e_\lambda^{(r)}(\bar{k})=0$.

The gauge invariance requires $M(k, k, p)=0$ and this condition gives

$$a_1(0) = b_1(0) = 0 .$$

So, our matrix element becomes

$$M^{(r)}(e, k, p) = ieG\bar{u}_{\mathcal{N}}(p)(A - \gamma_5 B)\sigma_{\lambda\mu}k_\mu u_Y(q)e_\lambda^{(r)}(\bar{k}) .$$

---

([1]) G. Quareni, A. Quareni-Vignudelli, G. Dascola and S. Mora: *Nuovo Cimento*, **14**, 5 1178 (1959).

([2]) J. Schneps and Y. W. Kong: *Nuovo Cimento*, **19**, 1218 (1961).

([3]) G. Feldman, P. T. Matthews and A. Salam: *Phys. Rev.*, **121**, 1, 302 (1961).

Moreover time reversal requires $A$ and $B$ to be « relatively real », that is practically real.

In the standard way we may obtain the total decay rate

$$w = \frac{(\Sigma^2 - \mathcal{N}^2)}{4\pi\Sigma^3} e^2 G^2 (A^2 + B^2) , \tag{3}$$

the angular distribution of the emitted protons, in the rest system of the hyperon

$$P(\theta) = 1 + \alpha P_Y \cos\theta ,$$

were $\theta$ is the angle between the proton direction and the polarization vector $\boldsymbol{P}_Y$, with the asymmetry parameter

$$\alpha = \frac{2AB}{A^2 + B^2} , \tag{4}$$

and the longitudinal polarization of the nucleon

$$P_{\mathcal{N}} = - \frac{\alpha + P_Y \cos\theta}{1 + \alpha P_Y \cos\theta} . \tag{5}$$

If $P_Y = 0$ (unpolarized hyperons)

$$P_{\mathcal{N}} = - \alpha .$$

Our task is now the interpretation and, possibly, the evaluation of the unknown coefficients $A$ and $B$. Let's use the dispersive approach suggested by FELDMAN, SALAM and MATTHEWS, whose argument is the following.

The decay amplitude can be written

$$M_{FI} = (2\pi)^4 i\delta(p + k - q) \langle pk | H_W(0) | q \rangle ,$$

at the first order in $H_W$. We assume analytical properties for this matrix element in the three external particle masses and write a tridimensional integral representation for it, in these variables. Then, we limit ourselves to the «poles » contribution.

The location of the singularities depends on the decay particle nature.

If we take into consideration the $\Sigma^+ \to p + \gamma$ process, we have the following situation: ($\mathcal{N}$, $\Sigma$, $\pi$ ... are the masses of the corresponding particles).

For the variable $\xi = q^2$

$$\text{pole } \xi = \mathcal{N}^2 , \qquad \text{cut } \xi \geqslant (\mathcal{N} + \pi)^2 .$$

For the variable $\eta = p^2$

$$\text{pole } \eta = \Sigma^2 , \qquad \text{cut } \eta \geqslant (\Sigma + \pi)^2 .$$

For the variable $\zeta = k^2$

$$\text{cut } \zeta \geqslant (K + \pi)^2 .$$

Moreover, for the decay $\Sigma^0 \to n + \gamma$ we could have the pole $\eta = \Lambda^2$ corresponding to the $\Sigma^0\Lambda^0\gamma$ vertex.

As Feymann graphs, the lowest singularities, for $\Sigma^+ \to p + \gamma$, are represented by Fig. 1:

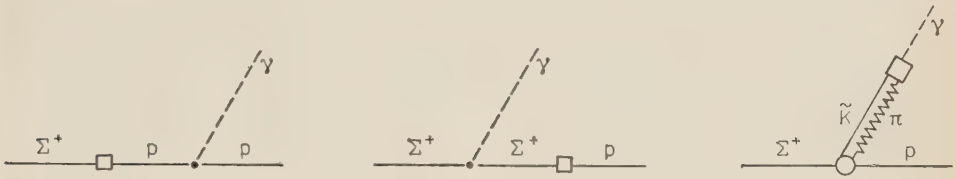


Fig. 1.

The electromagnetic vertices have the general expression

$$\langle p' | j_\mu(0) | p \rangle = ie\bar{u}(p') \left[ F_1(0)\gamma_\mu + \sigma_{\mu\nu}(p' - p)_\nu \frac{x}{2m} F_2(0) \right] u(p) ,$$

$x$: anomalous magnetic moment and $F_i(0) = 1$ and we put for the weak vertex

$$\langle p | H_W(0) | \Sigma \rangle = G\bar{u}_{\mathcal{N}}(p)[a(\Sigma^2) + \gamma_5 b(\Sigma^2)]\, u_\Sigma(q) .$$

with $a, b$ scalar coefficients to be determined.

Taking into account only the barion poles, we obtain for the matrix element:

$$M_{FI} = (2\pi)^4 i\delta(p + k - q) \frac{eG}{\Sigma^2 - \mathcal{N}^2} \bar{u}_{\mathcal{N}}(p) \left\{ \left[ \gamma_\mu - \frac{x_{\mathcal{N}}}{2\mathcal{N}} \sigma_{\mu\nu} k_\nu \right] \cdot \right.$$
$$\cdot [a(\Sigma^2)(\Sigma + \mathcal{N}) + \gamma_5 b(\Sigma^2)(\mathcal{N} - \Sigma)] - [a(\mathcal{N}^2)(\Sigma + \mathcal{N}) + \gamma_5 b(\mathcal{N}^2)(\Sigma - \mathcal{N})] \cdot$$
$$\left. \cdot \left[ \gamma_\mu - \frac{x_\Sigma}{2\Sigma} \sigma_{\mu\nu} k_\nu \right] \right\} u_\Sigma(q) e_\mu^{(r)}(\bar{k}) .$$

Gauge invariance requires

$$a(\Sigma^2) = a(\mathcal{N}^2) , \qquad b(\Sigma^2) = b(\mathcal{N}^2) ,$$

so that we can finally identify

$$(7) \qquad \begin{cases} A = \dfrac{a}{\Sigma - \mathcal{N}} \left( \dfrac{x_\Sigma}{2\Sigma} - \dfrac{x_{\mathcal{N}}}{2\mathcal{N}} \right) , \\ B = -\dfrac{b}{\Sigma + \mathcal{N}} \left( \dfrac{x_\Sigma}{2\Sigma} + \dfrac{x_{\mathcal{N}}}{2\mathcal{N}} \right) . \end{cases}$$

In this way, our results depend on the three quantities $a$, $b$ and $x_\Sigma$, anomalous magnetic moment of the $\Sigma$-hyperon.

While $x_\Sigma$ is unknown at all, « $a$ » and « $b$ » can be related to the decay mode $\Sigma^+ \to p + \pi^0$, if we use for this process the « pole » approximation.

In particular, following FELDMAN *et al.* [3] we can easily see that the branching ratio $\Sigma^+ \to p + \gamma / \Sigma^+ \to p + \pi^0$ is

$$R = \frac{e^2(\Sigma+\mathcal{N})^2 \left\{ \left(\frac{a}{b}\right)^2 (\Sigma+\mathcal{N})^2 \left(\frac{x_\Sigma}{2\Sigma} - \frac{x_\mathcal{N}}{2\mathcal{N}}\right)^2 + (\Sigma-\mathcal{N})^2 \left(\frac{x_\Sigma}{2\Sigma} + \frac{x_\mathcal{N}}{2\mathcal{N}}\right)^2 \right\}}{g^2 \left(1 + \frac{g_{\pi\Sigma}}{g_{\pi\mathcal{N}}}\right)^2 [(\Sigma+\mathcal{N})^2 - \pi^2] \sqrt{(\Sigma^2 - \mathcal{N}^2 - \pi^2)^2 - 4\pi^2\Sigma^2(\Sigma^2 - \mathcal{N}^2)}} \quad (8)$$

Experimentally this ratio seems to be 1/100.

In order to give some rough numerical evaluation we assume global symmetry, $g_{\pi\Sigma} = g$. From the (8) ($R = 1/100$) we obtain, variying $a/b$ (*), the following figures

| $a/b$ | 1 | 2 | 3 | 4 | $\frac{\Sigma+\mathcal{N}}{\Sigma-\mathcal{N}} \simeq 8.44$ |
|---|---|---|---|---|---|
| $x_\Sigma$ in $\mu_0 = \frac{e}{2\mathcal{N}}$ units | − 6.27<br>9.76 | − 2.25<br>5.81 | − 0.90<br>4.47 | − 0.228<br>3.80 | 0.97<br>2.61 |
| $\alpha$ | 0.18<br>0.27 | 0.056<br>0.15 | 0.005<br>0,11 | − 0.032<br>0.090 | − 0.150<br>0.094 |

These numbers should not be taken too seriously. However if more experimental data will be available, the knowledge of the asymmetry parameter for example could give a further independent condition to determine $a/b$ and $x_\Sigma$. Moreover we would like to cite a recent dispersive calculation, given by TANAKA [4], on the magnetic moment of the $\Lambda$ and $\Sigma$-hyperons. This author finds values between $1.53\mu_0$ and $-0.83\mu_0$ for the $\Sigma^+$, values depending both on the calculation method and on the hypothesis on the $\Sigma K \mathcal{N}$ coupling.

The reported approach is the simplest we may use. It's obvious that if we introduce the contribution of the higher intermediate states, our coefficients $A, B$ of eq. (1) will contain a greater number of parameters, some of which unknown. The terms we have neglected are the states of the continuum for the $\xi$, $\eta$ variables and

(*) If we make a perturbative evaluation of the matrix element $\langle p | H_W(0) | \Sigma \rangle$ using the weak coupling $V - A$ between the $\Sigma^0\Sigma^+$ and $p\Sigma^0$ currents

$$\langle p | H_W(0) | \Sigma \rangle = \bar{u}(p)[(1 - \alpha'\gamma_5) S_F(x=0)(1 + \alpha''\gamma_5)] u_\Sigma(q) ,$$

with $\alpha'$, $\alpha''$ unknown at all, we get

$$a/b = \frac{1 - \alpha'\alpha''}{\alpha'' - \alpha'} .$$

(4) Y. TANAKA: *Phys. Rev.*, **122**, 705 (1961).

completely those deriving from the $\zeta$ variable. In the first case we had to take into account for example the $\pi\mathcal{N}$ state with $j=\frac{1}{2}$, whose contribution depends on the photo-production amplitude $j=\frac{1}{2}$.

More important are probably the terms in the « photon mass » variable. The contribution of this first intermediate state $\widetilde{\mathrm{K}}\pi$ can be studied resolving further the weak vertex $\widetilde{\mathrm{K}}\pi\to\gamma$ in this way: $\widetilde{\mathrm{K}}\pi\to\pi\pi\to\gamma$ so that finally we have the strong interaction $\Sigma\widetilde{\mathrm{p}}\to\widetilde{\mathrm{K}}\pi$, the weak vertex $\widetilde{\mathrm{K}}\pi\to\pi\pi$ and the electromagnetic pion form factor $\pi\pi\to\gamma$. The situation in complicated also if, in the interest of simplicity, we admit the existence of the neutral boson of Lee and Yang $W$, transmitter of weak interactions. Then if its mass is $<\mathrm{K}+\pi$ it gives a pole in $\zeta=W^2$ following the graph of Fig. 2.

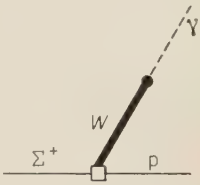

Fig. 2.

It is easily shown that adding this pole, our coefficients $A$ and $B$ are now depending on eight independent parameters.

Similar considerations can be applied to the radiative decay $\Sigma^+\to\mathrm{p}+\pi^0+\gamma$ and a comparison between these processes will be possibly discussed later.

IL NUOVO CIMENTO Vol. XXI, N. 4 16 Agosto 1961

# Some Consequences of Nuclear Forces due to Pion-Pion Interaction.

Y. Fujii

*Department of Physics, College of Science and Engineering, Nihon University - Tokyo*

(ricevuto il 4 Luglio 1961)

**1.** – We have that shown the pion-pion resonance in the state $I=J=1$ affects considerably the nuclear potentials in the regions I and II [1] (*). In particular, the prediction of a repulsive central potential in the $^3$O-state and a strong repulsive tensor potential in the $^3$E-state seems to offer a test for the theory by a re-analysis of the nucleon-nucleon scattering data at low energies. In this note we shall make a preliminarly report concerning these two potentials together with the $L$-$S$ potential in the $^3$E-state.

**2.** – From the recent analysis of Otsuki *et al.* [2], there is no longer any objection to the repulsive central potential in the $^3$P-state. They have shown by an analysis more careful than the previous one [3], that at present no definite conclusion can be drawn as to the sign of the two-pion-exchange potential.

**3.** – Tamagaki has suggested that the strong repulsive $L$-$S$ potential appearing in the $^3$E-state may compensate the effect of the strong repulsive tensor potential, as far as the deuteron is concerned [4]. In the following we shall give the results of his calculation (Case 1 below) together with consideration on somewhat more general cases.

In the case of the deuteron ($^3S_1 + {}^3D_1$ state) the Schrödinger equation reads as follows

$$(1)\ (**) \qquad \frac{\mathrm{d}^2u}{\mathrm{d}r^2} + \gamma^2 u = J_s(r)\ , \qquad \frac{\mathrm{d}^2w}{\mathrm{d}r^2} + \gamma^2 w - \frac{6}{r^2}\, w = J_d(r)\ ,$$

(1) Y. Fujii: *Progr. Theor. Phys.*, 25, 441 (1961).
(*) Hereafter referred to as A.
(2) S. Otsuki, M. Taketani, R. Tamagaki and W. Watari: *Progr. Theor. Phys.*, 25, 427 (1961).
(3) For example, *Progr. Theor. Phys.*, Suppl. no. 3 (1956).
(4) R. Tamagaki: private communication.
(**) We use units in which the pion mass is equal to unity.

where

$$(2)\qquad \begin{cases} J_s(r) = U_C(r)\,u(r) + 2\sqrt{2}\,U_T(r)\,w(r)\,, \\ J_d(r) = [U_C(r) - 2U_T(r) - 3U_{LS}(r)]\,w(r) + 2\sqrt{2}\,U_T(r)\,u(r)\,. \end{cases}$$

Here $u(r)$ and $w(r)$ are the usual deuteron wave functions, and $U(r)$ and $\gamma^2$ are respectively given by

$$U(r) = MV(r)\,,$$

$$\gamma^2 = ME\,.$$

We shall first evaluate $J_s(r)$ and $J_d(r)$ from $V_C$, $V_T$ and $V_{LS}$ as calculated in the ρ-meson formalism with $m=600$ MeV and $h^2=5$ (solid curves in Fig. 6*b* in A), referred to as Case I. Tentatively we use the conventional deuteron wave functions as calculated, for example, by HAMADA [5]. Strictly speaking this procedure is never justified since the conventional wave functions are calculated taking into account only $V_C$ and $V_T$, but neglecting $V_{LS}$. However we shall use them to see the characteristic features of the potentials considered. The numerical results are displayed in Table I for $r=1$ and 1.5. These should be compared with the values calculated from the one-pion-exchange potential (OPEP).

TABLE I

| Case | $(U_C - 2T_T - 3U_{LS})w$ | $2\sqrt{2}\,U_T u$ | $J_d$ | $U_C u$ | $2\sqrt{2}\,U_T w$ | $J_s$ |
|---|---|---|---|---|---|---|
| OPEP | + 0.58 | — 2.31 | — 1.72 | — 0.114 | — 0.894 | — 1.01 |
| | + 0.102 | — 0.559 | — 0.457 | — 0.046 | — 0.163 | — 0.208 |
| I | — 0.99 | + 1.04 | + 0.05(— 2.9) | — 0.51 | + 0.40 | — 0.11(+ 11) |
| | — 0.066 | + 0.097 | + 0.031(— 6.8) | — 0.065 | + 0.028 | — 0.037(+ 18) |
| II | — 0.74 | + 0.81 | + 0.07(— 4.1) | — 0.408 | + 0.31 | — 0.095(+ 9.4) |
| | — 0.034 | + 0.048 | + 0.015(— 3.2) | — 0.034 | + 0.014 | — 0.020(+ 9.5) |
| III | — 1.52 | + 0.68 | — 0.84(+ 49) | — 1.08 | + 0.26 | — 0.82(+ 81) |
| | — 0.088 | + 0.060 | — 0.028(+ 7.6) | — 0.109 | + 0.018 | — 0.091(+ 53) |
| IV | — 0.70 | + 0.59 | — 0.11(+ 6.4) | — 0.27 | + 0.23 | — 0.04(+ 4) |
| | — 0.039 | + 0.052 | + 0.013(+ 3.6) | — 0.027 | + 0.015 | — 0.012(+ 6.9) |

In each case the upper line corresponds to $r=1$, the lower to $r=1.5$. In parentheses the ratios to the corresponding values in the OPEP are written in percentages.

[5] T. HAMADA: *Progr. Theor. Phys.*, **24**, 126 (1960).

4. – We find that each term in $J_d(r)$, for example, $(U_C - 2U_T - 3U_{LS})w$ or $2\sqrt{2}U_T u$ is of comparable order (even larger in some cases) and opposite sign to the corresponding term in the OPEP, but that they cancel each other to give a very small $J_d(r)$ as compared with that in the OPEP (smaller than 10%). The situation is very similar also in the case of $J_s(r)$. These results suggest that the potentials due to the pion-pion resonance, though considerably strong, have only a small effect as far as the static properties of the deuteron are concerned. A re-analysis taking an $L$-$S$ potential into account is strongly suggested.

5. – As noted already in A the calculated potentials involve some uncertainties concerning the mass of the pion-pion resonance, the treatment of the 3-3 resonance and the charge of the pion cloud $2G_1(0)$. In view of these uncertainties we also made the above calculations in the following cases.

Case II: The potentials are calculated with $m \to \infty$, and $T(0)/4\pi = 0.272$ (dotted curves in Fig. 6*b* in A).

Case III: $G_\alpha(k^2)$, the form factor with the pion-pion interaction neglected, is calculated in the Born approximation with the 3-3 resonance neglected (cf. Table III of A). In this case $G_1(0) = 0.66e$, which corresponds to a pion charge of $1.32e$ requiring a negative charge in the core part of the nucleon. The pion-pion resonance is taken into account in the same way as in Case I. This case is interesting because the contribution from the 3-3 resonance seems to be overestimated.

Case IV: Case III is modified by tentatively reducing $G_1(k^2)$ to a half scale, corresponding to a pion charge of $0.66e$.

The numerical results are displayed also in Table I. We find that in Cases II and IV the deviations from the OPEP are not larger than 10%, whereas in Case III the potentials considered give $J_d$ and $J_s$ both drastically different from those of the OPEP. We may, thus, conclude that we should be particularly interested in further developing the calculation of $G_1(0)$.

6. – As shown in the preceeding sections the strong repulsive $L$-$S$ potential in the $^3$E-state plays an important role in the deuteron problem. This character of the $L$-$S$ potential is a consequence of the pion-pion resonance in the $I=J=1$ state (the potentials are proportional to $\tau\tau$, which assumes the value $-3$ in the $^3$E-state). This seems not consistent with the phenomenological $L$-$S$ potentials in that state presented so far ([6]). It should be noted that the $L$-$S$ potential derived from the « ω-meson » with $I=0$ and $J=1$ ([7]), is an attractive one both in the $^3$O-state and in the $^3$E-state. (The magnitudes are also equal.) Therefore a careful analysis of the $L$-$S$ force in the $^3$E-state is strongly suggested. In view of the difficulty of the pn scattering in the high energy region we are interested again in the deuteron problem.

Feshbach has estimated the deuteron magnetic moment arising from the $L$-$S$

([6]) J. Gammel and R. Thaler: *Phys. Rev.*, **107**, 291, 1337 (1957); P. S. Signell and R. E. Marshak: *Phys. Rev.*, **109**, 1229 (1958).

([7]) Y. Nambu: *Phys. Rev.*, **106**, 1366 (1957); Y. Fujii: *Progr. Theor. Phys.*, **21**, 232 (1959); J. J. Sakurai: *Ann. Phys.*, **11**, 1 (1960).

potential ([8]),

$$(\Delta\mu)_{LS} \simeq (M/6)\int_0^\infty \mathrm{d}r\, u^2(r) r^2 V_{LS}(r)\,, \tag{3}$$

in nuclear magnetons. Assuming an $L$-$S$ potential identical to the one fitted to the pp scattering data around 150 MeV ([6]), he obtained the result,

$$(\Delta\mu)_{LS} = -0.036 \div -0.056\,,$$

which is so negative that a *negative* $D$-state probability is necessitated if the other contributions are ignored.

In the case of the pion-pion resonance in the $I=J=1$ state, $V_{LS}$ for the deuteron is repulsive and three times larger in magnitude than $V_{LS}$ in pp scattering. Substituting $V_{LS}$ as calculated in the ρ-meson formalism with $m=600$ MeV and $h^2=5$ in eq. (3) we obtain

$$(\Delta\mu)_{LS} = +0.086\,.$$

This leads to a $D$-state probability of $\sim 19\%$, if the other contributions are ignored (*).

* * *

The author would express his sincere thanks to Dr. R. Tamagaki for informing the author of his calculation before publication. He is also indebted to Dr. S. Otsuki and Dr. W. Watari for their valuable discussions.

---

([8]) H. Feshbach: *Phys. Rev.*, **107**, 1626 (1957).

(*) Among many other contributions we would point out that the $\gamma$-$3\pi$ interaction, required to explain the isoscalar electromagnetic structure of the nucleon, produces a considerable amount of the deuteron magnetic moment ([9])([10]).

([9]) M. Kawaguchi, Y. Miyamoto and Y. Fujii: *Nuovo Cimento*, **20**, 408 (1961).

([10]) Y. Fujii and M. Kawaguchi: *Progr. Theor. Phys.*, to be published.

# LIBRI RICEVUTI E RECENSIONI

## Libri ricevuti.

G. R. Screaton: *Dispersion Relations*; Oliver and Boyd, London, 1961; pp. xiii-290; 55 s.

J. Wilks: *The Third Law of Thermodynamics*; Oxford University Press, Oxford, 1961; pp. 142; 15 s.

E. Fermi: *Notes on Quantum Mechanics*; University of Chicago Press, Chicago, 1961; vii-171; $ 1.50.

S. S. Schweber: *Relativistic Quantum Field*; Row Peterson and Company, Evanston, Ill., 1961; pp. x-905; $ 13.75.

J. Thewlis: *Encyclopaedic Dictionary of Physics*; Vol. 1; Pergamon Press Ltd., Oxford, 1961; pp. xv-800.

R. L. Chase: *Nuclear Pulse Spectrometry*; Mc Graw-Hill Co., New York, N.Y., 1961; pp. vii-221; 66 s.

P. L. Copeland and W. E. Bennett: *Elements of Modern Physics*; Oxford University Press, Oxford, 1961; x+507; 68 s.

D. J. Thouless: *The Quantum Mechanics of Many-Body Systems;* Accademic Press, New York, N.Y.; 1961, ix+175, $ 5.50.

## Recensioni.

*Nuclear Spectroscopy.* Edited by F. Ajzenberg-Selove. Academic Press Inc. Publishers, New York, 1960. Two volumes (Part A pp. xxi-621; part B pp. 625-1147), $ 16.

Questo libro colpisce subito il lettore, fin dalla prima sommaria scorsa dell'indice, per la varietà di argomenti trattati, in uno spazio relativamente piccolo; la parte A, infatti, in sole 624 pagine, raccoglie ben 23 articoli (sotto 17 titoli diversi), raggruppati in 4 sezioni principali (*The Spectroscopy of Charged Particles, Gamma Ray Spectroscopy, Neutron Spectroscopy, Other Topics*; quest'ultima comprendente le reazioni fotonucleari, la misura di vite brevissime e la misura dei momenti elettromagnetici degli stati nucleari) e compilati da 22 autori diversi; la parte B raccoglie in due sezioni principali (*Analisi teorica dei dati* e *Modelli nucleari*), 13 articoli (sotto 12 titoli) e 2 appendici con 13 autori diversi per complessive 523 pagine: la parte A è corredata del proprio indice per argomenti e per autori e la parte B del proprio indice per autori e dell'indice cumulativo per argomento.

Non si può evitare quindi un iniziale scetticismo sulla possibilità di una trattazione adeguata di sì vasto campo, ma occorre dire subito che un'attenta lettura dei vari articoli dissipa largamente tale diffidenza. Infatti il coordinatore (Editor F. Ajzenberg-Selove) dichiara nella prefazione che il libro si propone di

fornire « *un aggiornato resoconto delle presenti conoscenze* » dedicato specialmente a coloro che « *s'incamminano su questo campo senza esteso contatto con la marea di letteratura che è apparsa negli ultimi anni* » e più particolarmente ancora ai neo-laureati « *che si preparano alla ricerca sperimentale in spettroscopia nucleare* » e « *agli specialisti che desiderano acquistare una più ampia comprensione dell'intero campo* ». Tale scopo è stato, in generale, ottimamente conseguito.

Alcuni rilievi che si possono qua e là fare, derivano in gran parte dal fatto che molti articoli danno una sintesi così efficace da far dimenticare che il libro vuol essere solo un aggiornato testo introduttivo alla complessa materia. Ad esempio la bibliografia alla fine dei singoli articoli è generalmente ben curata, pur non pretendendo di essere completa; sarebbe costato molto poco, tuttavia, aggiungere ad ogni articolo la data di chiusura, il che è fatto solo per l'eccellente articolo di Bohr e Mottelson su *Moto collettivo e spettri nucleari*.

Il coordinatore (Editor) riconosce nella prefazione le ovvie difficoltà create dalla molteplicità degli autori, come la disuniformità nel livello e nella profondità di trattazione, ma ritiene che il vantaggio della competenza specializzata nei singoli argomenti fossa fornire un adeguato compenso; bisogna riconoscere che, in generale, tali inconvenienti si riscontrano solo in misura molto ridotta mentre anche molti articoli specializzati sono presentati in forma generale notevolmente sintetica e chiara, senza perdere in precisione.

Certamente se si nota ad esempio che il passaggio attraverso la materia è trattato da autori diversi per le particelle pesanti e per gli elettroni, e lo stesso accade per le interazioni dirette (suddivise in « scattering anelastico » e « stripping and pick-up reactions »), non si può fare a meno di pensare che la sola esigenza di assicurare ad ogni argomento un autore esperto nel ramo non sarebbe stata sufficiente a giustificare una così fine divisione: essa, invece, è forse un indice della difficoltà di trovare persone che, essendo altamente competenti ed attive in un certo ramo di ricerca trovino poi il tempo per un lavoro come quello di una vasta rassegna e di un buon testo.

Ma possiamo aggiungere che scorrendo l'elenco dei singoli autori ci si consola facilmente anche di una eccessiva suddivisione; troviamo infatti ad esempio C. S. Wu e C. Geoffrion per le misure di spettri beta, D. E. Alburger per gli spettri gamma, G. A. Bartholomew per i gamma da cattura neutronica, W. E. Stephens per le reazioni fotonucleari, H. Feshbach per il nucleo composto e per il modello a potenziale complesso, I. C. Biedeuharn per le correlazioni angolari, M. E. Rose per l'analisi dei decadimenti beta e per la conversione interna, D. H. Wilkinson per l'analisi dei dati dei raggi gamma, A. Bohr e B. R. Mottelson per i moti collettivi e spettri nucleari e D. Strominger per l'utilissima tavola degli isotopi, posta in appendice alla parte B.

Quando si è detto che tali autori fanno onore al loro nome, anche per chiarezza di esposizione, e ripetuto che il livello, anche per gli altri articoli, è sensibilmente uniforme, credo si sia detto abbastanza per incoraggiare qualunque lettore.

Il coordinatore precisa ancora nella prefazione che gli argomenti specifici della spettroscopia beta e gamma non sono discussi a lungo per non duplicare l'eccellente libro pubblicato a cura del Siegbahn, ma dato il carattere introduttivo del presente testo, il recensore ritiene che qualche pagina di più e una maggior cura avrebbe potuto esser dedicata a tali argomenti. Ad esempio le 18 pagine complessivamente dedicate ai contatori a scintillazione, suddivise, come sono, fra tre articoli, non bastano a dare un'idea chiara dell'argomento a chi ne sia inizialmente digiuno, anche

se i punti essenziali sono messi abbastanza bene in risalto; solo 4 pagine sono dedicate alla spettrometria gamma con scintillatori ed in essa non compare nessuno spettro tipico che metta almeno in evidenza la relativa importanza del «full energy loss peak», del continuo Compton, etc., nelle varie condizioni sperimentali; la molto opportuna (e interessante per la sua novità) inclusione della camera a bolle a idrogeno come rivelatore di neutroni veloci è trattata però con abbondanza di particolari elementari, mentre la Camera di Wilson a idrogeno (p. 379) viene liquidata con una spiegazione troppo semplice e termodinamicamente insoddisfacente.

I contatori di Čerenkov che, a rigore, avrebbero potuto essere omessi in una trattazione del genere, trovano stranamente, un posto nell'articolo sull'interazione delle particelle beta con la materia, mentre nell'articolo sui rivelatori di particelle cariche, per molti aspetti efficace ed interessante, si trova l'affermazione seguente: «for a particle having the rest mass of a proton the energy of the particle must be of the order of *several hundred million electron volts before such radiation is even possible* with materials of index of refraction about 2»; ciò sorprende non poco in quanto l'applicazione della ben nota condizione $(v/c)(1/n)$, riportata anche nel testo, porta ad una soglia di solo 145 MeV ed è ben noto che a *qualche* centinaio di MeV (da 200 a 340 MeV) MATHER ha addirittura usato l'effetto Čerenkov (sia pure con fasci di particelle e non con particelle singole) (in un mezzo con $n=1.88$) per la taratura in energia del fascio stesso.

Buona la veste tipografica; si nota qualche raro, e non grave, errore di stampa.

Queste osservazioni di carattere marginale nulla tolgono al valore complessivo del libro, per il quale può dirsi che, non solo consegue ottimamente lo scopo dichiarato nella prefazione (e sopra riportato in corsivo), ma raggiunge un livello e un'abbondanza informativa tale da renderne utile la lettura e la consultazione anche a chi lavori già negli specifici argomenti trattati nei singoli articoli.

M. MANDÒ

*X-Ray Microscopy and X-Ray Microanalysis – Proceedings of the Second International Symposium (Stockholm, 1960)*. Edited by A. ENGSTRÖM, V. COSSLETT and H. PATTEE. Elsevier Publishing Company, Amsterdam, 1960; pp. 542, f. 52.50.

Già da vari anni l'interesse di numerosi ricercatori si è rivolto alle possibilità di estendere l'osservazione di oggetti piccolissimi al di là di quanto permetta un microscopio ottico, utilizzando un sistema che, al pari del microscopio ottico, non richieda una preparazione dell'oggetto da osservare che ne generi necessariamente una sensibile alterazione, come accade nel caso della microscopia elettronica, e che dia la possibilità di eseguire sull'oggetto medesimo delle determinazioni di carattere chimico o strutturale.

I raggi X hanno le qualità necessarie per costituire un mezzo atto allo scopo, ma la loro utilizzazione presenta notevoli difficoltà tecniche.

Un primo congresso sull'argomento fu tenuto nel 1956 a Cambridge (Inghilterra) col nome di «Symposium on Microscopy and Microradiography». Furono allora presentati i metodi atti ad ottenere immagini ingrandite mediante raggi X, e discusse le possibilità di avere informazioni sulla costituzione chimica degli oggetti osservati dallo studio di immagini ottenute per assorbimento. In questo secondo congresso invece l'interesse dei ricercatori si è rivolto, in buona parte, a metodi di microanalisi per emissione e per dif-

frazione. Il congresso, relativo ai tre argomenti presentati, è stato diviso in tre sezioni: microassorbimento, microemissione, e microdiffrazione, alle quali presiedettero, rispettivamente, H. Pattee, V. E. Cosslett, A. Engström. Il volume è perciò diviso in tre parti, presentata ciascuna dal relativo presidente di sezione, nella quale viene introdotto l'argomento e accennato ad alcuni risultati.

Nel primo capitolo, che comprende 44 relazioni, dopo alcune osservazioni di carattere teorico sulle proprietà dei raggi X molli, sono presentati vari perfezionamenti della tecnica microradiografica per proiezione, della quale era già stato ampiamente trattato nel precedente congresso. A ciò si aggiungono due note sulla teoria e tecnica della microscopia per riflessione fatta mediante raggi X.

Seguono i risultati ottenuti mediante questi metodi, nel campo della metallurgia e della biologia.

I perfezionamenti dei mezzi tecnici non sono stati tali da offrire nuove effettive possibilità di indagine: infatti non si è ancora raggiunto un potere risolutivo sensibilmente migliore di quello dato dal microscopio ottico. Si è insistito tuttavia con resultati interessanti, nell'usare vari tipi di resine sintetiche o altre sostanze organiche come mezzo sensibile ai Raggi X, allo scopo di superare il limite dato dalla grana della lastra fotografica alla risoluzione ottenibile in una immagine fatta con raggi X, e quindi utilizzare il potere risolutivo del microscopio elettronico per l'osservazione di tale immagine.

Le applicazioni dei metodi d'assorbimento dei raggi X molli sono per la maggior parte di carattere biologico e riguardano in parte tessuti mineralizzati (osso) in parte tessuti osservati con mezzi di contrasto: in parte sono fatte sempre su tessuti, con raggi X mollissimi (700-1 000 V). I resultati che si ottengono offrono dati assai utili per completare le osservazioni che possono essere fatte sugli stessi preparati con metodi ben noti di osservazione al microscopio a luce.

Il secondo capitolo, sulla microemissione, presenta 15 relazioni su quanto si è raggiunto estendendo il ben noto metodo della sprettrometria dei raggi allo studio di oggetti microscopici. Raggi X provenienti da una sorgente che può essere più piccola di un micron quadro ($10^{-6}$ mm$^2$) colpiscono l'oggetto da osservare il quale emette le sue righe caratteristiche. In questo modo può essere analizzato un volume di $10^{-12}$ cm$^3$. Il metodo ha larga applicazione in metallurgia, tanto che microanalizzatori a raggi X vengono ora prodotti commercialmente in varie nazioni. Naturalmente per analizzare l'oggetto si può o muoverlo meccanicamente sotto al fascio esploratore o muovere il fascio rispetto ad esso come si fa per le immagini televisive.

I raggi X vengono a formare una immagine su un tubo catodico. Logicamente i risultati più estesi si hanno con gli elementi pesanti, tuttavia notevoli progressi dobbiamo ormai aspettarci anche per l'osservazione degli elementi leggeri che interessano in modo particolare i soggetti biologici.

Il terzo capitolo, sulla microdiffrazione, presenta l'estensione della tecnica della diffrazione per lo studio di strutture molecolari al caso in cui il materiale in studio sia costituito di cristalli minutissimi eventualmente mescolati ad altro materiale. È necessario a questo scopo che il fascetto di raggi X primario sia ben collimato, e vengono proposti vari tipi di diffrattometri di ampia applicazione pratica in buona parte previsti ad uso dei metallurgici. Si sono però estese le possibilità di questo metodo allo studio della diffrazione sotto piccoli angoli fino a risolvere distanze reticolari dell'ordine di 10 000 Å, risultato di particolare interesse per lo studio di grosse molecole quali si presentano in biologia.

Il volume è senza dubbio di notevole interesse, si presenta con ottima veste tipografica, con brillanti riproduzioni del materiale fotografico; è stimolo a dirigere l'attività dei ricercatori in un campo che ha grandi possibilità di sviluppo.

D. Steve Bocciarelli

Y. W. Lee – *Statistical Theory of Communication*; John Wiley and Sons, Inc. Publ., New York, pp. xviii-510.

La Teoria statistica delle Comunicazioni è quella parte della Teoria delle Comunicazioni che viene spesso chiamata Teoria dell'Informazione. Essa è dovuta essenzialmente ai lavori di C. E. Shannon e N. Wiener ed ha come fine l'utilizzazione migliore di un certo sistema di comunicazioni, considerando il complesso dei segnali e dei disturbi o rumori. Come tale questa teoria (che deriva da moderni sviluppi della Teoria della Probabilità) interessa non solo l'ingegnere delle Comunicazioni, ma anche il Fisico e l'Astronomo. Invero qualunque osservazione può considerarsi come la sovrapposizione di due fenomeni: uno è il fenomeno che vogliamo osservare (per es. la distribuzione dell'energia nel profilo di una riga spettrale di un determinato atomo nell'atmosfera di una stella) e l'altro il disturbo (nel nostro esempio, l'effetto di altri atomi, quello del mezzo interstellare e terrestre che la luce deve attraversare, i vari effetti ottici, fotografici, ecc.). Da ciò l'importanza che la Teoria delle Informazioni sta assumendo negli ultimi anni anche per le tecniche sperimentali (specialmente nella Spettroscopia). Questo libro del Lee, allievo e collaboratore di Wiener, si dirige soprattutto agli Ingegneri, ai quali presenta un quadro dettagliato degli elementi matematici della teoria. Un Fisico-Matematico potrà, forse, trovare un po' troppo tediosi tutti gli sviluppi dei calcoli, alcuni dei quali sono elementari e potevano essere omessi. D'altra parte i testi di N. Wiener sono, per contro, un po' troppo sintetici e la loro lettura riesce alquanto difficile. Pertanto molti preferiranno, probabilmente, la trattazione più elementare, ma completa e tutt'altro che superficiale, di Lee, omettendo eventualmente quelle parti che possono essere già note e troppo evidenti.

L'esposizione è sempre chiara e può essere seguita facilmente da una persona che possieda una cultura matematica corrispondente al 1° biennio di Ingegneria delle nostre Università.

L. Gratton



Direttore responsabile: G. POLVANI Tipografia Compositori - Bologna

Questo fascicolo è stato licenziato dai torchi il 2-IX-1961